NAVAL POSTGRADUATE SCHOOL
Monterey, California

THESIS

BROADBAND HF AND VHF ANTENNA DESIGN WITH TERRAIN MODELING

by

Theodore S. Kline

December 1995

Thesis Advisors: Richard W. Adler
Rasler W. Smith

Approved for public release; distribution is unlimited

DISCLAIMER NOTICE

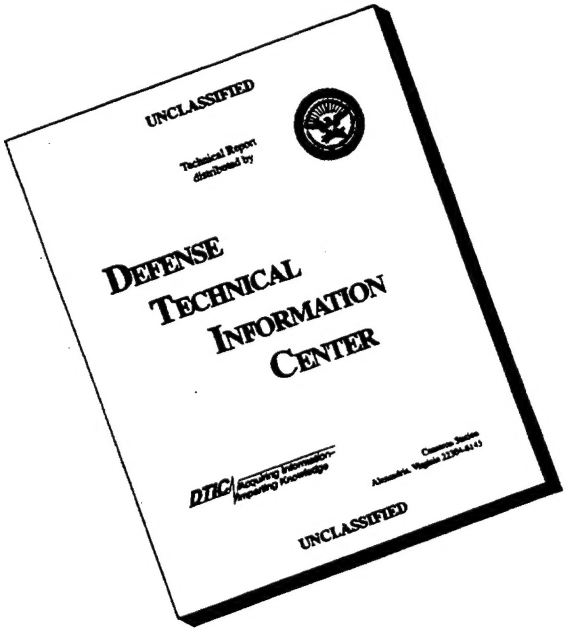

THIS DOCUMENT IS BEST QUALITY AVAILABLE. THE COPY FURNISHED TO DTIC CONTAINED A SIGNIFICANT NUMBER OF PAGES WHICH DO NOT REPRODUCE LEGIBLY.

REPORT DOCUMENTATION PAGE

Form Approved
OMB No. 0704-0188

1. AGENCY USE ONLY *(Leave blank)*	2. REPORT DATE	3. REPORT TYPE AND DATES COVERED
	December, 1995	Master's Thesis

4. TITLE AND SUBTITLE
BROADBAND HF AND VHF ANTENNA DESIGN WITH TERRAIN MODELING

5. FUNDING NUMBERS

6. AUTHOR(S)
Kline, Theodore S.

7. PERFORMING ORGANIZATION NAME(S) AND ADDRESS(S)
Naval Postgraduate School
Monterey, Ca. 93943-5000

8. PERFORMING ORGANIZATION REPORT NUMBER

9. SPONSORING / MONITORING AGENCY NAME(S) AND ADDRESS(S)

10. SPONSORING / MONITORING AGENCY REPORT NUMBER

11. SUPPLEMENTARY NOTES
The views expressed in this thesis are those of the author and do not reflect the official policy or position of the Department of Defense or the U.S. Government.

12a. DISTRIBUTION / AVAILABILITY STATEMENT
Approved for public release; distribution unlimited

12b. DISTRIBUTION CODE

13. ABSTRACT *(Maximum 200 words)*

The objective of this thesis was the design and analysis of broadband antennas to be used with sounders for trans-equatorial propagation research. Sites have been identified in Oahu and Rarotonga. A four step process is used in the design of the antennas. The four steps are: theoretical design, preliminary analysis with ELNEC software, detailed analysis with NEC-4 software and finally terrain modeling with PAINT, MN and TA software.

Preliminary work led to the decision to use two antennas at each site. On Oahu a HF log-periodic antenna is used for the 2-25 MHz band and a VHF log-periodic antenna is used for the 25-60 MHz band. On Rarotonga a VHF log-periodic antenna is also used for the 25-60 MHz band, however a sloping V antenna is used for the 2-25 MHz band. Computer generated impedance values and radiation patterns are presented.

14. SUBJECT TERMS	15. NUMBER OF PAGES
broadband antenna, antenna design, terrain modeling, equatorial propagation	133
	16. PRICE CODE

17. SECURITY CLASSIFICATION OF REPORT	18. SECURITY CLASSIFICATION OF THIS PAGE	19. SECURITY CLASSIFICATION OF ABSTRACT	20. LIMITATION OF ABSTRACT
UNCLASSIFIED	UNCLASSIFIED	UNCLASSIFIED	UNLIMITED

Approved for public release; distribution is unlimited

BROADBAND HF AND VHF ANTENNA DESIGN WITH TERRAIN MODELING

Theodore S. Kline
Captain, United States Marine Corps
B.S., The Pennsylvania State University, 1987

Submitted in partial fulfillment of the
requirements for the degree of

MASTER OF SCIENCE IN ELECTRICAL ENGINEERING

from the

NAVAL POSTGRADUATE SCHOOL
December 1995

Author: Theodore S. Kline
Theodore S. Kline

Approved by:
Basler W. Smith, Thesis Co-Advisor

Richard W. Adler, Thesis Co-Advisor

Herschel H. Loomis, Jr., Chairman
Department of Electrical and Computer Engineering

ABSTRACT

The objective of this thesis was the design and analysis of broadband antennas to be used with sounders for trans-equatorial propagation research. Sites have been identified in Oahu and Rarotonga. A four step process is used in the design of the antennas. The four steps are: theoretical design, preliminary analysis with ELNEC software, detailed analysis with NEC-4 software and finally terrain modeling with PAINT, MN and TA software.

Preliminary work led to the decision to use two antennas at each site. On Oahu a HF log-periodic antenna is used for the 2-25 MHz band and a VHF log-periodic antenna is used for the 25-60 MHz band. On Rarotonga a VHF log-periodic antenna is also used for the 25-60 MHz band, however a sloping V antenna is used for the 2-25 MHz band. Computer generated impedance values and radiation patterns are presented.

TABLE OF CONTENTS

LIST OF FIGURES

LIST OF TABLES

I. INTRODUCTION

A. DISCUSSION OF THE PROBLEM

Communication and surveillance via the ionosphere require an understanding of conditions necessary for radio wave propagation. Currently mid-latitude conditions are adequately understood to facilitate modeling and prediction programs. Equatorial ionospheric conditions are not currently understood well enough to use condition information for prediction. One reason for the difficulty of prediction near the equator is the "Appleton" or "Equatorial" anomaly. This anomaly is caused by electrons rising over the equator then drifting north and south due to the earth's electric and magnetic fields. The anomaly is also known as the "fountain effect" and the result is "electron clumps" located about 10 to 20 degrees north and south geomagnetic latitude.[Ref. 1] The Naval Postgraduate School is currently conducting research to better understand and predict the equatorial ionosphere.

B. RESEARCH OBJECTIVES

One method of studying the ionosphere is through remote sensing by radio waves from an ionosonde. A swept-frequency ionosonde probes the ionosphere using a synchronized transmitter and receiver. An oblique ionosonde uses a separated transmitter and receiver and can provide observations of all propagation modes being supported by the ionosphere at that time, maximum usable frequencies (MUF's) for each mode, and electron density information. Ionosondes can also be useful in measuring scintillations which are variations in amplitude, phase, polarization or angle of arrival. [Ref. 2]

Research being conducted by the Naval Postgraduate School requires a transmitter placed on Rarotonga in the Cook Islands and a receiver placed on Oahu in Hawaii. As shown in Figure 1, Rarotonga and Oahu are nearly conjugate to the magnetic equator. These two sites are ideal locations for placement of sounders to study trans-equatorial propagation (TEP).

The objective of this thesis is to design and analyze broadband antennas to be used with the sounders for 2-60 MHz. The required elevation pattern is 0-45 degrees to support propagation of various modes. Since the circuit is point-to-point, the antenna azimuth patterns should be very narrow. The sounders require 50 ohm antennas. This thesis uses several programs to model the antennas including: NEC-4, ELNEC, and MN. Additionally, terrain modeling will be done with the Performance of Antennas In Non-ideal Terrain (PAINT) program and the Terrain Analyzer (TA) program.

Chapter II will discuss trans-equatorial propagation between Rarotonga and Oahu. Chapter III will discuss antenna design theory for long wire antennas, log-periodic antennas and effects of terrain. Chapter IV will show preliminary antenna designs and ELNEC results. Chapter V will discuss antenna selection and show NEC-4 results. Chapter VI will discuss terrain modeling and show the effect of terrain on the elevation patterns for the Oahu and Rarotonga sites. Chapter VII will present conclusions, sample comparative analysis and recommendations.

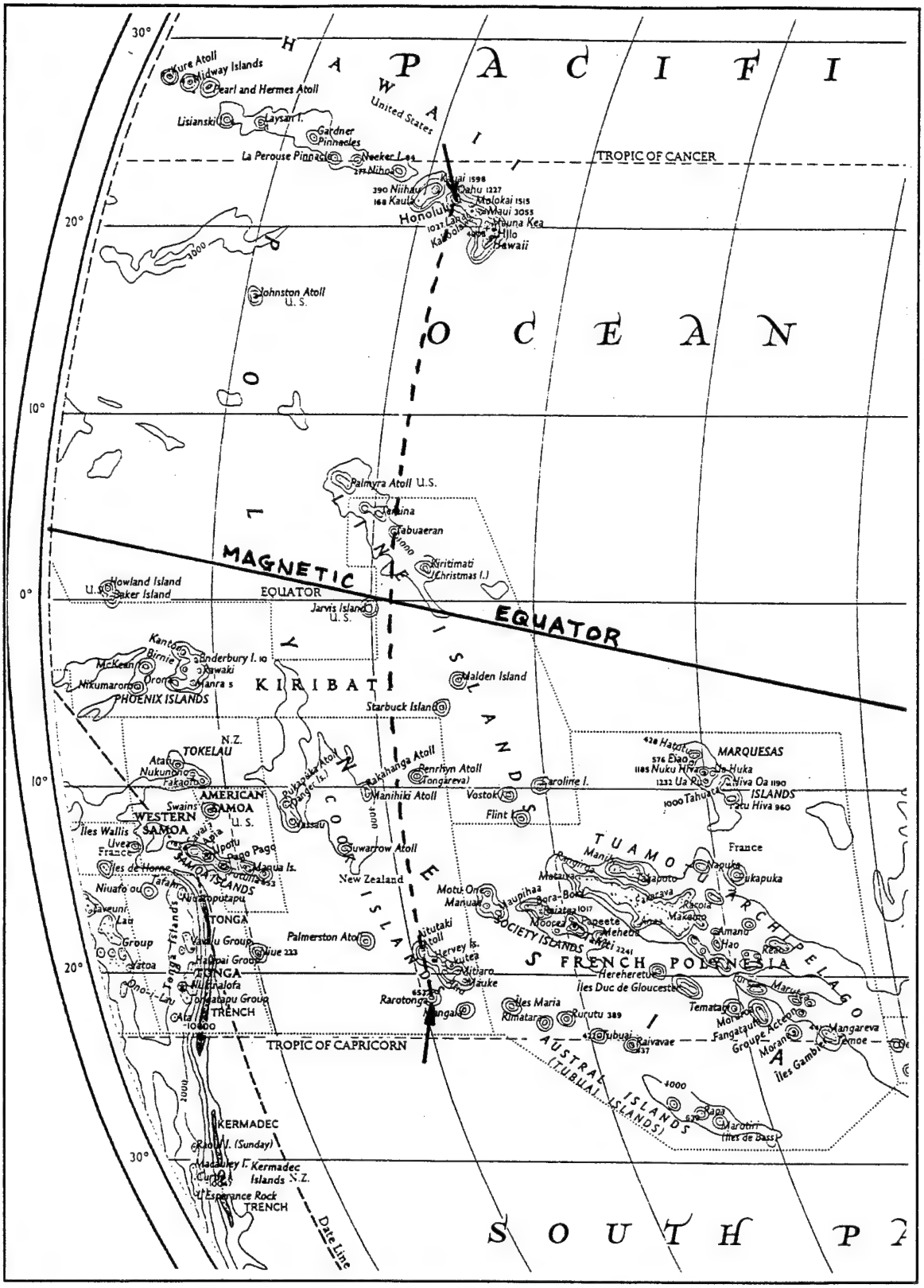

Figure 1. Locations of Rarotonga and Oahu.

II. TRANS-EQUATORIAL PROPAGATION

A. OVERVIEW OF IONOSPHERIC PROPAGATION

The ionosphere is formed when extreme ultraviolet (EUV) light from the sun strips electrons from the neutral atoms of the Earth's atmosphere. When an EUV photon hits a neutral atom, energy is transferred to an electron which escapes from the atom producing a positively charged ion. These free electrons refract radio waves. The ions are too massive to respond to the rapid oscillations of a radio wave. [Ref. 1]

Figure 2 is a simplified illustration of how the ionosphere may reflect a skywave enabling radio wave propagation over long distances. Although a ground wave is shown in the figure, these waves normally dissipate before reaching the receiver. Point "P" is defined as the point of reflection a distance "h" above the earth. In reality the skywave is not reflected at "P" but continuously refracted or bent towards the ground as it propagates within the ionosphere. In this thesis, the term "reflection" is adequate to describe refraction and subsequent return to earth.

The electron density determines the maximum frequency that can be reflected. The critical frequency is defined as the maximum frequency that will be reflected at vertical incidence and is determined by [Ref. 1]:

$$f_c \approx 9\sqrt{N_m} \qquad (1)$$

where f_c is in Hz and N_m is the electron density (electrons $/m^3$) and is a function of height. Frequencies higher than f_c will pass through the ionosphere at vertical incidence.

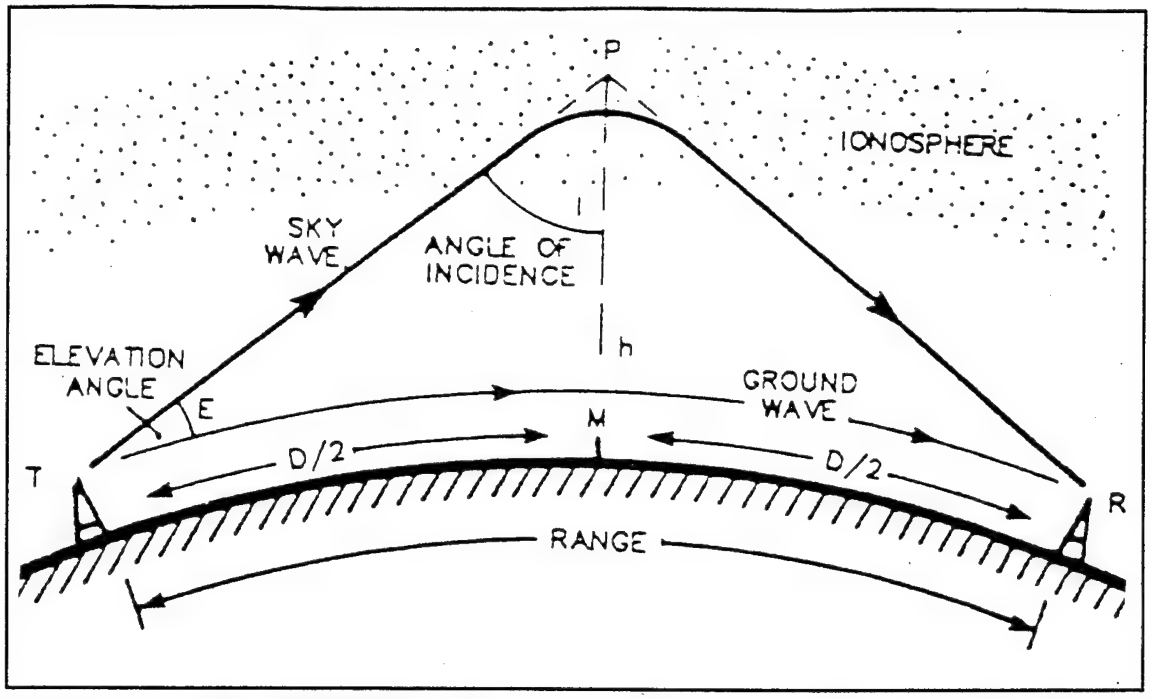

Figure 2. Simplified Model of Skywave and Groundwave Paths. From Ref. [1]

For oblique angles of incidence the maximum usable frequency (MUF) is defined as :

$$MUF = f_c / \cos\theta_i = f_c \sec\theta_i \qquad (2)$$

where θ_i = angle of incidence ($\theta_i = 0$ degrees for vertical incidence). As shown in Figure 3 for a fixed circuit, higher frequency rays (rays 2 and 3) penetrate further into the ionosphere than the lower frequency ray (ray 1). The frequency ray higher than the MUF penetrates through the ionosphere (ray 4).

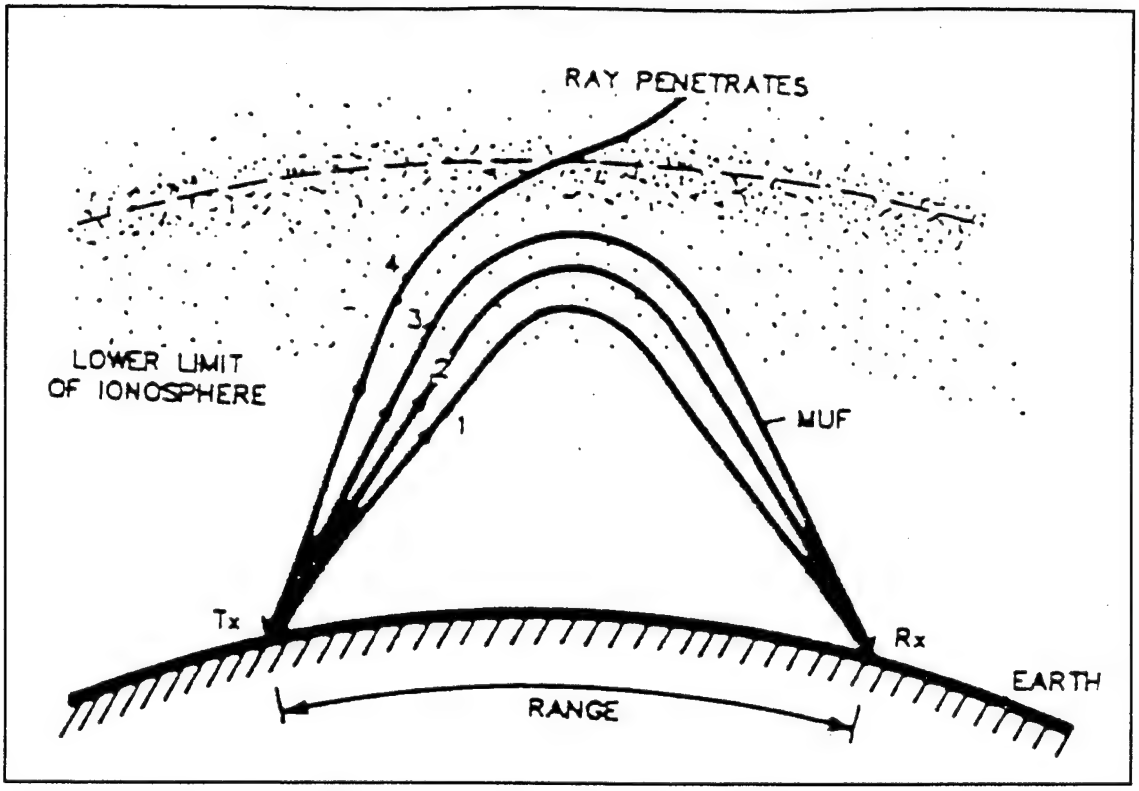

Figure 3. Raypaths for Increasing Frequency. From Ref. [1]

B. CHARACTERISTICS OF THE EQUATORIAL IONOSPHERE

The equatorial ionosphere, as other regions of the ionosphere, has five main variations. The ionosphere varies with location, season, height, solar activity, and time of day. The main basic difference between the equatorial ionosphere and the mid-latitude ionosphere is the "fountain effect" which redistributes electrons at low latitudes, moving electrons from over the magnetic equator, north and south 10 to 20 degrees latitude. As illustrated in Figure 4, electrons produced near the equator by photoionization drift upwards under the combined influence of horizontal electric and magnetic fields. The electrons then diffuse down along lines of force of the Earth's magnetic field north and

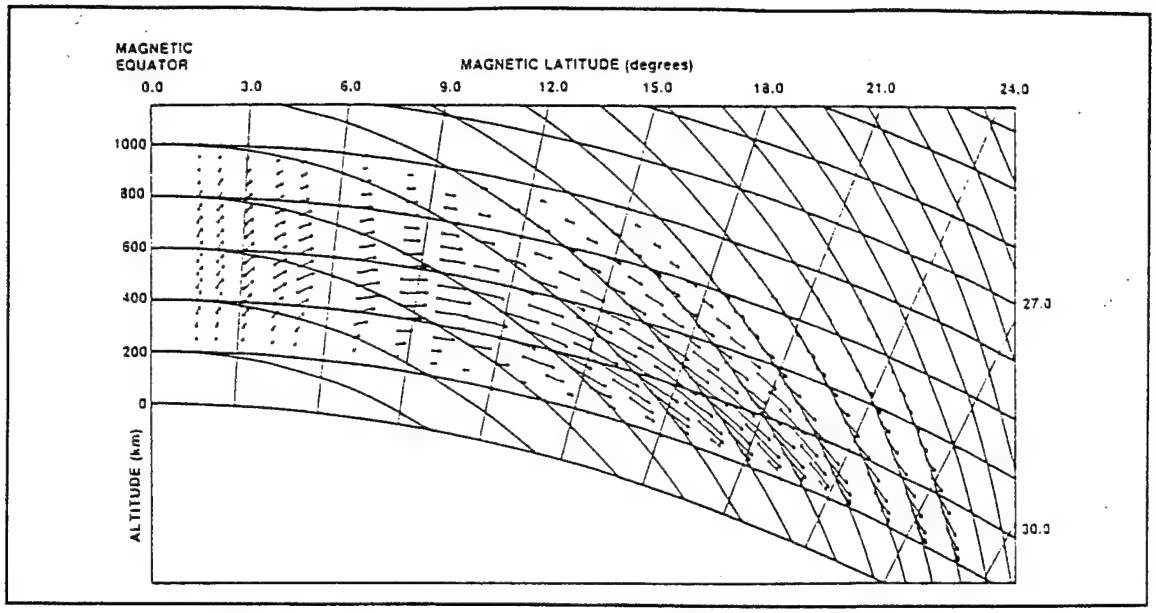

Figure 4. The Equatorial "Fountain Effect". From Ref. [1]

south. As a result, large numbers of electrons produced near the equator end up in crests or clumps of electrons north and south of the magnetic equator. [Ref. 1]

C. RAROTONGA - OAHU PROPAGATION MODES

Two unusual trans-equatorial propagation modes have been identified. These two modes can facilitate use of a higher MUF than normal multi-hop modes. The modes are called "afternoon-type TEP" and "evening-type TEP".

The afternoon-type TEP normally peaks around 1700 to 1900 local time, near the equinoxes and around solar cycle maximum. The propagation mode for the afternoon-type TEP is a super F or FF mode as shown in Figure 5. The signal is reflected twice by the F layer electron crests on opposite sides of the equator. [Ref. 1] The electron crests are formed by the fountain effect described in the previous section.

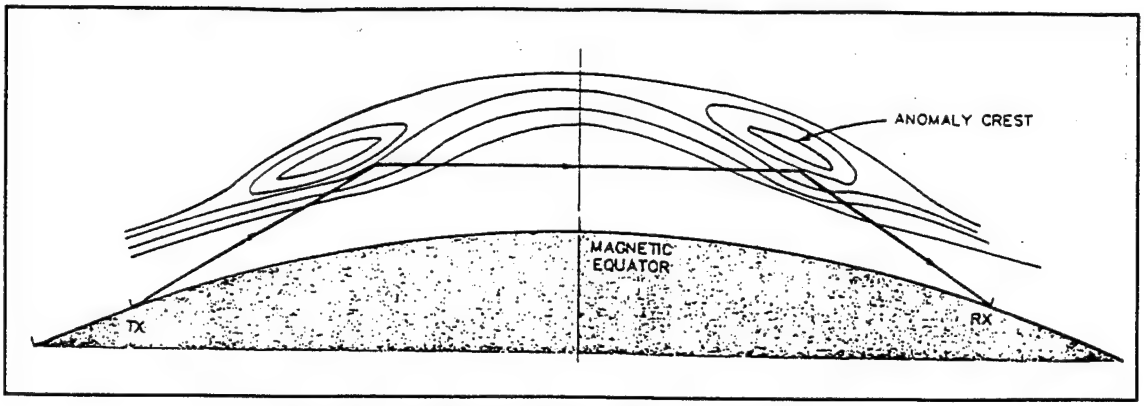

Figure 5. Afternoon-type TEP. From Ref. [1]

The evening-type TEP occurs around 2000 to 2300 local time near equinoxes and around solar maximum. As shown by Figure 6, the evening-type TEP is caused by a "tube" or "bubbles" of electron depletion regions. These tubes are formed after sunset as the F layer rapidly rises and diffuses along the Earth's magnetic field lines. Radio waves propagate through the tubes by reflecting off the walls. [Ref. 1] The evening-type TEP between Hawaii and Rarotonga was observed as early as 1958 when Hawaiian TV stations were received in Rarotonga in the evening hours. [Ref. 3]

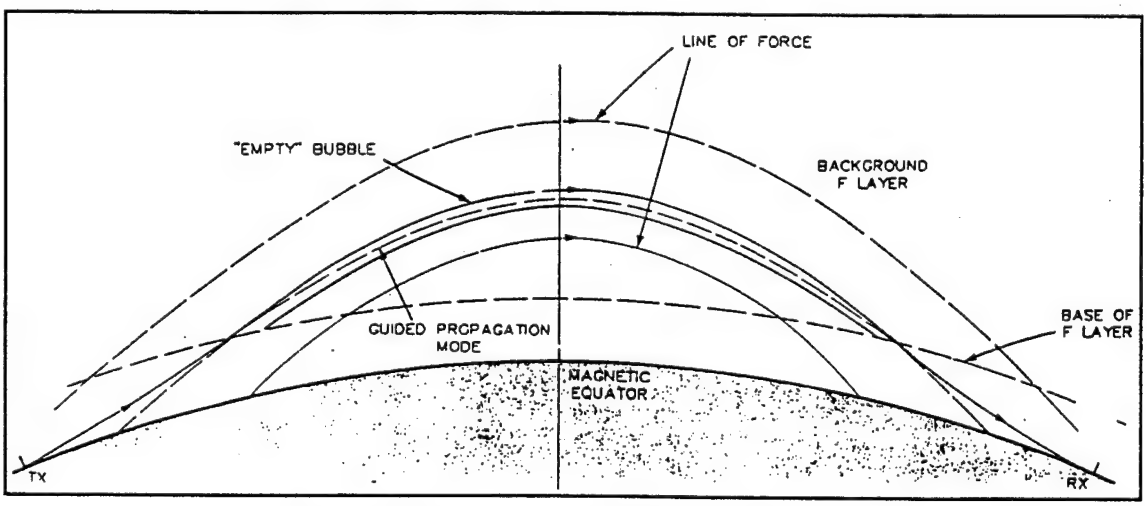

Figure 6. Evening-type TEP. From Ref. [1]

Another phenomenon affecting low latitude propagation is the sporadic E layer. The equatorial sporadic E layer is made up of electron clouds a few kilometers thick and a few hundred kilometers across. It is caused by a plasma instability due to the high electron drift velocity. It is essentially a daytime occurrence. Sporadic E layers are very patchy and transparent to vertically incident signals. To oblique radio waves a sporadic E layer is very reflective and can affect propagation on long circuits.

III. ANTENNA DESIGN THEORY

A. LONG WIRE RADIATORS

1. Electrical Length

Long wire antennas have been proven to be effective in long range HF ionospheric propagation. Various configurations have been used including the rhombic, sloping V, horizontal V, inverted V, and others. The electrical length of a single wire determines the radiation pattern produced around the wire. Figure 7 shows some examples of the cones of radiation lobes produced around a single wire. There is a lobe for each half wavelength of wire length. As the wire length increases the first major lobe becomes narrower and makes a smaller angle with respect to the wire axis. [Ref. 4] The angle between the first major lobe and the wire is approximately given by [Ref. 5]:

$$\cos\theta \approx 1 - \frac{0.37\lambda}{L} \qquad (3)$$

where L is the wire length and λ is the wavelength.

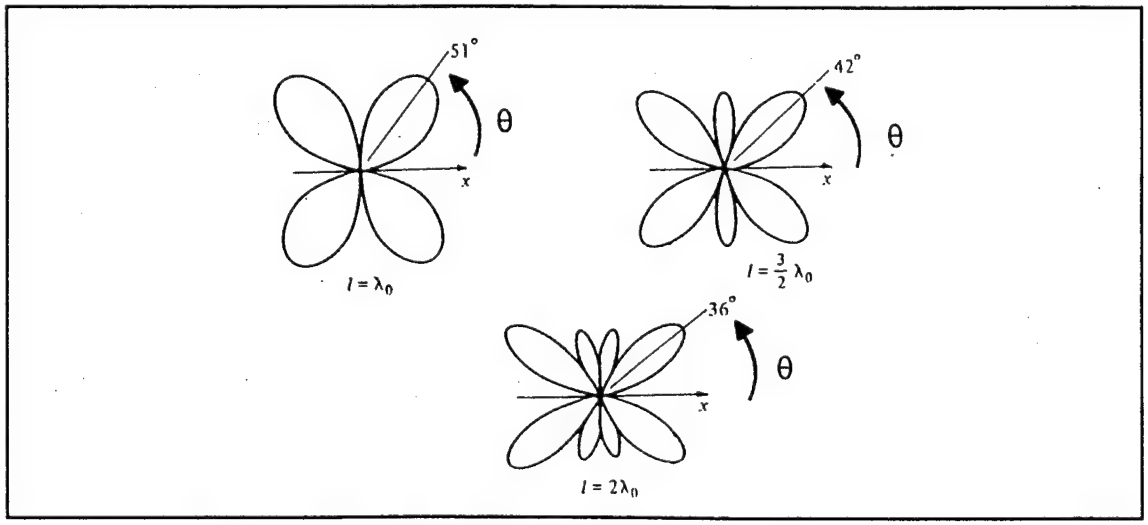

Figure 7. Long Wire Radiation Patterns. From Ref. [4]

Several wires can be oriented to produce a maximum in a particular direction. Figure 8 shows the resulting pattern when two wires are combined in a V shape. The combination will produce a maximum when the wires are positioned so that the main lobes will add. In this case, the wires are two wavelengths long. With Equation (3) it can be determined that the angle between the wires should be about 72 degrees for maximum major lobe addition.

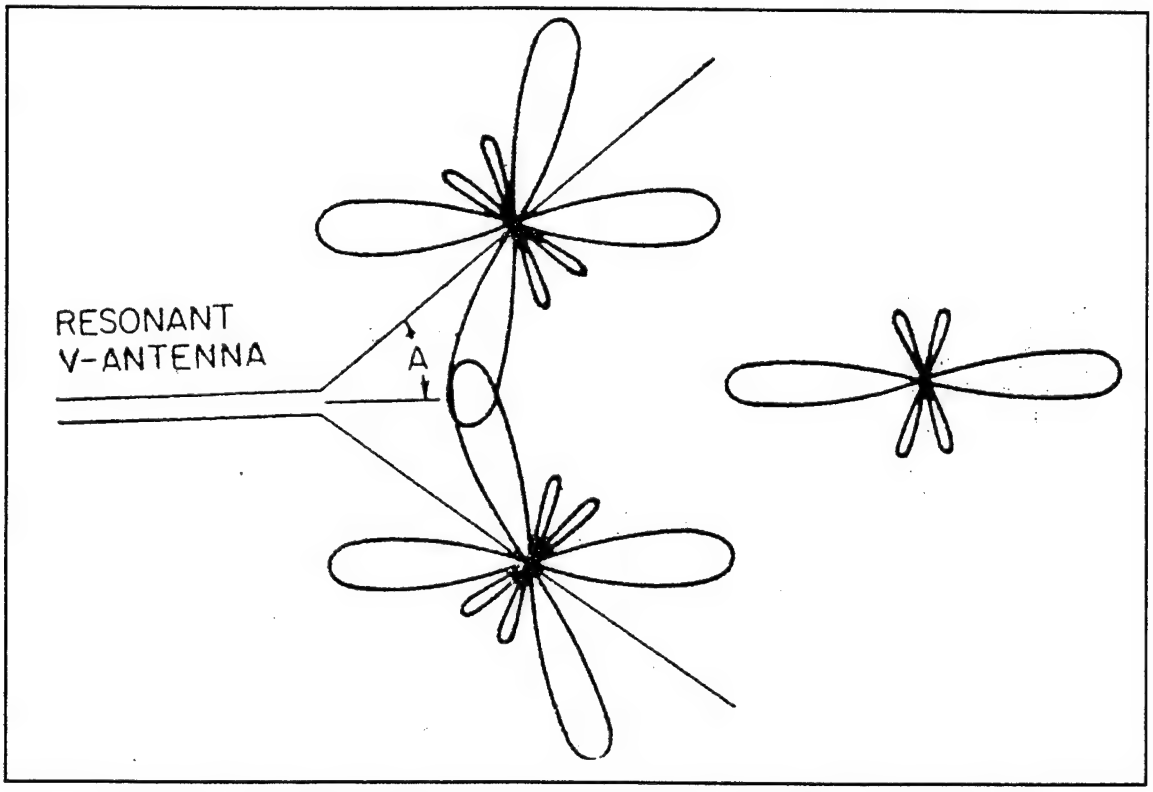

Figure 8. Resulting Pattern From Combining Long Wires. From Ref. [6]

2. Standing vs. Traveling Waves

A long wire antenna that is not terminated through a load is called a resonant or standing wave antenna. Standing wave antennas are designed for single frequency operation because a slight change in frequency causes a change in input impedance.

A long wire antenna that is terminated through a resistor is called a non-resonant or traveling wave antenna. In a traveling wave antenna the wave propagates along in one direction only because any remaining power at the far end is absorbed in the load and nothing is reflected. The benefit of using a traveling wave antenna is that the input impedance varies only slightly with frequency. [Ref. 5]

As shown in Figure 9, a traveling wave antenna produces lobes in the same location as a standing wave antenna. However, the lobes in the backward direction are greatly reduced as the wave is not reflected back but instead absorbed by the load.

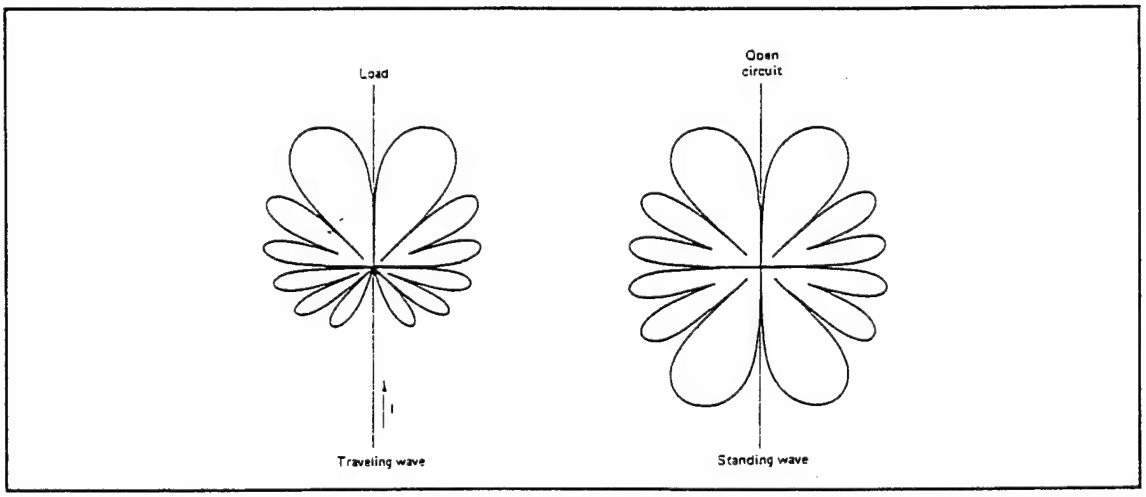

Figure 9. Traveling Wave and Standing Wave Radiation Patterns. From Ref. [6]

3. Feeding Wire Antennas

There are two primary concerns in connecting a wire antenna to a transmitter or receiver. The first is the impedance match between the antenna and the transmission line for maximum power transfer. The second is the excitation of a balanced current distribution on the antenna. [Ref. 7]

a. Impedance Match

The problem with impedance matching is that the antenna impedance changes with frequency. As discussed in the previous section, a long wire antenna that is grounded through a load will have an impedance that is less sensitive to frequency changes than a standing wave antenna. The antenna reflection coefficient is defined as:

$$\Gamma = \frac{Z_{in} - Z_o}{Z_{in} + Z_o} \tag{4}$$

where Z_{in} is the antenna input impedance and Z_o is the transmission line characteristic impedance. A mismatch will result in a partial standing wave on the transmission line with a voltage standing wave ratio (VSWR) given by:

$$\text{VSWR} = \frac{1+|\Gamma|}{1-|\Gamma|} \tag{5}$$

b. Balanced Antenna Currents

A symmetrical antenna should be fed so that the currents are balanced because unbalanced currents will change the antenna radiation pattern. Some transmission lines are balanced and some are unbalanced. A parallel pair of wire lines of the same diameter are inherently balanced and will excite balanced currents on a symmetrical antenna. A coaxial transmission line is one type of unbalanced line. A wave traveling down a coax line may have currents on the inner conductor and inside the outer conductor that have equal magnitude and opposite phase. The problem arises when the wave reaches the antenna and currents flow back on the outside of the outer conductor. This current may radiate and unbalances the current distribution on the antenna. A device called a

balun (**BA**Lanced to **UN**balanced) may be used to suppress the outside current. Different types of baluns have been used and many types are frequency dependent. [Ref. 8]

B. LOG-PERIODIC DIPOLE ANTENNAS

1. Theory

A log-periodic antenna has a structural geometry such that its impedance and radiation characteristics repeat as the logarithm of frequency. Log-periodic antennas are generally considered to be frequency independent over an operating band because variations are minor over the band. [Ref. 7] Figure 10 shows the geometry of a log-periodic dipole array. The structure is fed at the vertex end and energy travels along the structure until it reaches a resonant portion. The resonant portion radiates the energy back towards the vertex, leaving only insignificant power in the larger sections beyond. [Ref. 5]

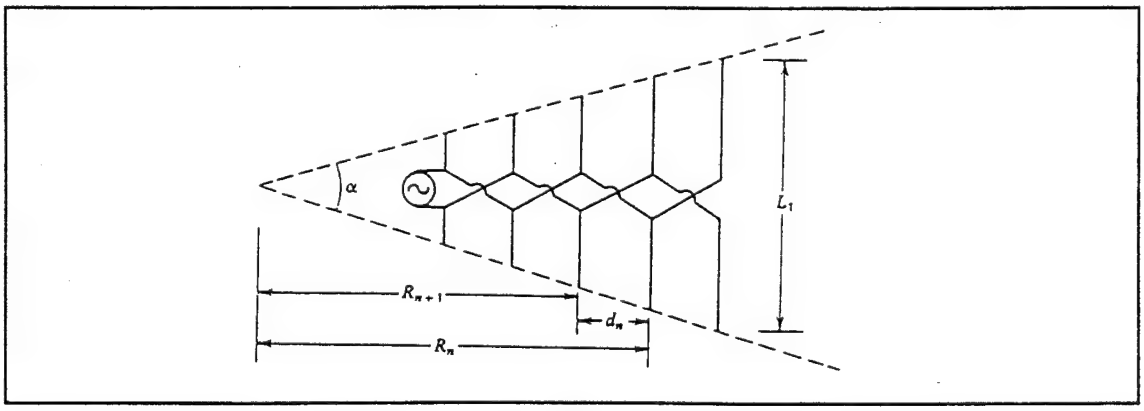

Figure 10. Log-periodic Dipole Array. From Ref. [7]

An important design parameter for the log-periodic is the taper ratio which is [Ref. 7]:

$$\tau = \frac{R_{n+1}}{R_n} = \frac{L_{n+1}}{L_n} = \frac{d_{n+1}}{d_n} < 1 \qquad (6)$$

where R is the distance from the virtual apex, L is the dipole element length, and d is the

spacing between elements. The taper ratio is normally between 0.80 and 0.98. The size of the longest and shortest elements are determined by the frequency band limits [Ref. 7]:

$$L_1 \approx \frac{\lambda_L}{2} \qquad \text{and} \qquad L_N \approx \frac{\lambda_U}{2} \tag{7}$$

where λ_L is the lower frequency wavelength and λ_U is the upper frequency wavelength. Another important design parameter is the spacing factor which is used to determine the spacing d, once the element lengths are known [Ref. 7]:

$$\sigma = \frac{d_n}{2L_n} \tag{8}$$

Figure 11 can be used to obtain the spacing factor for an optimum gain given a taper ratio.

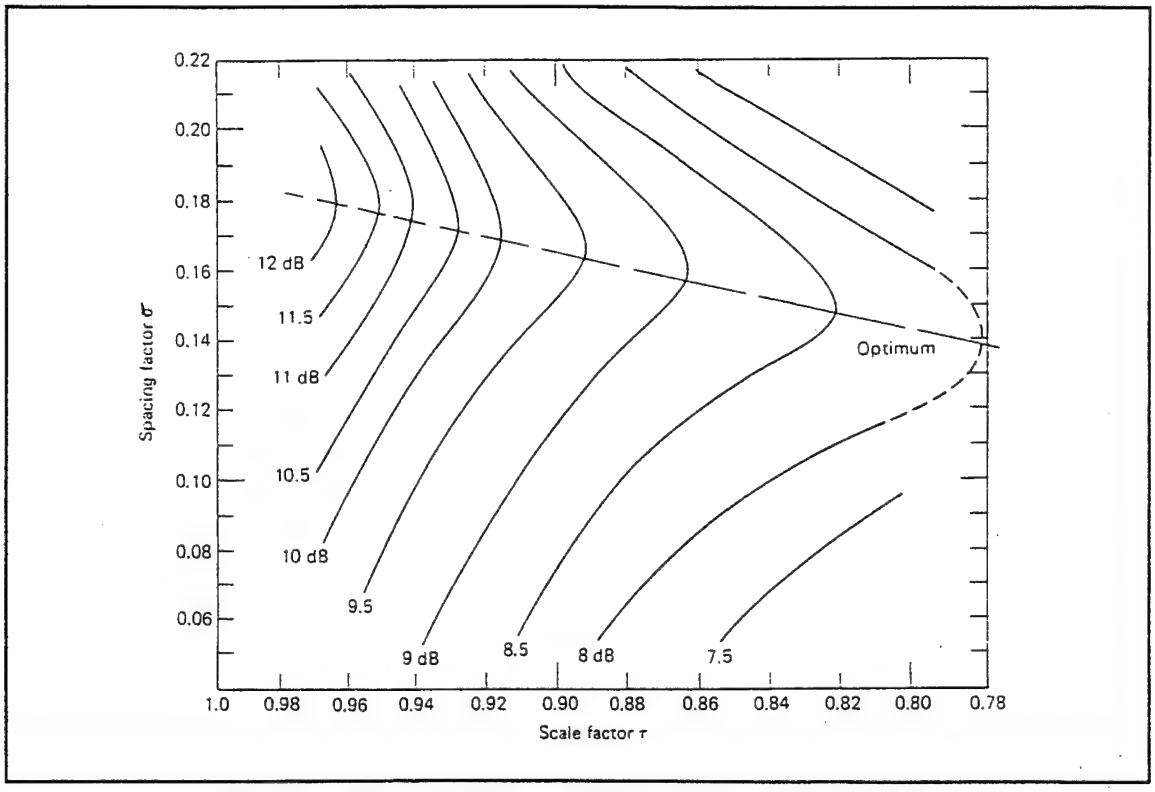

Figure 11. Spacing Factor vs. Taper Ratio. From Ref. [7]

2. Feeding the Log-periodic Antenna

The transmission line feeds between elements of the log-periodic antenna are crisscrossed as shown in Figure 10. This results in mutual cancellation of backlobe components from the individual elements. [Ref. 5] HF log-periodic antennas usually consist of complex wire arrays. This type of antenna can be fed with a balanced twin lead transmission line. VHF log-periodic antennas may require a different feed arrangement. A coax feed and an infinite balun can be used. As shown in Figure 12, the direction of the elements on the outer shield of the coax feeder and dummy coax is alternated to achieve the crisscross. [Ref. 6]

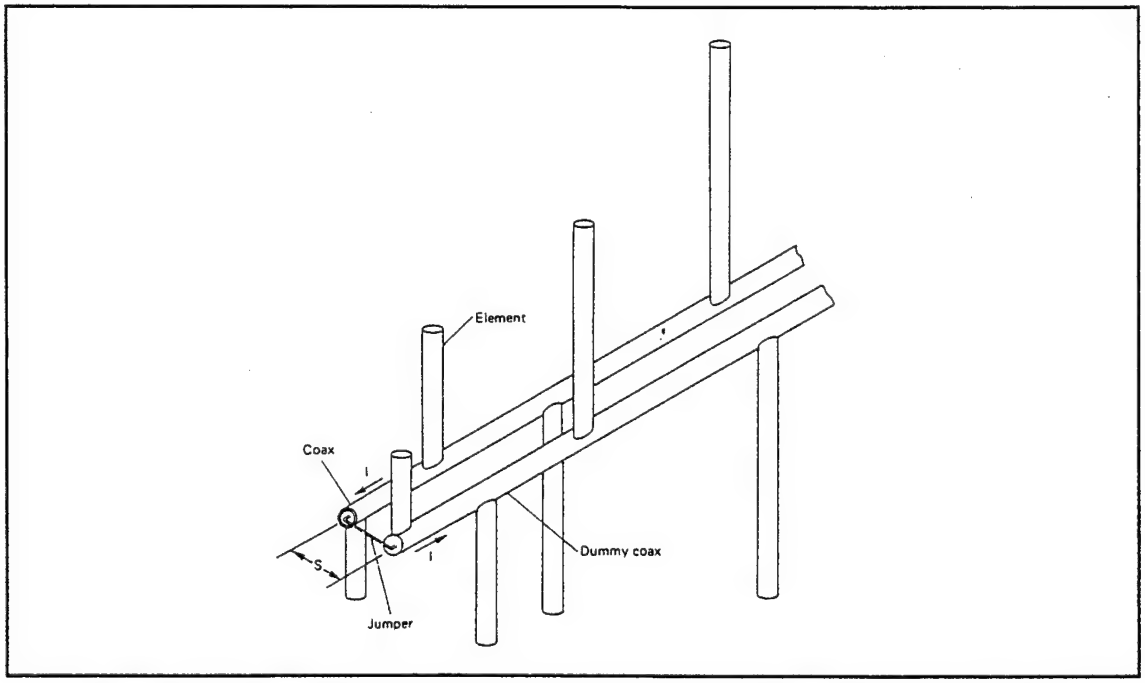

Figure 12. Log-periodic Antenna Feed with an Infinite Balun. From Ref. [6].

C. EFFECT OF THE TERRAIN

1. Antenna Height and Array Theory

Array theory can be used to predict radiated fields from an antenna over flat ground. Figure 13 illustrates how a reflected ray and direct ray at an elevation angle can add. For a perfect conducting surface the array factors will be [Ref. 4]:

$$|F(\psi)| = 2|\sin(k_o h \sin\psi)| \quad \text{for horizontal polarization} \qquad (9)$$

$$|F(\psi)| = 2|\cos(k_o h \sin\psi)| \quad \text{for vertical polarization} \qquad (10)$$

where $k_o = \frac{2\pi}{\lambda_o}$. These two equations are useful in determining the approximate height at which the rays will add constructively for a given elevation angle. The ground plane conductivity affects the strength of the reflected wave. Over real ground the strength of the reflected wave is less than over a perfectly conducting ground. [Ref. 8]

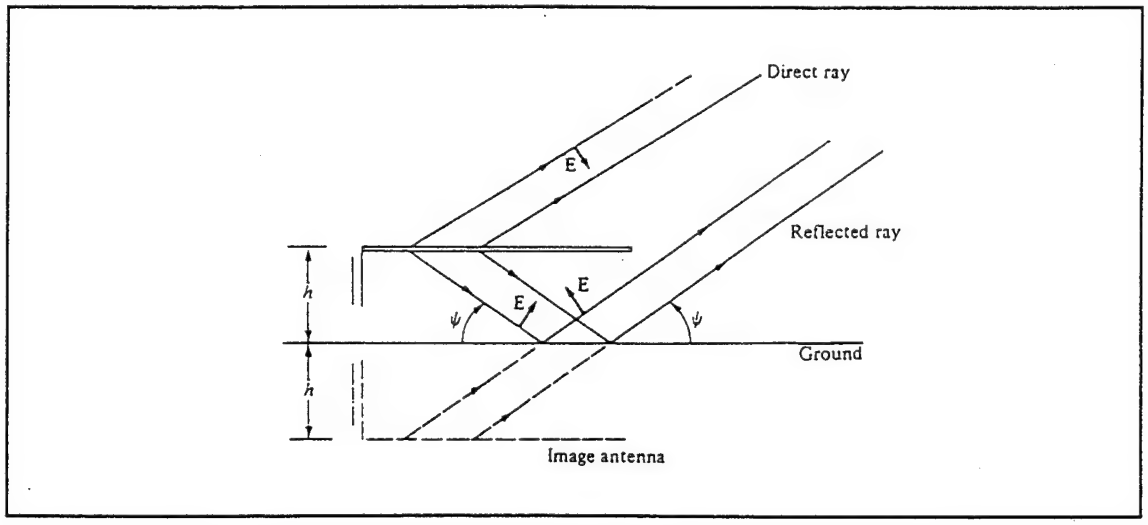

Figure 13. Illustration of Ground Reflection. From Ref. [4]

2. Ground Conductivity and Permittivity

Good conductors have conductivities on the order of 10^7 mho/m. Earth conductivity varies from about 10^{-1} mho/m with rich soil to about 10^{-3} mho/m in rocky or sandy soil. The relative permittivity varies from about 4 to 7 in dry sandy ground to about 10 to 20 in moist soil.

3. Terrain Modeling and the Geometric Theory of Diffraction

The effects of flat terrain can be modeled using geometric optic techniques. Geometric optics uses ray tracing to add direct rays and reflected rays, but has limitations in modeling irregular terrain. It can not model fields in shadowed regions where the direct and reflected fields are zero. The geometric theory of diffraction (GTD) overcomes the limitations of geometric optics by using diffraction and geometric optics to model fields in shadowed regions. Programs using GTD can model terrain by flat plates and dielectric layers. The total field at any point is the sum of the incident, reflected and diffracted fields [Ref. 9]:

$$U_{tot} = U_{inc} + U_{reflected} + U_{diff} \tag{11}$$

Figure 14 shows a source near a plate and the three fields contributing to the total field at an arbitrary point.

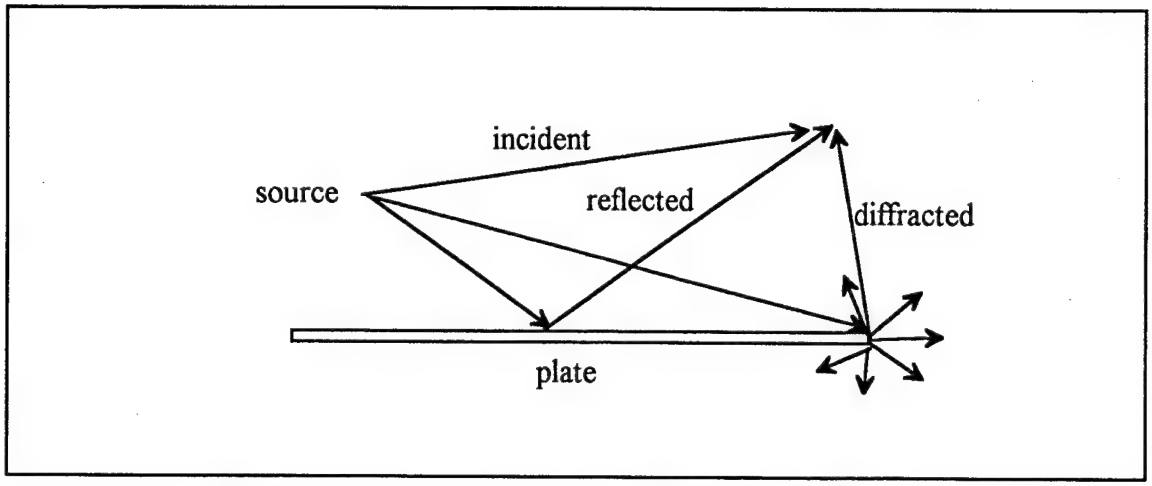

Figure 14. Geometric Theory of Diffraction Technique.

IV. PRELIMINARY ANTENNA DESIGN

A. DESIGN PROCESS

The first design decision was to use two broadband antennas to cover 2-60 MHz. One antenna was for 2-25 MHz and the other for 25-60 MHz. Several designs were examined for the 2-25 MHz band including a rhombic, a sloping V, and an HF log-periodic antenna. For the 25-60 MHz range a VHF log-periodic antenna was analyzed.

Several computer programs were used for design analysis. All preliminary work was done with ELNEC because of its simplicity and quick results. ELNEC antennas were modeled with segmented wires above a flat ground plane. Final designs were modeled and run on NEC-4 with a flat ground plane. Terrain modeling was also done with the PAINT and TA programs using terrain information at the two sounder sites.

B. COMPUTER MODELING OF ANTENNAS IN TERRAIN

1. NEC-4

The Numerical Electromagnetic Code (NEC) - Methods of Moments is a program used for analyzing the electromagnetic response of wire antennas and scatterers. NEC-4, the latest version, numerically solves integral equations for antenna currents by the method of moments. In NEC-4, wires are modeled as short straight segments and finite surfaces as perfectly conducting flat patches. The program operation is controlled by structure data and commands read from an input file which is normally created with a text editor. NEC-4 output files contain current distributions, impedance, power output, dissipation,

efficiency, radiation patterns and gains. Separate software is used to produce radiation plots from the output file. Antenna wires are specified by their endpoints and radii. Wires should be divided into 10-20 segments per wavelength. The segment lengths should also be at least several times longer than the wire radius. NEC-4 uses the thin wire approximation and neglects transverse currents on the wires. This is valid for $2\pi a << \lambda$, where a is the wire radius. Some other modeling guidelines are: segments may not overlap, a segment is required at each point where a source will be located, and the minimum separation between parallel wires should be at least several times the wire diameter. [Ref. 10]

NEC-4 can model a finitely conducting ground plane with a modified-image solution known as the Reflection Coefficient Approximation (RCA) or with a method based on the exact Sommerfield-integral solution for a source near an interface. The RCA solution can not be used to model long wire antennas close to ground because the RCA can produce an erroneous current that grows exponentially away from the source due to approximation errors. [Ref. 10]

2. PAINT

The Performance of Antennas In Non-ideal Terrain (PAINT) software models antennas located over 3-dimensional irregular terrain. The PAINT system is a collection of Fortran software programs written to run on a PC using the MS-DOS operating system. PAINT can access the United States Geological Survey (USGS) Digital Elevation Model (DEM) terrain data or the Defense Mapping Agency (DMA) Digital Terrain Elevation Data (DTED). A text file with x,y,z triplets can also be used by PAINT as

terrain input data. PAINT uses terrain data to create a terrain file consisting of triangular flat plates. Complex antennas can be defined by the user or by NEC output files. Terrain and antenna files are analyzed together by the Numerical Electromagnetic Code-Basic Scattering Code (NEC-BSC) which uses the geometric theory of diffraction. PAINT output patterns can be displayed in polar form on the screen or sent to a hard copy device. [Ref. 9]

3. ELNEC

ELNEC is an enhanced version of the MININEC antenna analysis program for the PC. It is faster than MININEC and easy to use. It has a menu-based system for describing and changing antennas. Special features allow fast and simple structure modifications. Antennas are modeled with segmented wires. The ELNEC rule of thumb is to have 20 segments per wavelength for pattern or gain analysis and about 40 segments per wavelength for more critical parameters such as impedance calculations. ELNEC has a wire segment-taper option for wires connecting at angles. ELNEC can model antennas over "real" flat ground. It assumes a perfect ground for impedance and current calculations and uses the ground parameters for determining shape and strength of the far field. ELNEC output patterns are plotted on the screen and can also be printed. [Ref. 11]

4. MN

MN is an enhanced version of MININEC for the PC . It too, is faster than MININEC, easier to use, and has additional features. Input to MN is via an input text file. MN computes and plots far field azimuth and elevation patterns. It also calculates impedance, VSWR, forward gain, front-to-back ratio, maximum sidelobe levels, and

beamwidth. MN free space output files can be imported into TA to observe the effects of terrain. [Ref. 12]

5. TA

Terrain Analyzer plots radiation patterns for antennas over irregular terrain. TA uses free space patterns from other programs (such as MN) and 2-dimensional terrain profiles to calculate elevation patterns over ground. Terrain is modeled by flat plates whose range and elevation coordinates are specified in a text file. TA models direct radiation, ground reflection, compound ground reflection, diffraction, compound diffraction, and real ground constants. The diffraction analysis is based on the geometric theory of diffraction. TA is mouse driven and allows quick changes to antenna location or changes in terrain profile. TA plots far field patterns on screen above the terrain profile and can easily be printed. [Ref. 13]

C. RHOMBIC DESIGN

1. Design Parameters

Figure 15 shows a top view of a rhombic antenna, with design parameters. Reference 7 describes a rhombic design technique for major lobe alignment at a specific elevation angle. The desired elevation takeoff angle is defined as α which is also the rhombic apex half angle. The height above ground is [Ref. 7]:

$$h = \frac{\lambda}{4\sin\alpha} \qquad (12)$$

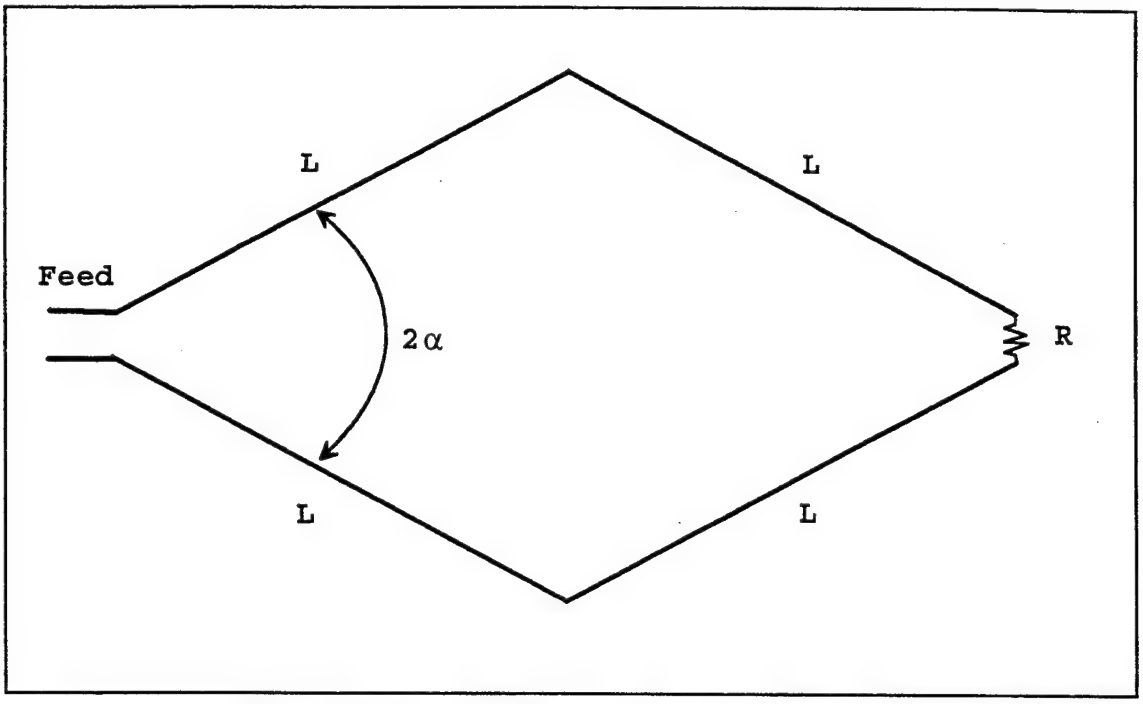

Figure 15. Rhombic Antenna Parameters, Top View.

and the leg lengths are:

$$L = \frac{0.371\lambda}{\sin^2\alpha} \tag{13}$$

The above equations are used to determine L and h. The case examined is a rhombic designed for 15 MHz and a takeoff angle of 22.5 degrees (since 0-45 degrees coverage is desired). The antenna modeled has the following parameters:

L = 50.7 meters
h = 13.1 meters
R = 600 Ω
wire diameter = 2 mm

Since the sounder has a 50 ohm characteristic impedance transmission line, the model assumes a 12:1 impedance transformer is used so that the antenna is fed from a 600 ohm

transmission line. Average ground is assumed for all preliminary ELNEC analysis (conductivity = 0.005 and permittivity = 13).

2. ELNEC RHOMBIC RESULTS

Appendix A contains the ELNEC input data that was used to generate the rhombic design results. Table 1 gives ELNEC impedance and VSWR information for various frequencies.

Frequency (MHz)	Impedance (ohms)	VSWR (for 600 ohm input)
2	1220.4 + j442.7	2.37
5	1122.2 + j154.0	1.92
10	869.6 - j443.5	2.02
15	603.8 - j167.1	1.32
20	895.1 - j237.6	1.67
25	595.0 - j300.6	1.65

Table 1. Impedance and VSWR for ELNEC Rhombic Model.

Figures 16 and 17 show the ELNEC elevation and azimuth patterns for increasing frequency. Dashed lines are used for vertical polarization, dotted lines are used for horizontal polarization and solid lines are used for total power. As the frequency increases, the takeoff angle lowers and the main lobe becomes narrower. These results indicate that the rhombic would perform well at the design frequency (15 MHz in this case) however, it does not have the bandwidth to perform well over the desired 2-25 MHz band.

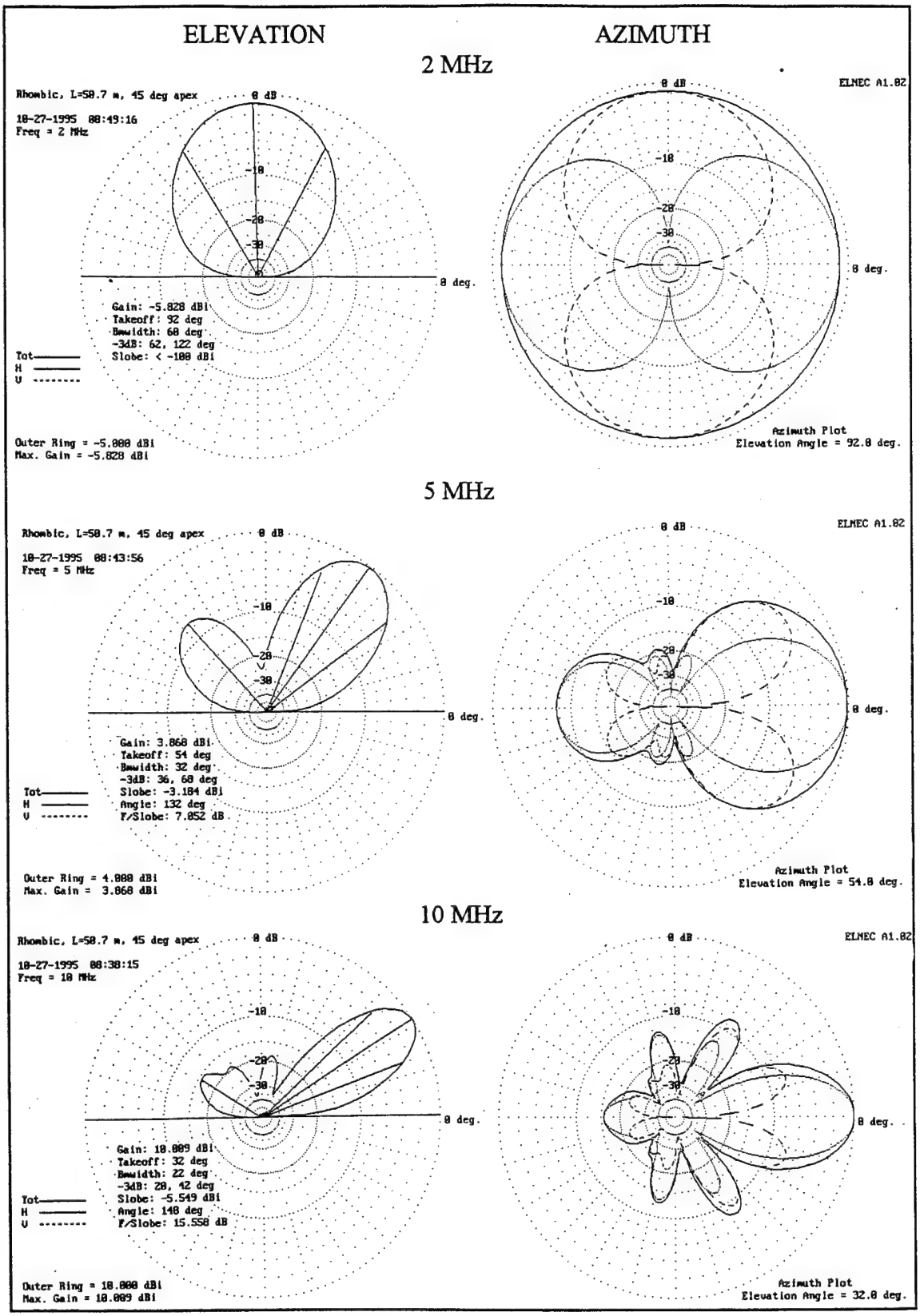

Figure 16. ELNEC Rhombic Radiation Patterns.

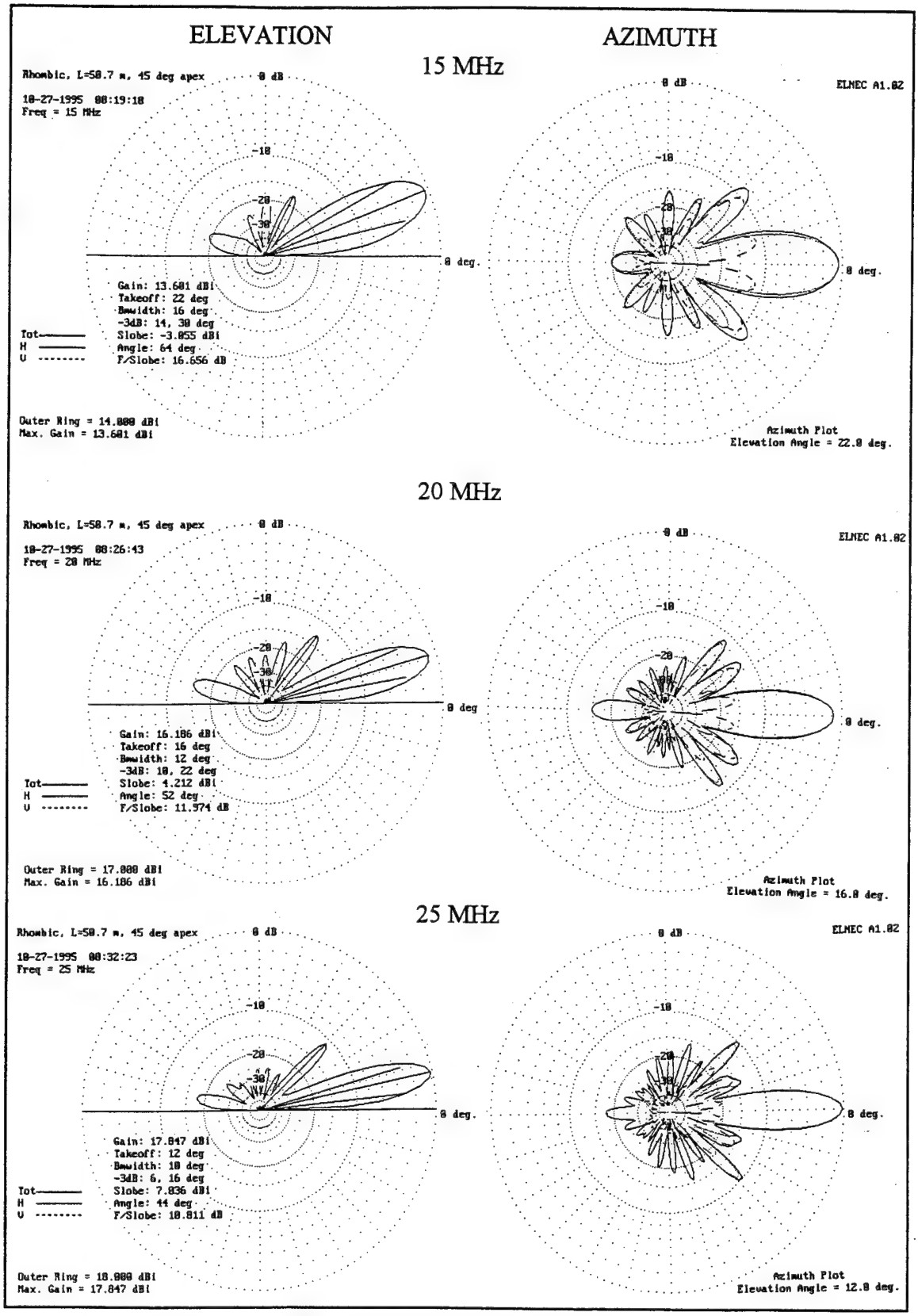

Figure 17. ELNEC Rhombic Radiation Patterns (Continued).

D. SLOPING V

1. Design Parameters

The band for this antenna is 2-25 MHz. Figure 18 shows the antenna configuration. Two wires of equal length are fed at the apex on the pole. The wires are grounded through terminating resistors. The design parameters are:

L = 80 m
H = 14 m
h = 1.8 m
α = 45 degrees
R = 600 ohms
wire dia. = 4 mm

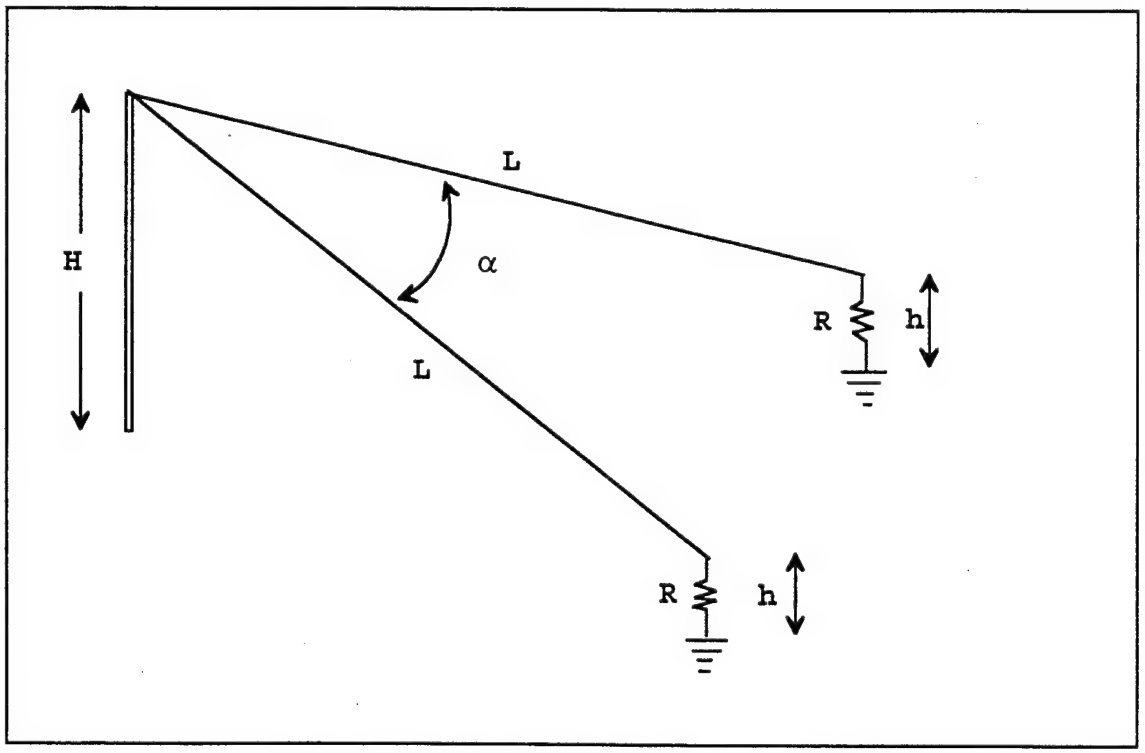

Figure 18. Sloping V Antenna Configuration.

2. ELNEC Sloping V Results

The ELNEC input data is in Appendix B. Table 2 lists ELNEC impedance and VSWR information for various frequencies. Figures 19 and 20 show the ELNEC elevation and azimuth pattern results. The ELNEC results show that the sloping V design has poor gain for the lower frequencies of the band. This is because long wire antennas should be at least a couple of wavelengths long and the electrical lengths of the legs of this antenna are too short (1.33 wavelengths at 5 MHz) at the lower frequencies.

Frequency (MHz)	Impedance (ohms)	VSWR (for 600 ohm input)
2	1010.8 - j456.2	2.16
5	883.9 + j61.0	1.49
10	523.6 - j150.6	1.35
15	615.3 - j646.1	2.77
20	887.9 - j381.1	1.90
25	448.4 - j350.9	2.06

Table 2. Impedance and VSWR for ELNEC Sloping V Model.

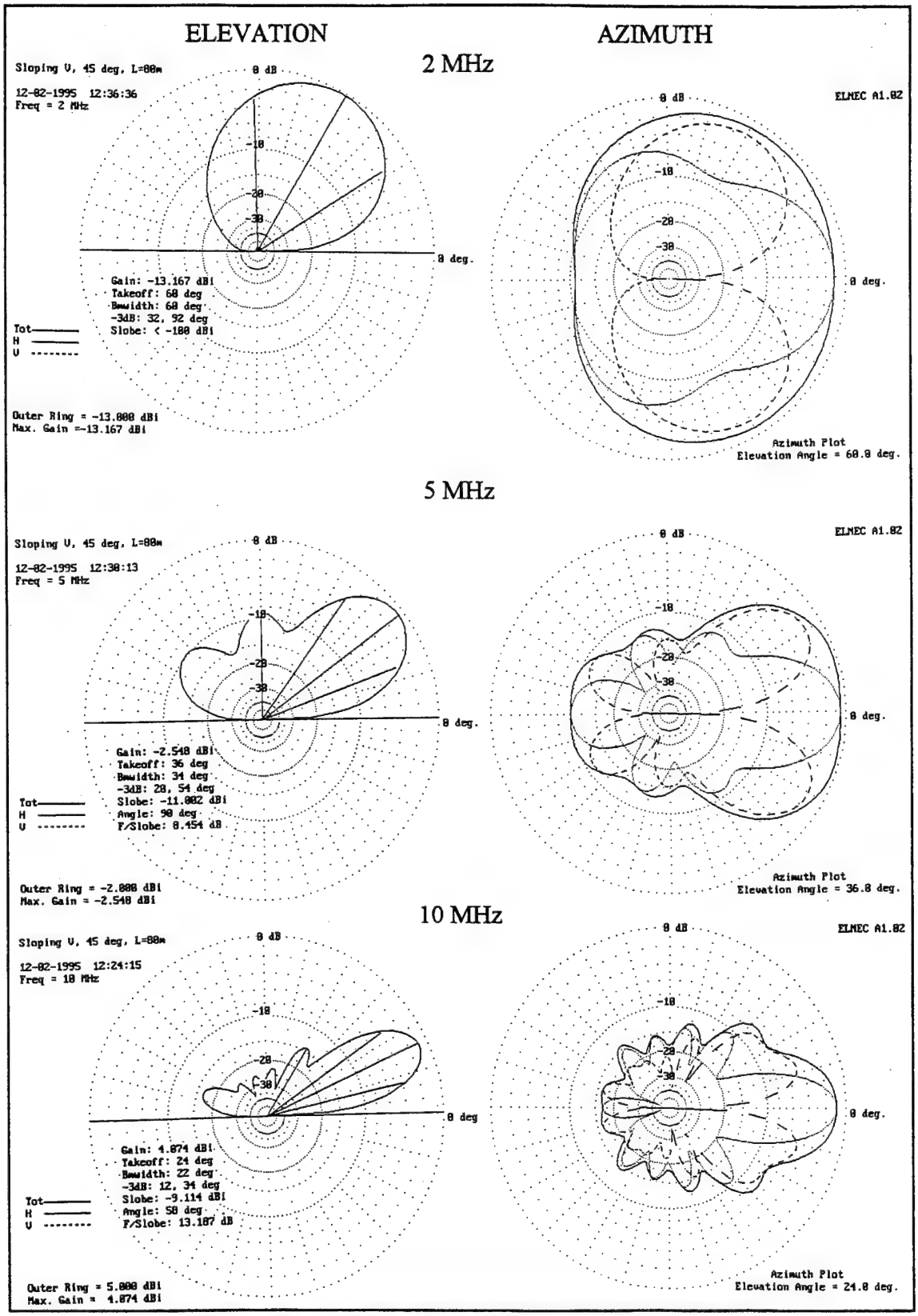

Figure 19. ELNEC Sloping V Radiation Patterns.

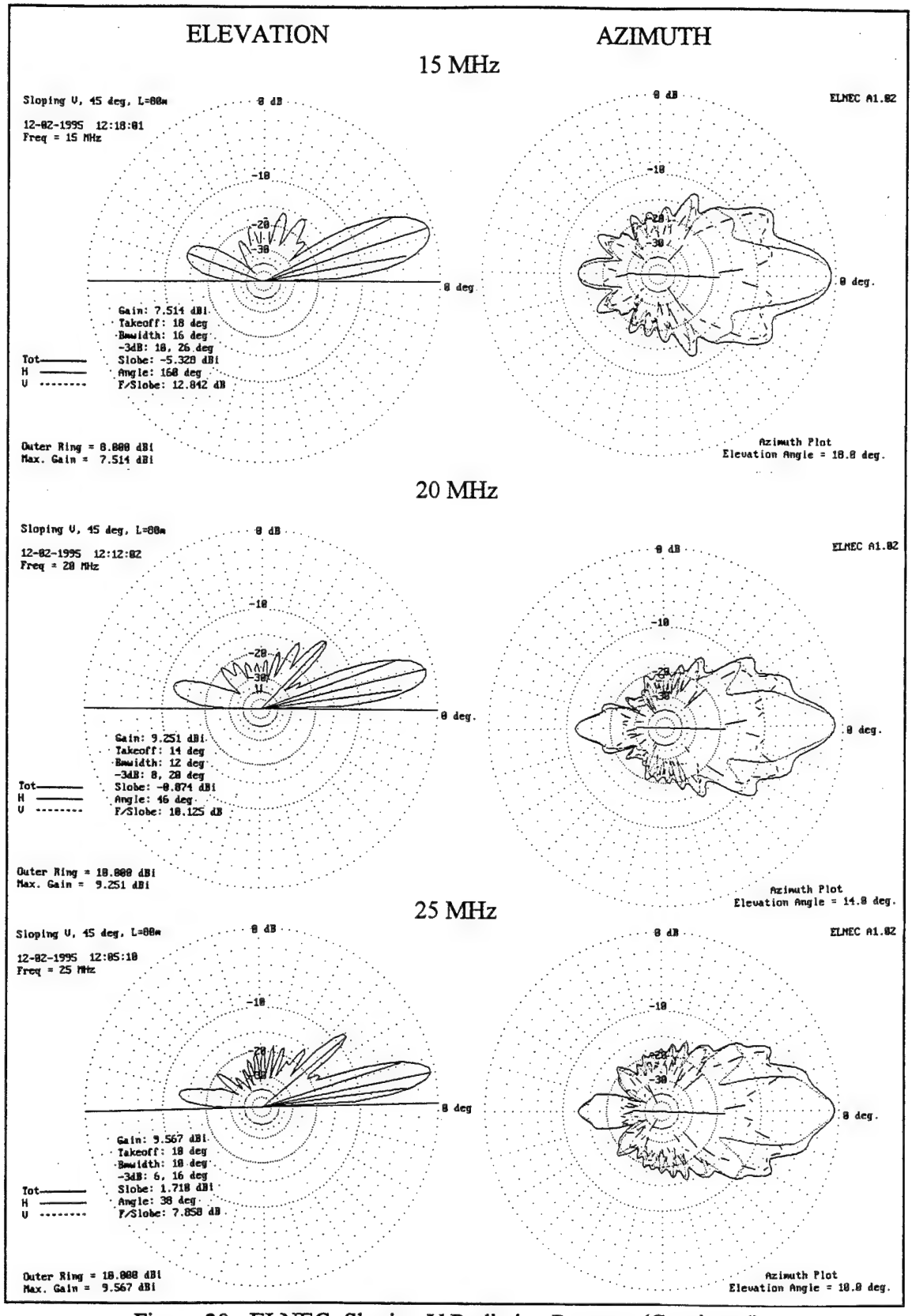

Figure 20. ELNEC Sloping V Radiation Patterns (Continued).

E. LOG-PERIODIC DESIGNS

Two log-periodic antennas are modeled. The first is a 12 element HF log-periodic antenna for 2-25 MHz. The second is a 6 element VHF log-periodic antenna for 25-60 MHz.

1. HF Log-periodic Design Parameters

The bandwidth limits determine the approximate size of the largest and smallest elements via Equation (8). If a taper ratio of 0.8 is used, 12 elements are required to cover the operating band. From Figure 11, the spacing constant of 0.145 is used in Equation (9) to find the element spacing for optimum gain. Table 3 lists the element lengths and spacing required.

Element # (n)	Element Length (feet)	Distance to Next Element (feet)
1	246	71
2	197	57
3	157	45
4	126	36
5	101	29
6	81	23
7	64	19
8	52	15
9	41	12
10	33	10
11	26	7.6
12	21	---

Table 3. HF Log-periodic Design Parameters.

As shown in Figure 21, the HF log-periodic model is sloping so that the electrical height of the radiating portion of the antenna remains approximately the same. For this model the longest element is at 100 feet and the shortest is at about 9.7 feet.

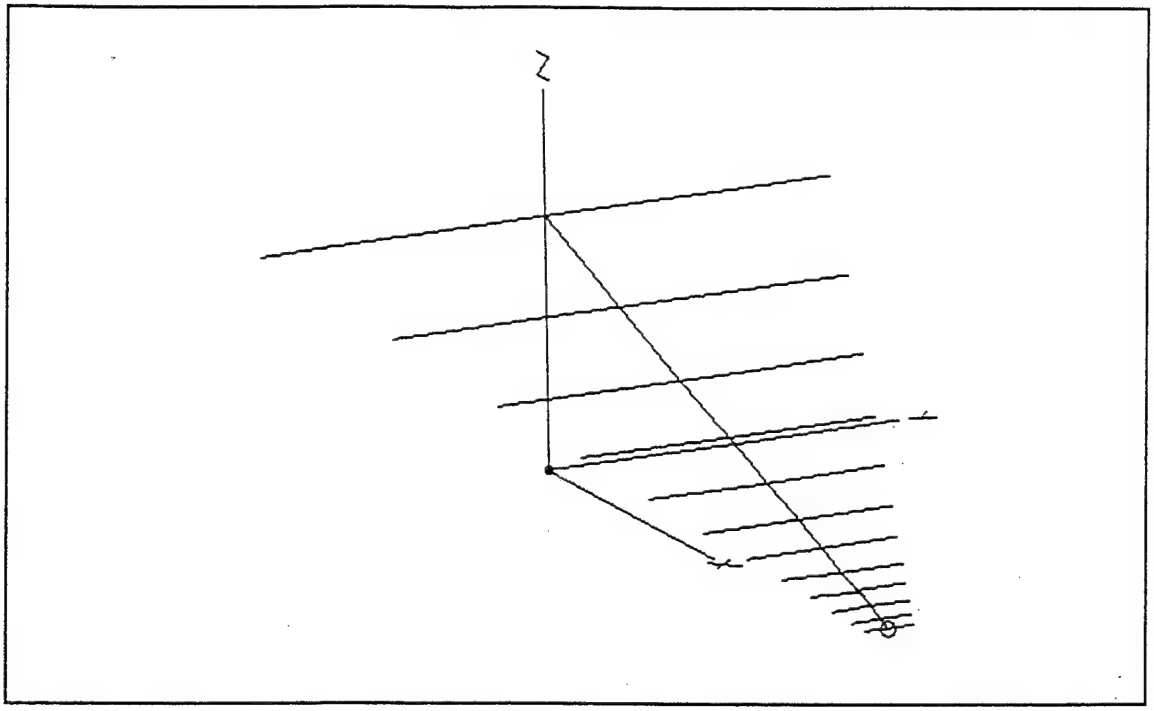

Figure 21. ELNEC Model of Sloping HF Log-periodic.

2. ELNEC HF Log-periodic Results

The ELNEC input data is in Appendix C. Table 4 lists ELNEC impedance and VSWR information for various frequencies.

Frequency (MHz)	Impedance (ohms)	VSWR (for 200 ohm input)
2	189.4 - j176.8	2.41
5	113.3 - j96.2	2.31
10	248.6 - j294.2	3.50
15	113.2 - j24.6	1.81
20	44.2 - j19.1	4.57
25	304.5 + j213.9	2.54

Table 4. Impedance and VSWR for ELNEC HF Log-periodic Model.

The ELNEC model of this antenna had about 20 segments per wavelength. It was not possible to use the recommended 40 segments per wavelength for accurate impedance analysis because 47 wires were required to model the dipole elements and the transmission lines, which exceeds the capability of ELNEC.

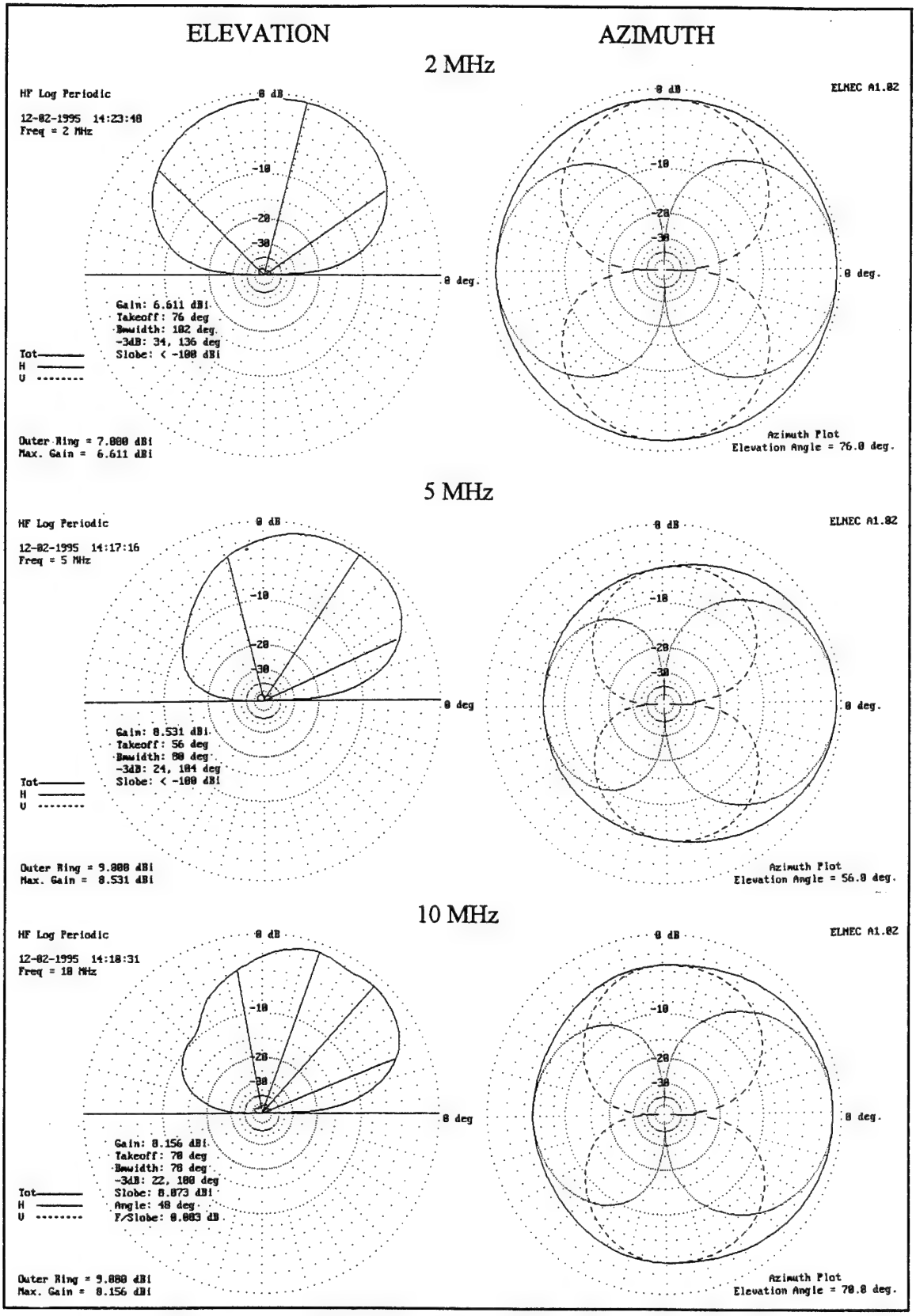

Figure 22. ELNEC HF Log-periodic Radiation Patterns.

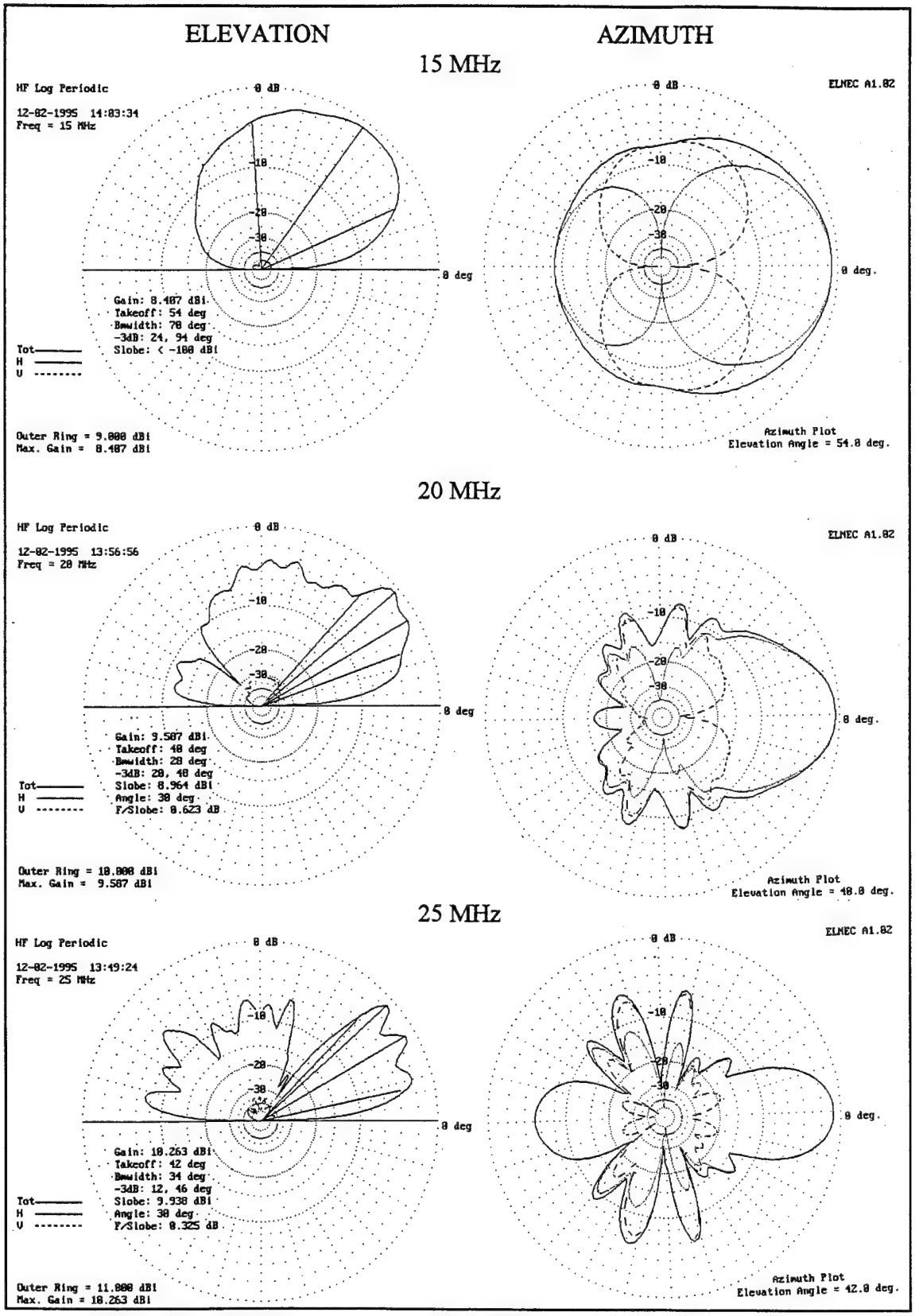

Figure 23. ELNEC HF Log-periodic Radiation Patterns (Continued).

3. VHF Log-periodic Design Parameters

The band for this antenna is 25-60 MHz. The design is a 6 element, horizontal log-periodic antenna. The taper ratio is 0.84 and the spacing constant is determined to be 0.157 from Figure 11. The element lengths and spacing distance is determined by Equations (6), (7), and (8). Table 5 lists the antenna design parameters. The antenna height is 10 feet which is less than half a wavelength for most of the band.

Element # (n)	Element Length (inches)	Distance to Next Element (inches)
1	236.2	74.2
2	198.4	62.3
3	166.6	52.4
4	140.0	44.0
5	117.6	36.9
6	98.8	---

Table 5. VHF Log-periodic Design Parameters.

4. ELNEC VHF Log-periodic Results

The ELNEC input data is in Appendix D. Table 6 lists ELNEC impedance and VSWR information for various frequencies. Figures 24 and 25 show the ELNEC elevation and azimuth pattern results. The ELNEC results show that the VHF log-periodic design has good elevation patterns throughout the 25-60 MHz band.

Frequency (MHz)	Impedance (ohms)	VSWR (for 50 ohm input)
25	62.4 - j2.6	1.25
31	105.1 + j10.1	2.13
38	111.7 - j2.2	2.23
45	73.3 - j19.0	1.64
52	85.3 - j11.3	1.75
60	51.6 + j61.4	3.15

Table 6. Impedance and VSWR for ELNEC VHF Log-periodic Model.

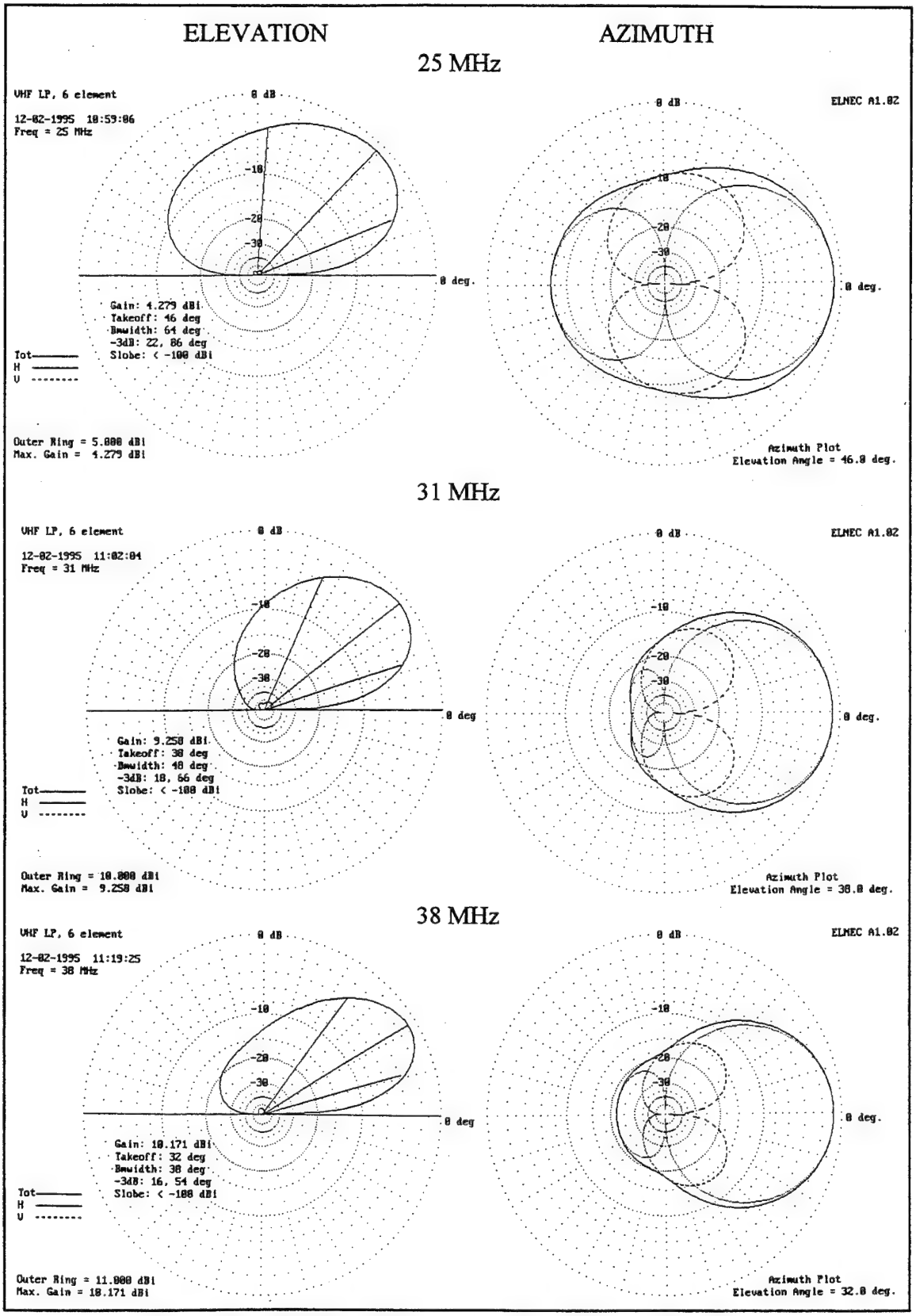

Figure 24. ELNEC VHF Log-periodic Radiation Patterns.

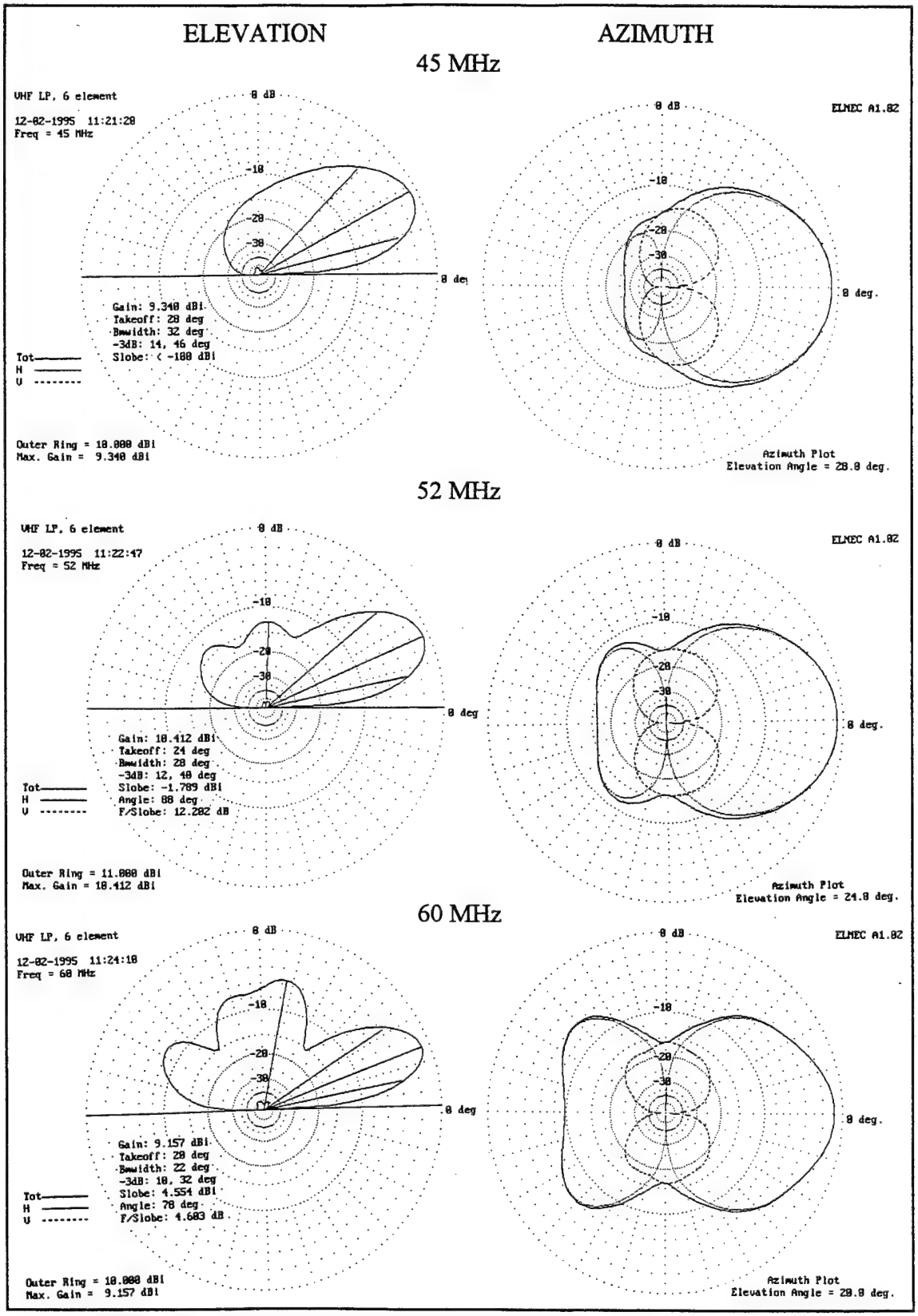

Figure 25. ELNEC VHF Log-periodic Radiation Patterns (Continued).

V. FINAL DESIGN ANALYSIS

A. ANTENNA SELECTION

Four broadband antennas were modeled in the preliminary design stage. The ELNEC results of the previous chapter show that the sloping V, the HF log-periodic, and the VHF log-periodic would be acceptable for the TEP soundings. The rhombic design was rejected because it does not have the bandwidth to perform well over the 2-25 MHz band. The problem with the rhombic is that the main lobe takeoff angle drops with increasing frequency and the beam becomes too narrow at higher frequencies.

At the Rarotonga site the sloping V antenna is used for 2-25 MHz and a VHF log-periodic antenna is used for 25-60 MHz.

On Oahu an HF log-periodic antenna and a VHF log-periodic antenna are used for the two bands.

B. NEC-4 VHF LOG-PERIODIC ANTENNA RESULTS

The NEC-4 input data file is in Appendix E. NEC-4 has a transmission line command that allows easy modeling of log-periodic antennas. Results were obtained for 6 frequencies throughout the 25-60 MHz range. The 6 element antenna has the same dimensions given in section IV.E.3. All NEC-4 models had wires with 2 mm. radius and an average real ground plane (conductivity = 0.005 and relative permittivity = 13). Table 7 shows the NEC-4 impedance data for the VHF log-periodic antenna.

Frequency (MHz)	Impedance (ohms)	VSWR (for 50 ohm input)
25	50.5 + j6.4	1.13
31	50.6 - j3.1	1.06
38	50.6 - j2.1	1.04
45	41.1 - j3.5	1.25
52	38.2 - j1.6	1.33
60	47.8 - j10.3	1.25

Table 7. Impedance and VSWR for NEC-4 VHF Log-Periodic Model.

Differences between the NEC-4 results and ELNEC results can be attributed to differences in which the transmission lines are modeled in each program. For this antenna the ELNEC transmission line characteristic impedance, which is determined by the model geometry does not match the specified NEC-4 transmission line characteristic impedance. The ELNEC wire radius and spacing could have been selected to closely match the NEC-4 model. Other factors such as element endpoint locations, number of segments and wire diameter are modeled the same for the VHF log-periodic antenna.

Figures 26 through 31 show NEC-4 elevation and azimuth patterns for the VHF log-periodic design.

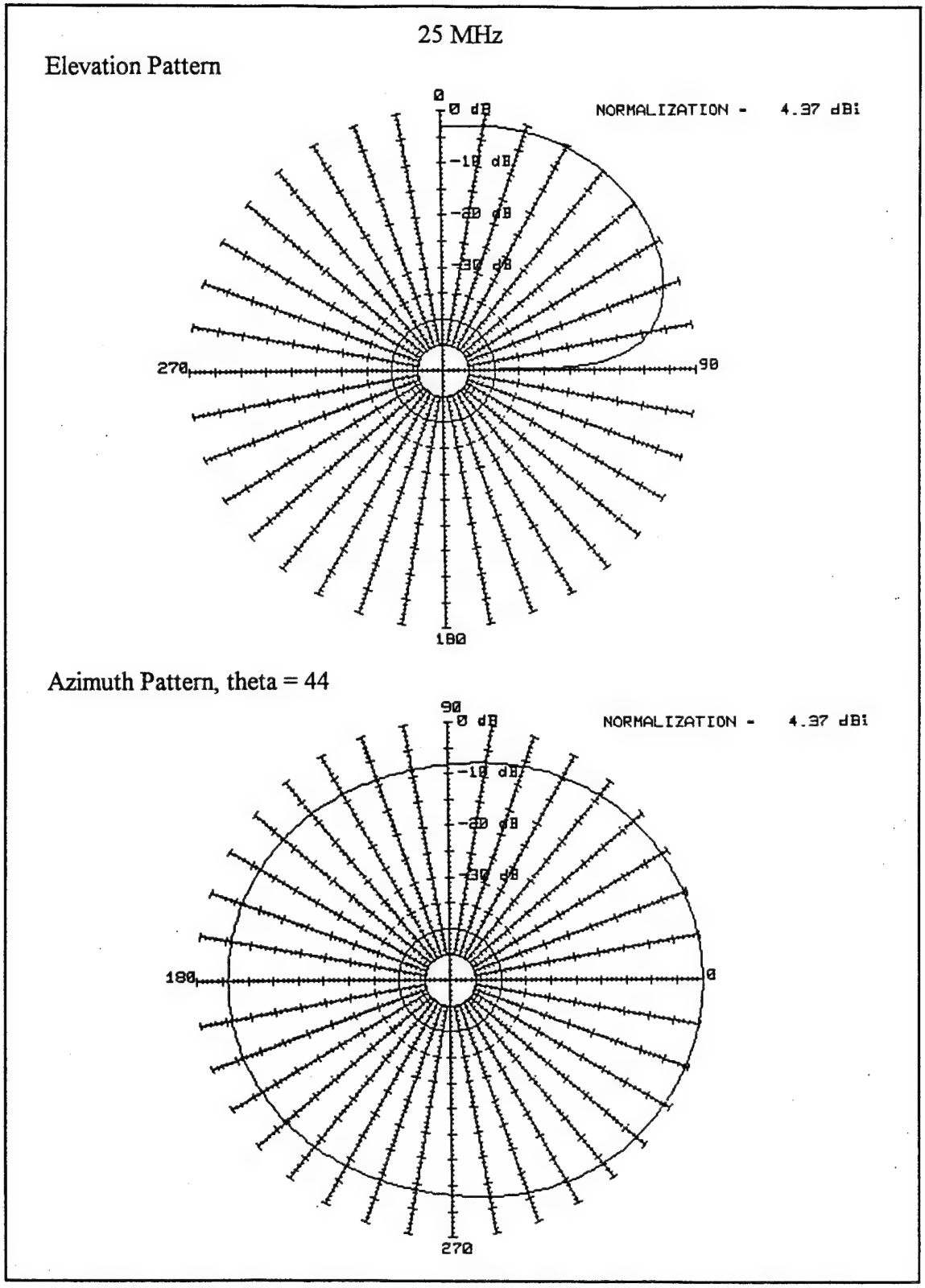

Figure 26. NEC-4 VHF Log-periodic Radiation Patterns, 25 MHz.

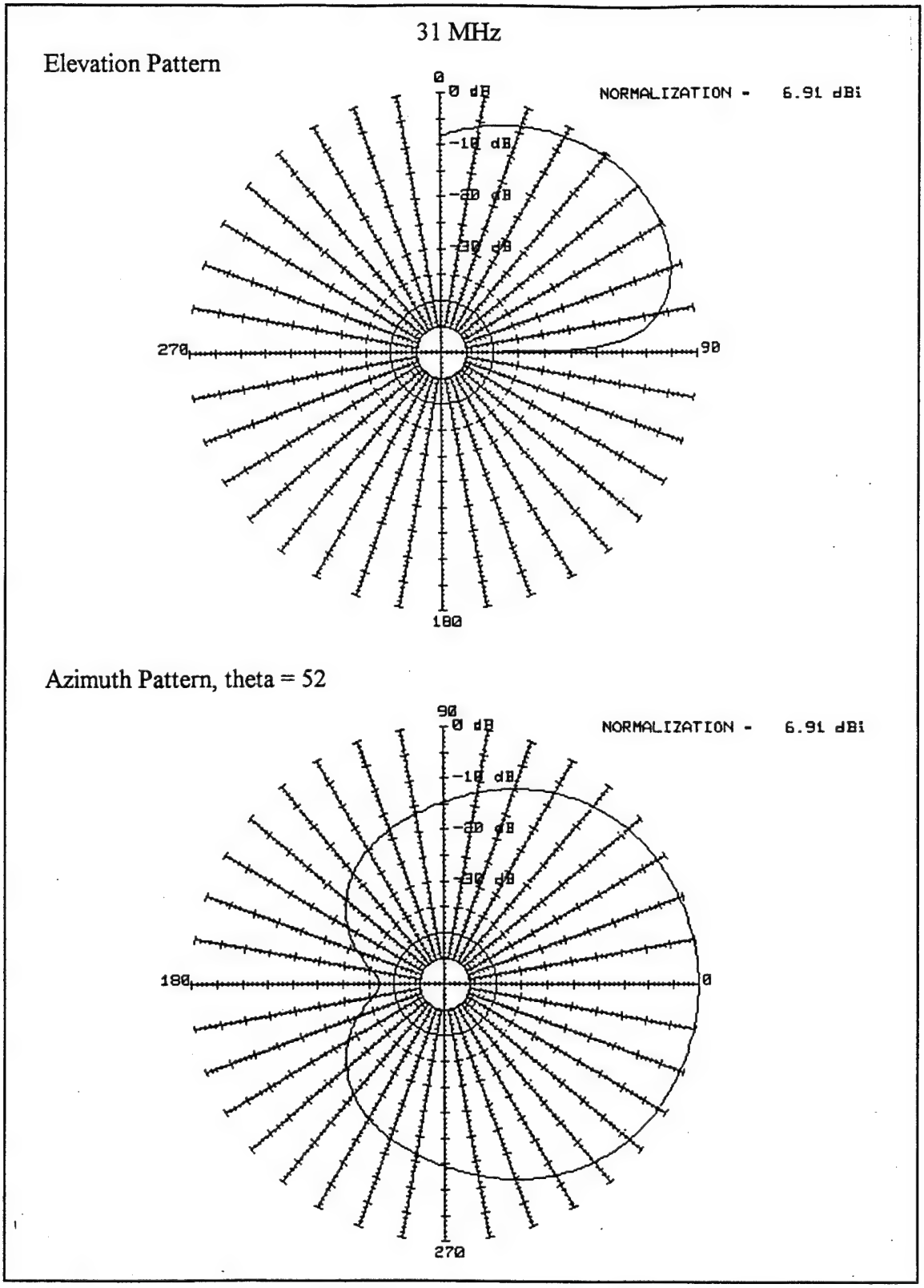

Figure 27. NEC-4 VHF Log-periodic Radiation Patterns, 31 MHz.

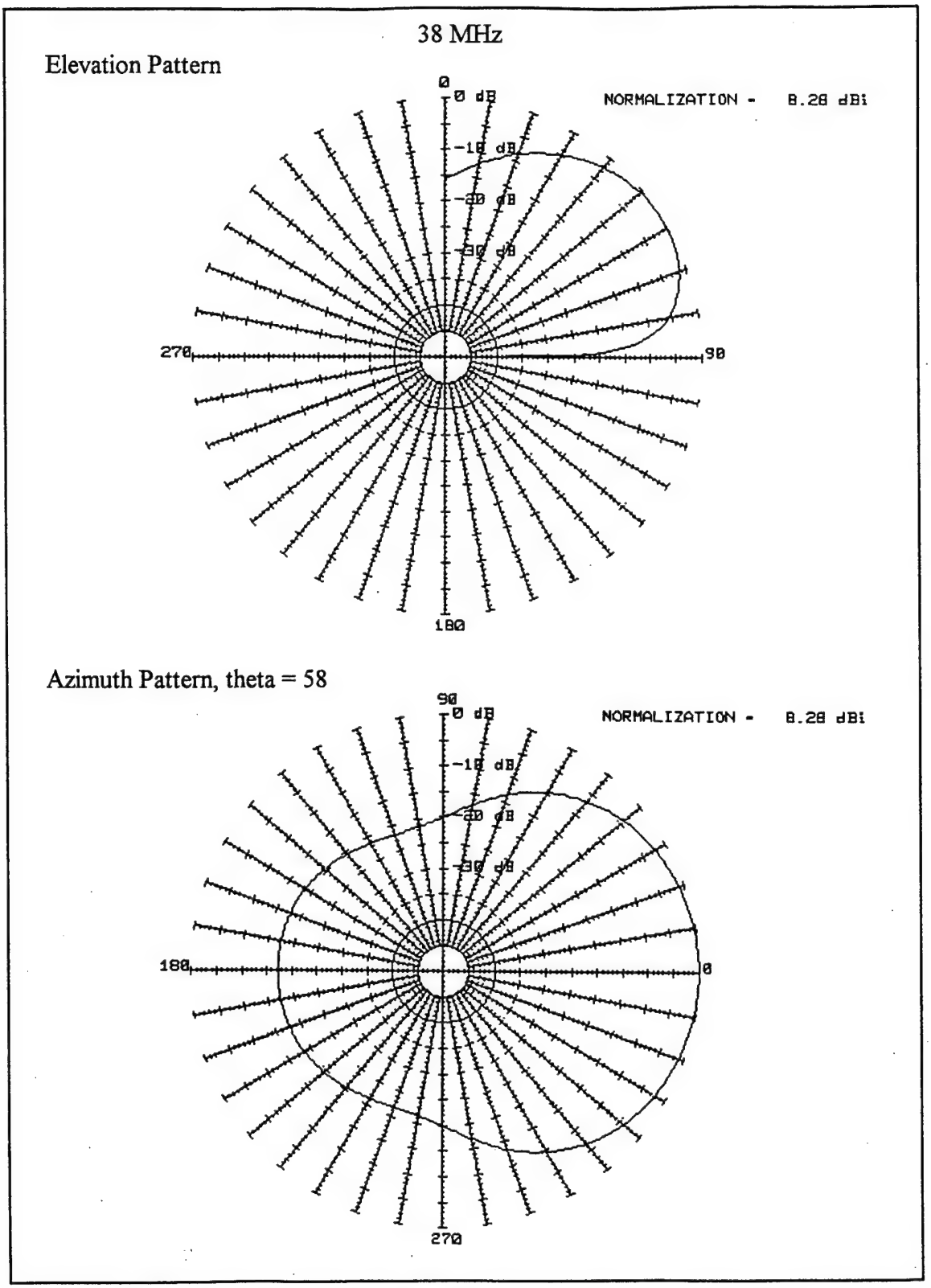

Figure 28. NEC-4 VHF Log-periodic Radiation Patterns, 38 MHz.

45 MHz

Elevation Pattern

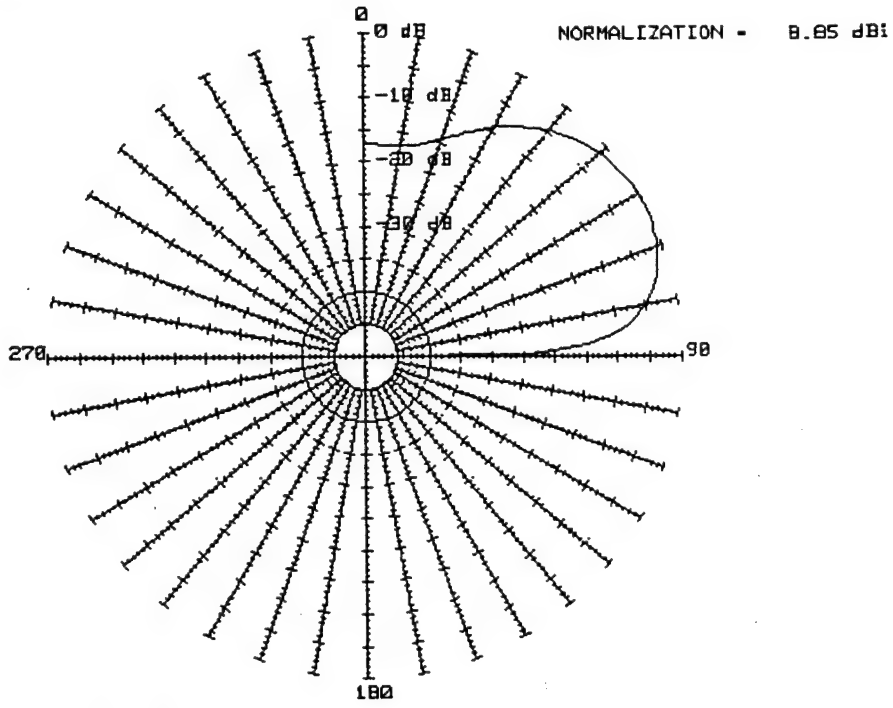

Azimuth Pattern, theta = 61

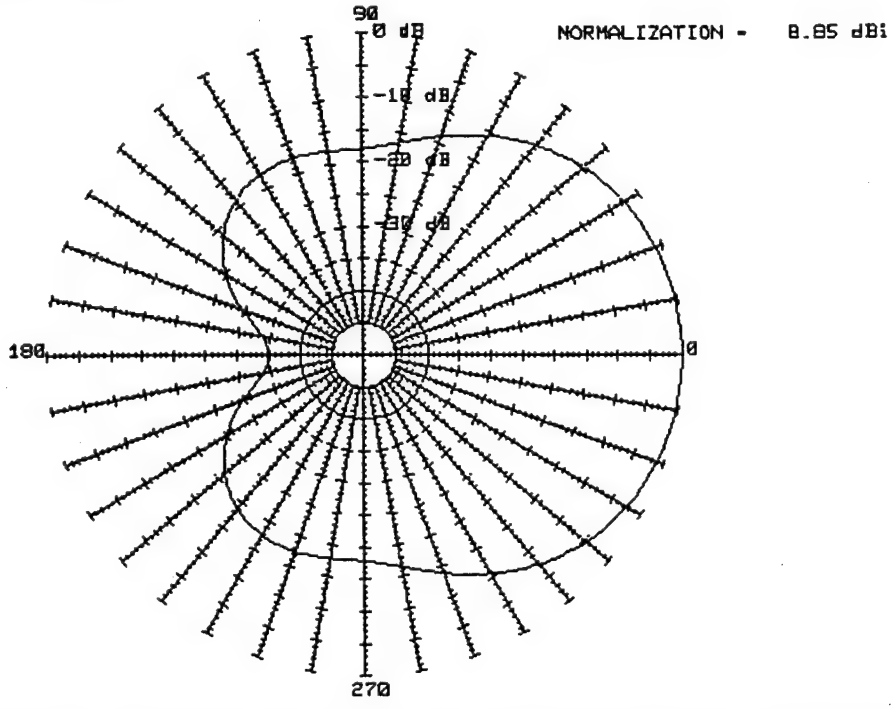

Figure 29. NEC-4 VHF Log-periodic Radiation Patterns, 45 MHz.

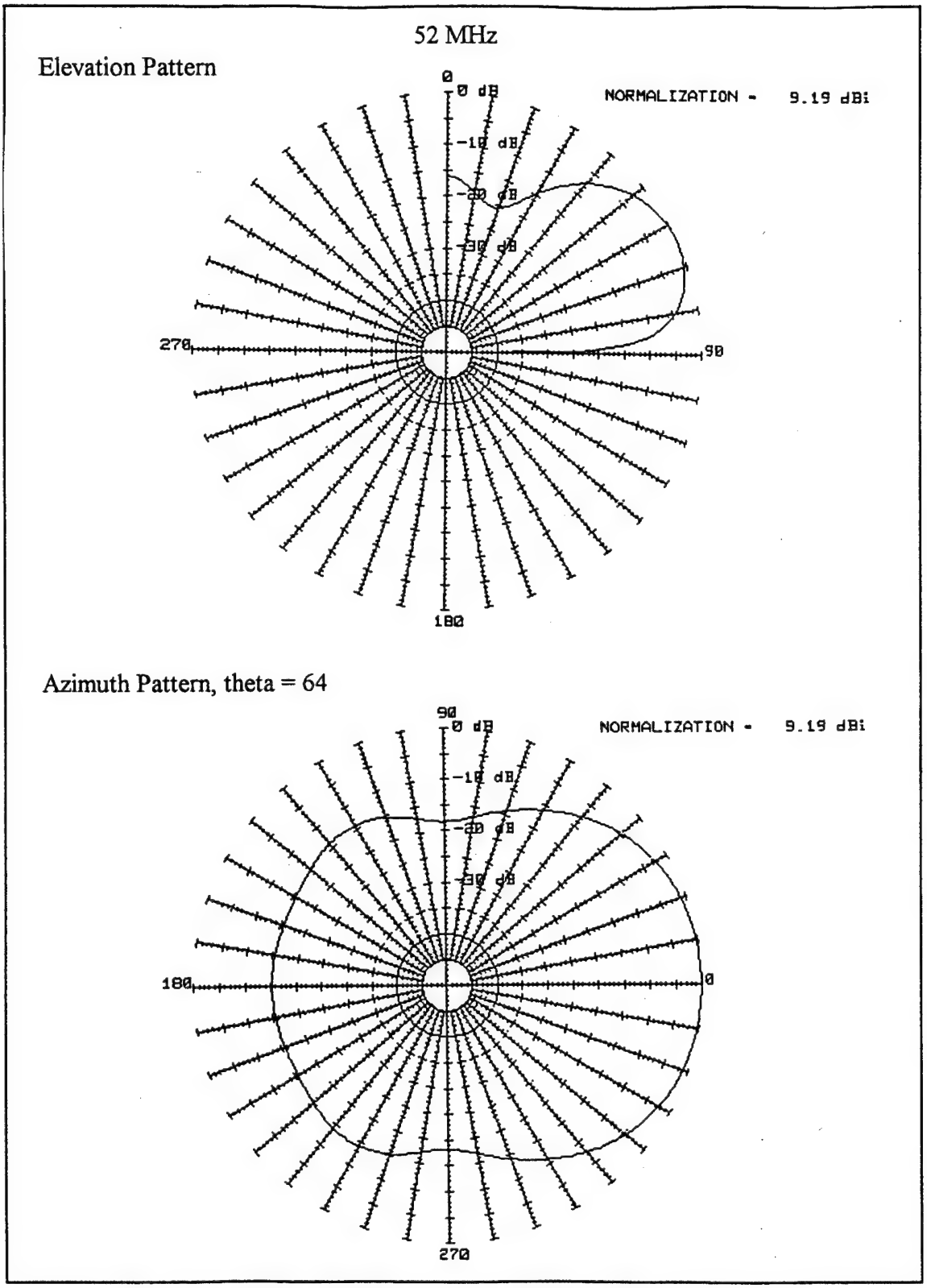

Figure 30. NEC-4 VHF Log-periodic Radiation Patterns, 52 MHz.

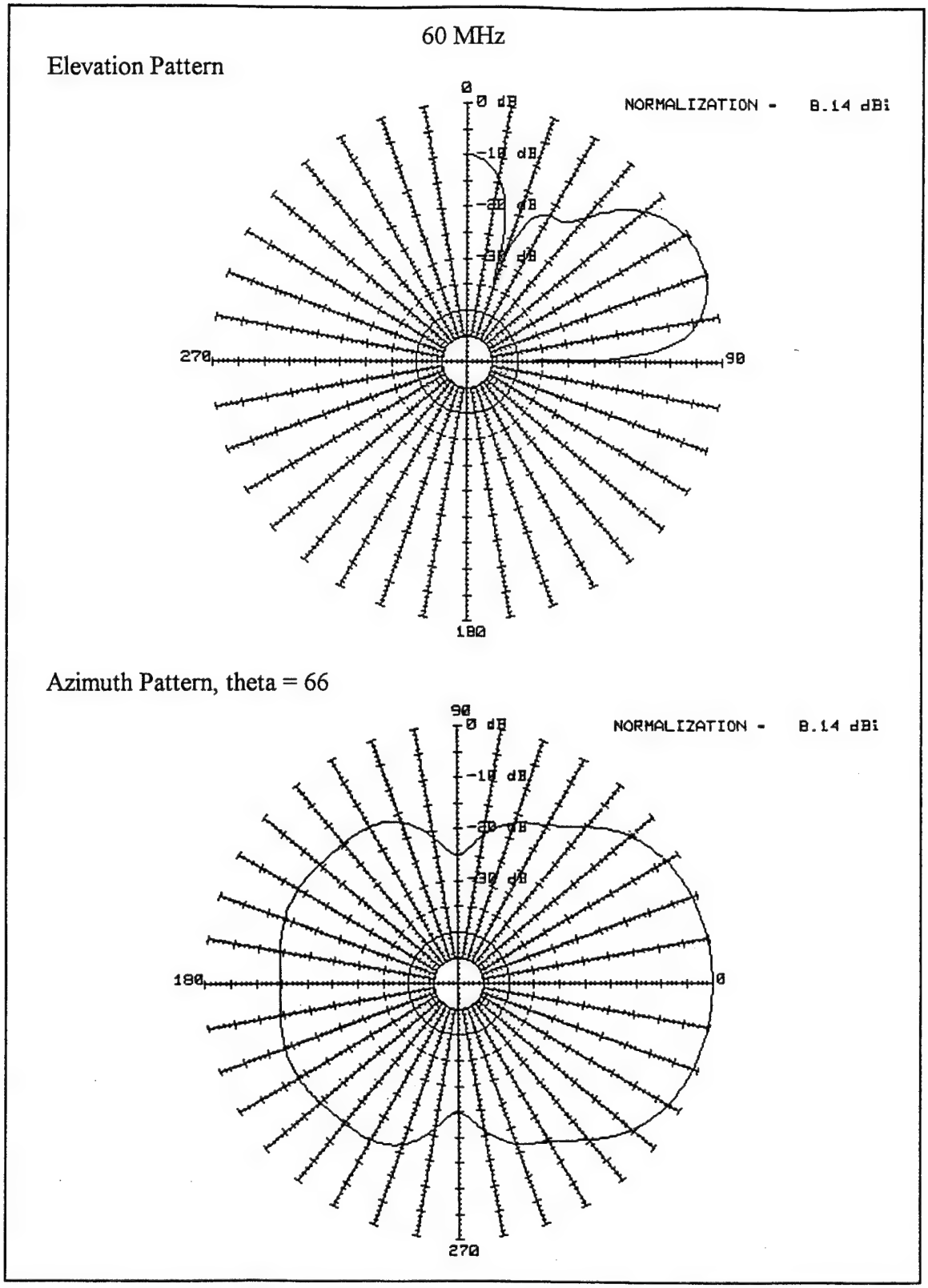

Figure 31. NEC-4 VHF Log-periodic Radiation Patterns, 60 MHz.

C. NEC-4 HF LOG-PERIODIC ANTENNA RESULTS

The NEC-4 input data file is in Appendix F. Results were obtained for 6 frequencies throughout the 2-25 MHz band. The 12 element antenna has dimensions given in section IV.E.1. Table 8 shows NEC-4 impedance data for the HF Log-periodic antenna.

Frequency (MHz)	Impedance (ohms)	VSWR (for 200 ohm input)
2	131.4 - j64.3	2.28
5	122.7 - j51.2	1.78
10	269.2 - j180.0	2.23
15	130.0 - j9.8	1.90
20	93.9 - j65.6	2.39
25	152.9 - j119.7	2.03

Table 8. Impedance and VSWR for NEC-4 HF Log-Periodic Model.

For this antenna model, ELNEC and NEC-4 differences are caused by the number of element segments being different and transmission line modeling differences. The ELNEC transmission line characteristic impedance, which is determined by the model geometry does not match the specified NEC-4 characteristic impedance. Figures 32 through 37 show NEC-4 elevation and azimuth patterns for the HF log-periodic design.

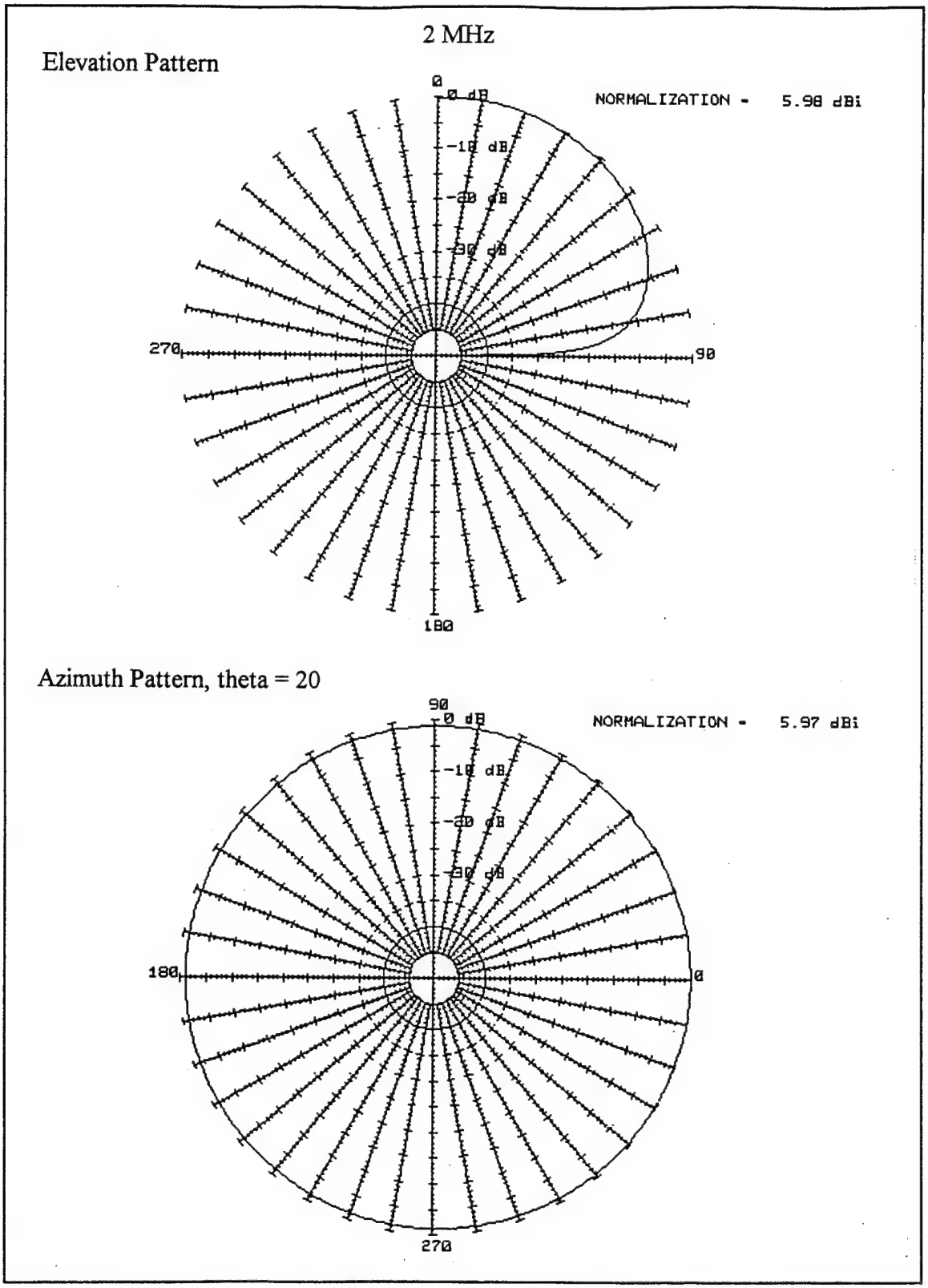

Figure 32. NEC-4 HF Log-periodic Radiation Patterns, 2 MHz.

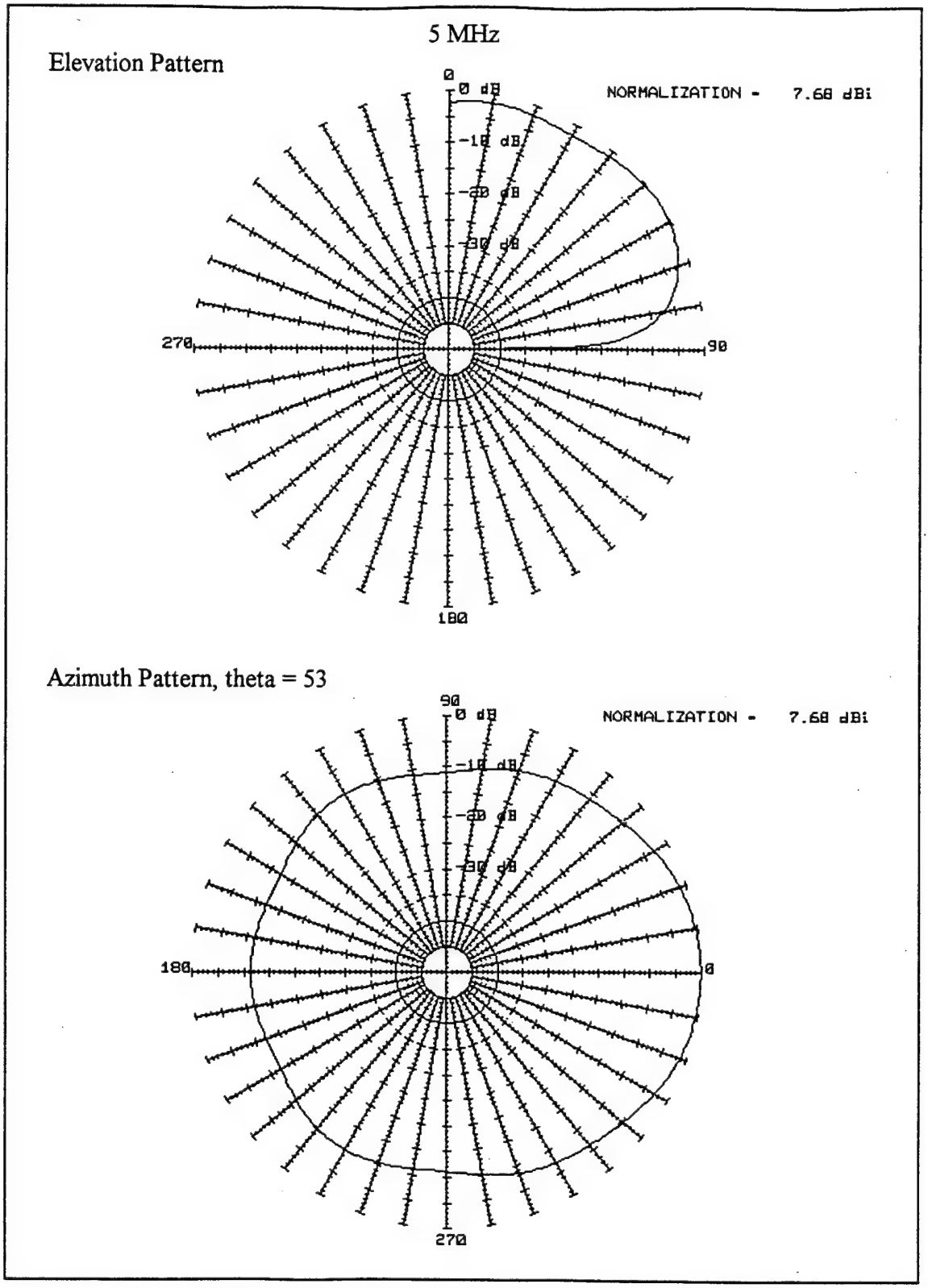

Figure 33. NEC-4 HF Log-periodic Radiation Patterns, 5 MHz.

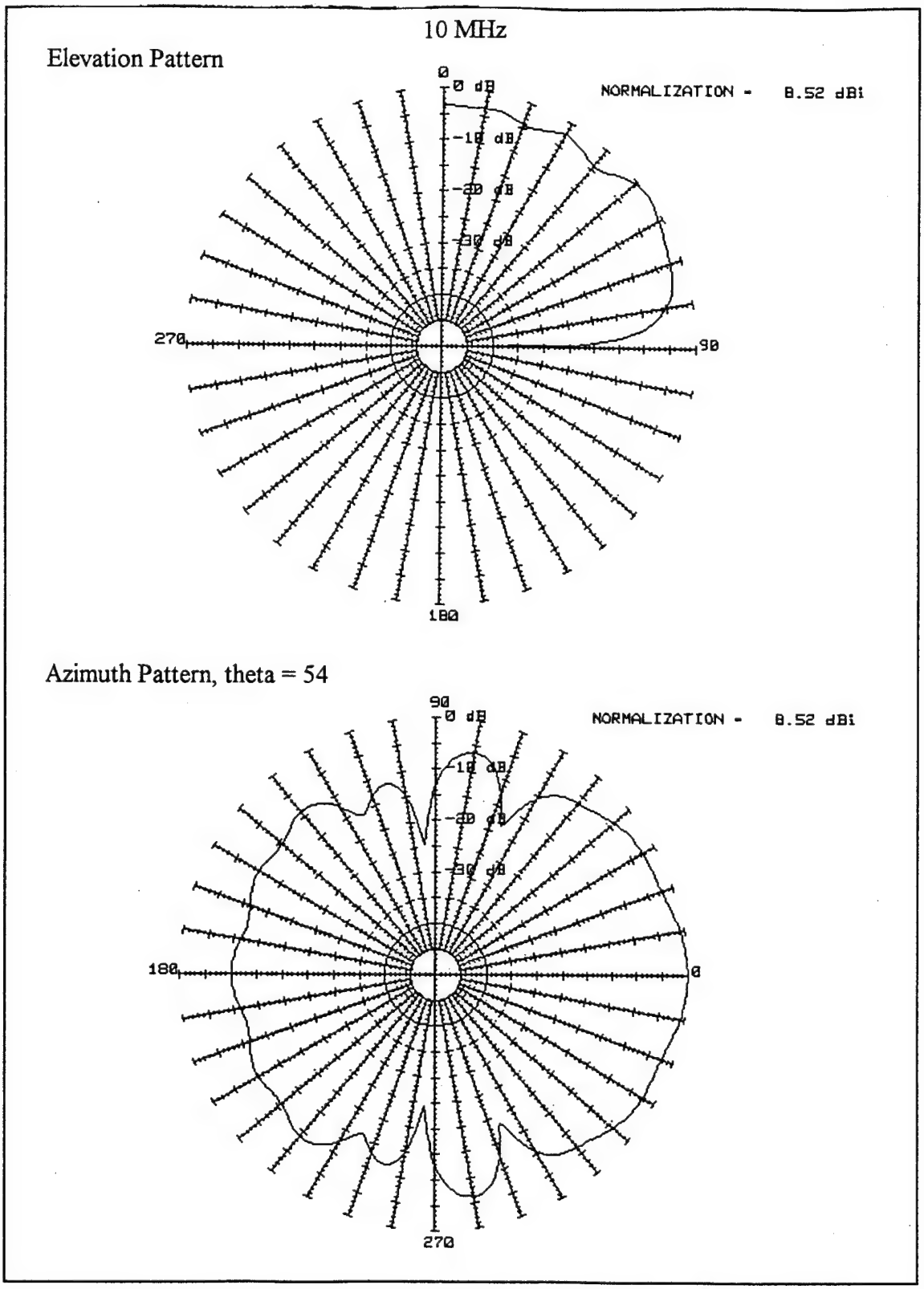

Figure 34. NEC-4 HF Log-periodic Radiation Patterns, 10 MHz.

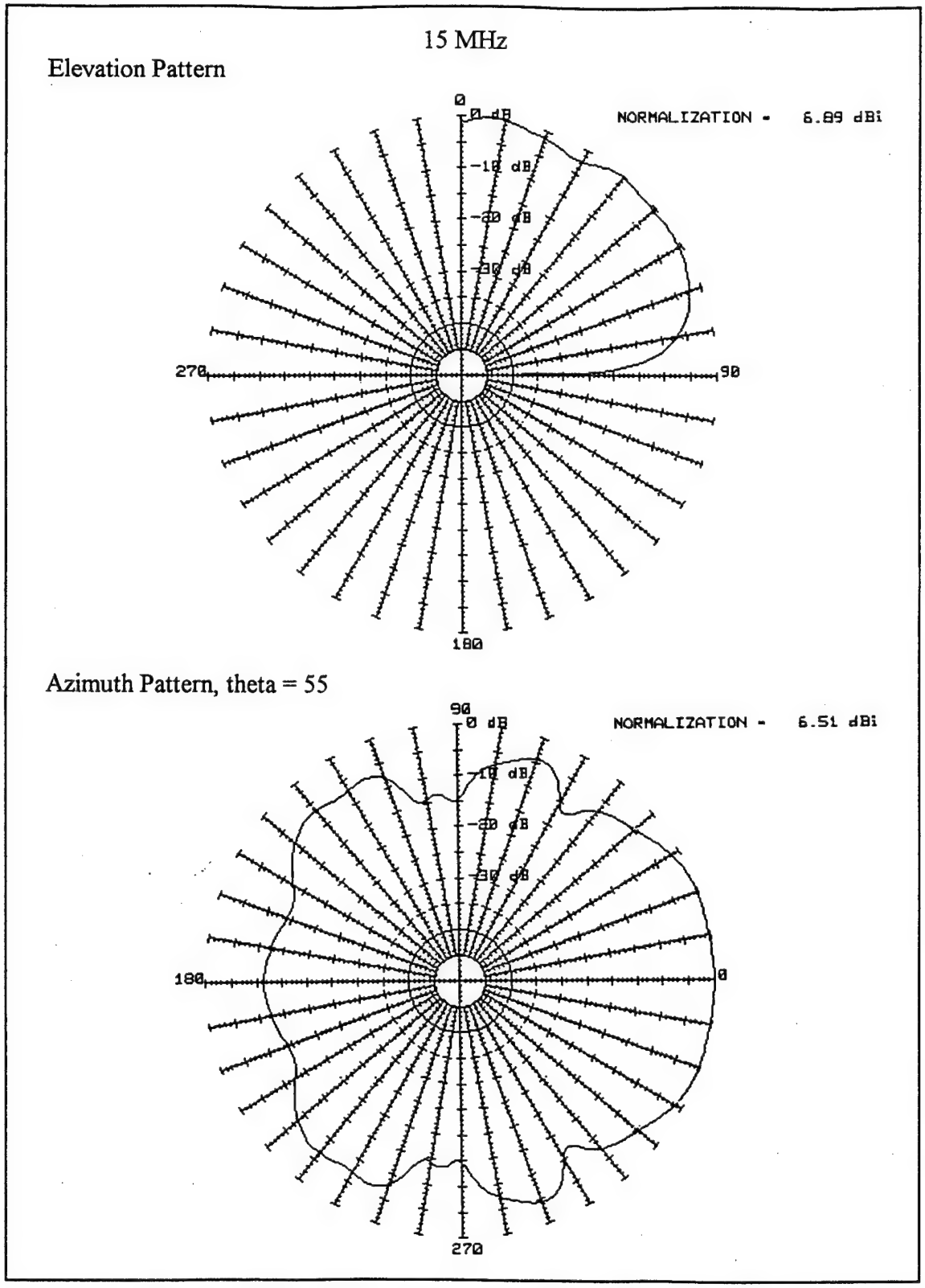

Figure 35. NEC-4 HF Log-periodic Radiation Patterns, 15 MHz.

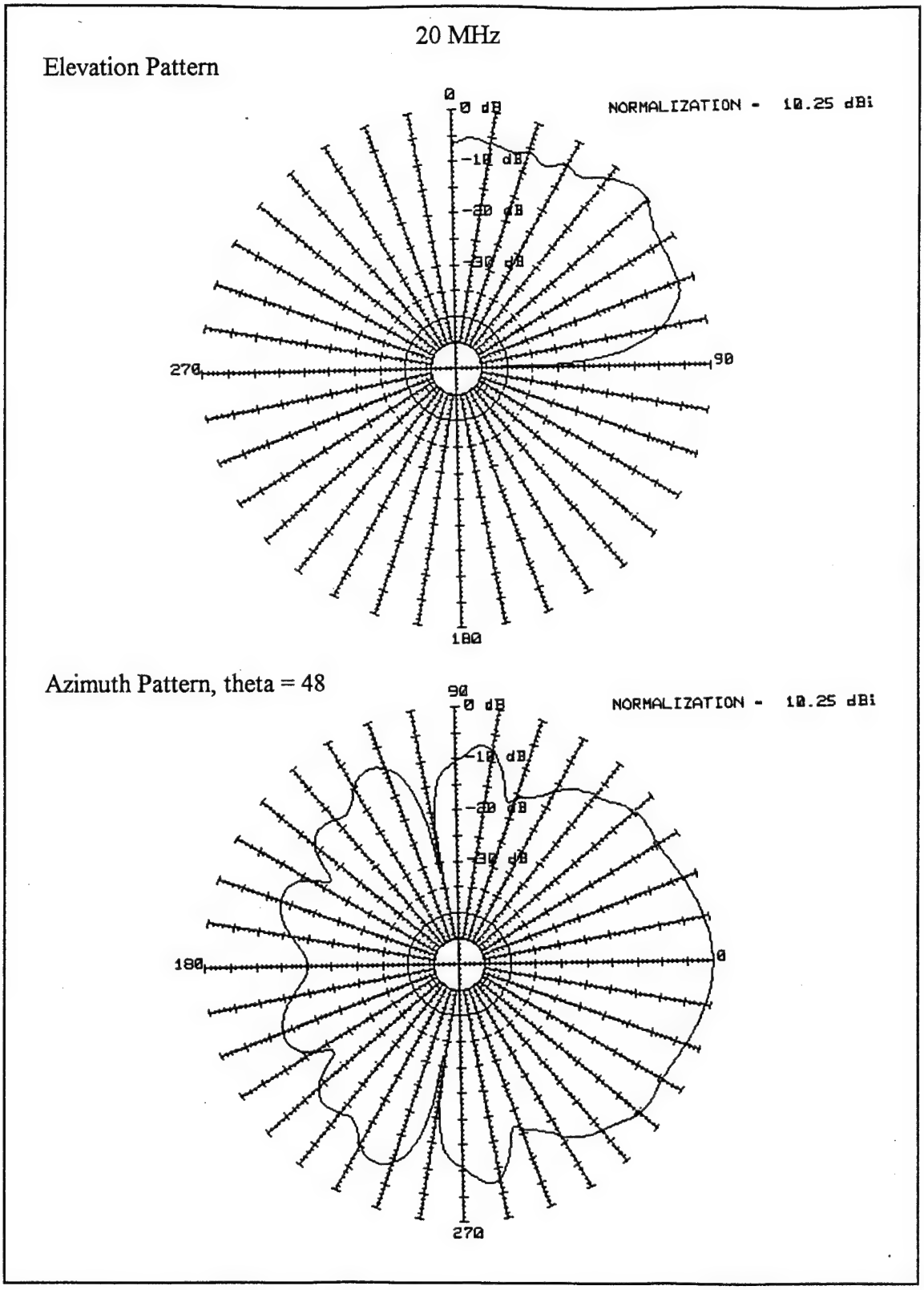

Figure 36. NEC-4 HF Log-periodic Radiation Patterns, 20 MHz.

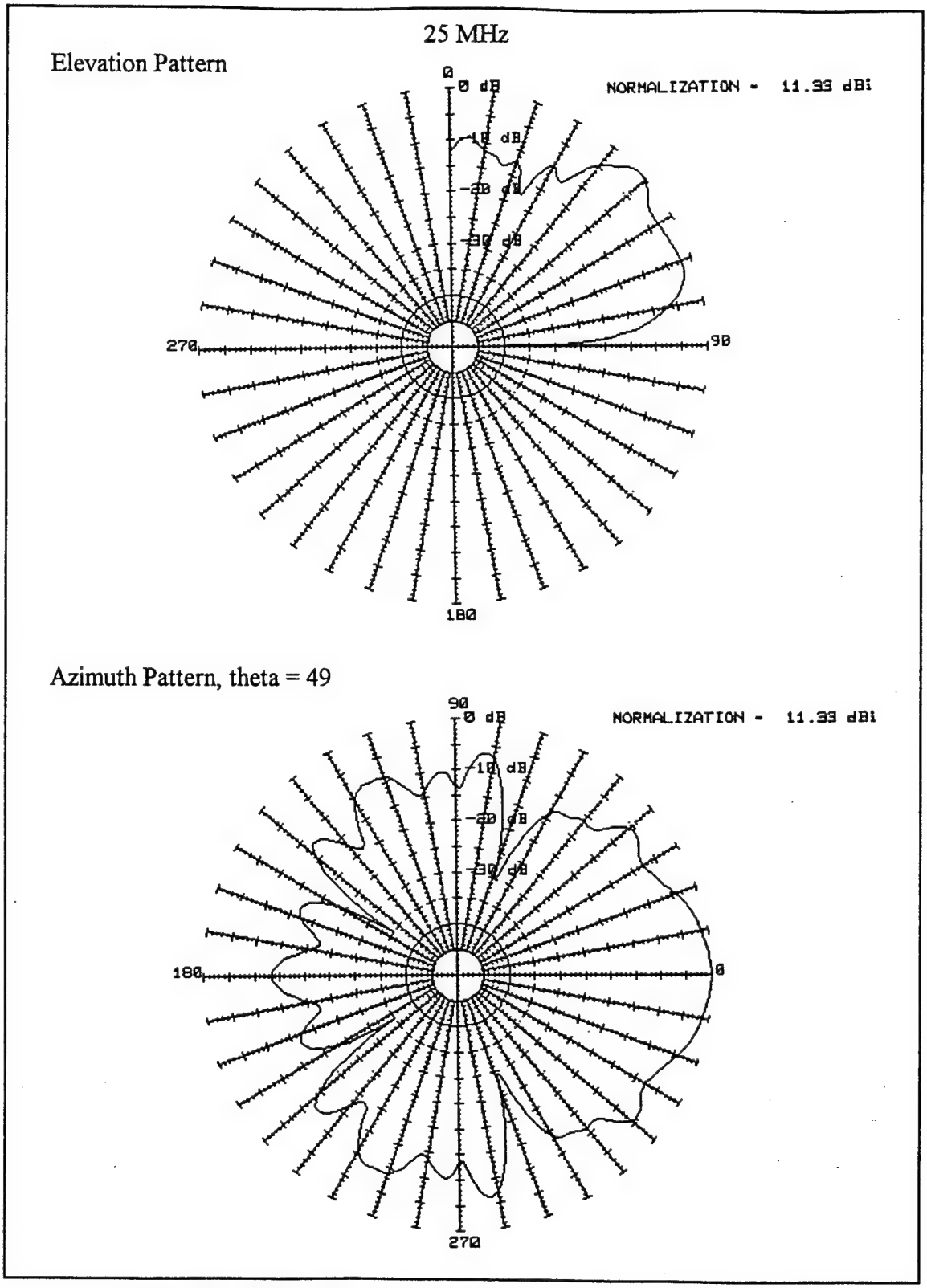

Figure 37. NEC-4 HF Log-periodic Radiation Patterns, 25 MHz.

D. NEC-4 SLOPING V ANTENNA RESULTS

The NEC-4 input data file is in Appendix G. Results were obtained for 6 frequencies throughout the 2-25 MHz band. The sloping V antenna dimensions are given in section IV.D.1. Table 9 shows the NEC-4 impedance data for the Sloping V antenna. The results show that the antenna has high VSWR values at the lower end of the frequency band. The electrical lengths of the legs of this antenna are shorter than required at the lower frequencies.

Frequency (MHz)	Impedance (ohms)	VSWR (for 600 ohm input)
2	320.5 - j1895.5	21.20
5	415.2 + j663.0	3.65
10	353.0 - j302.2	2.28
15	1104.7 - j340.7	2.08
20	522.0 + j19.5	1.09
25	610.2 - j298.5	1.63

Table 9. Impedance and VSWR for NEC-4 Sloping V Model.

Figures 38 through 43 show NEC-4 elevation and azimuth patterns for the sloping V design.

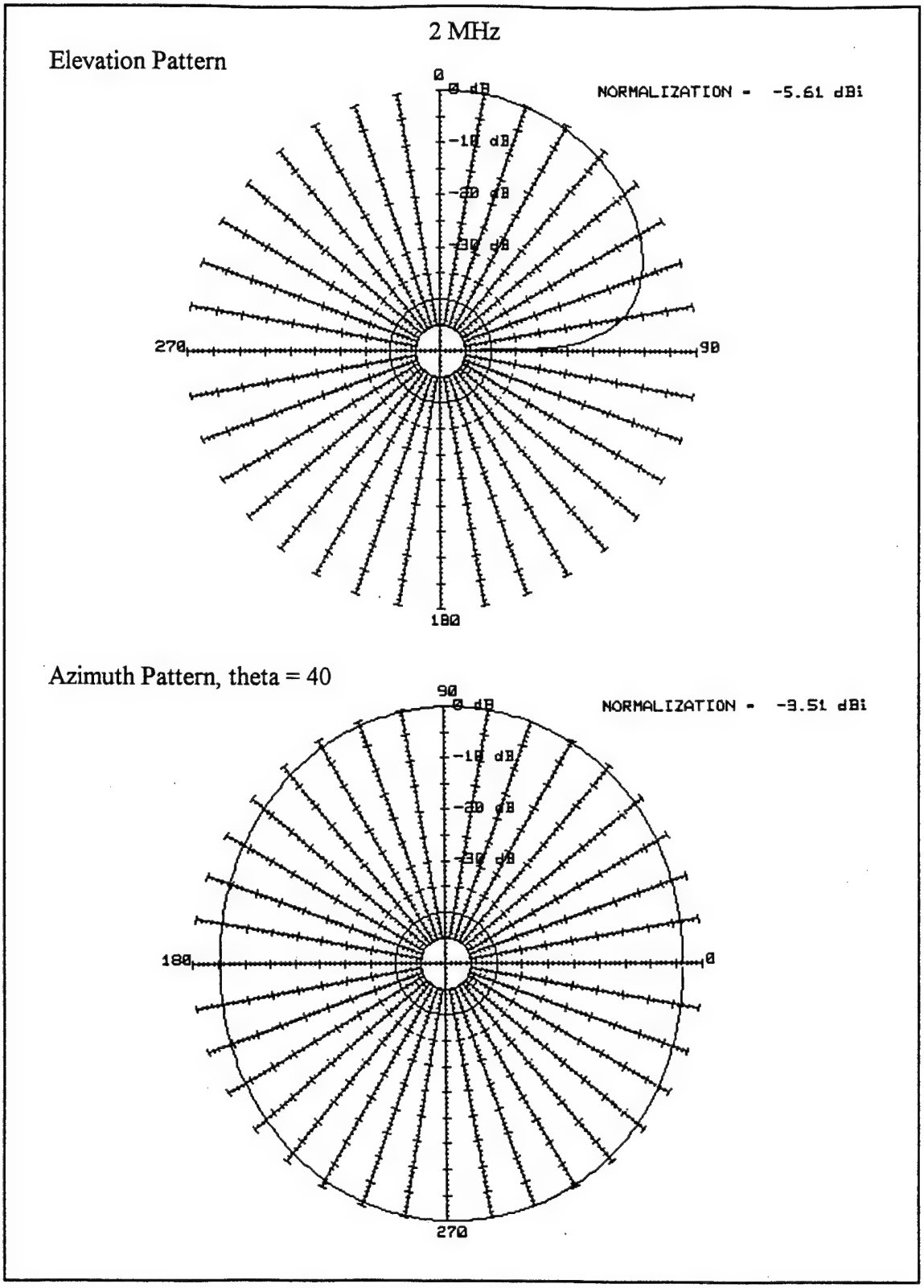

Figure 38. NEC-4 Sloping V Radiation Patterns, 2 MHz.

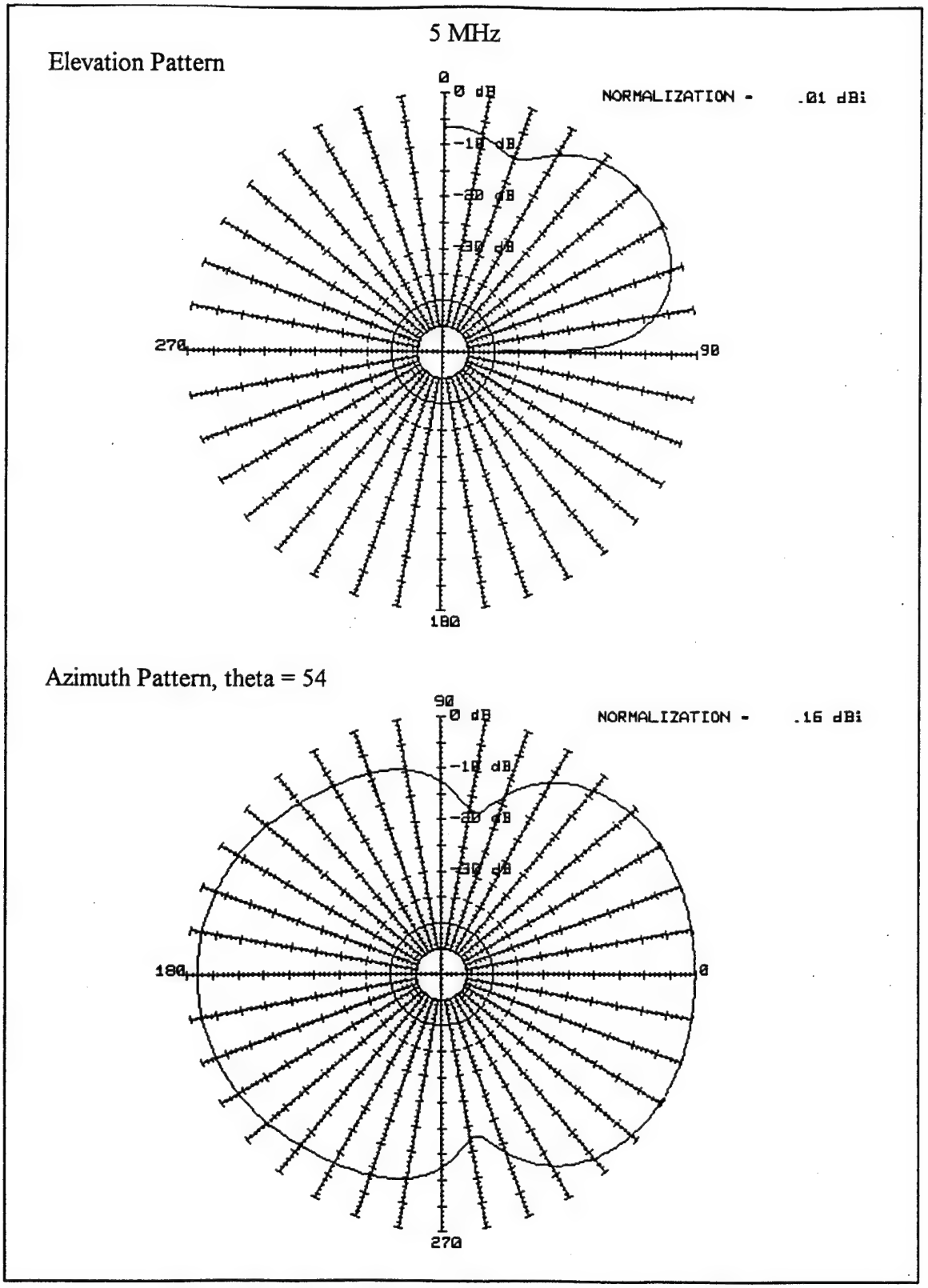

Figure 39. NEC-4 Sloping V Radiation Patterns, 5 MHz.

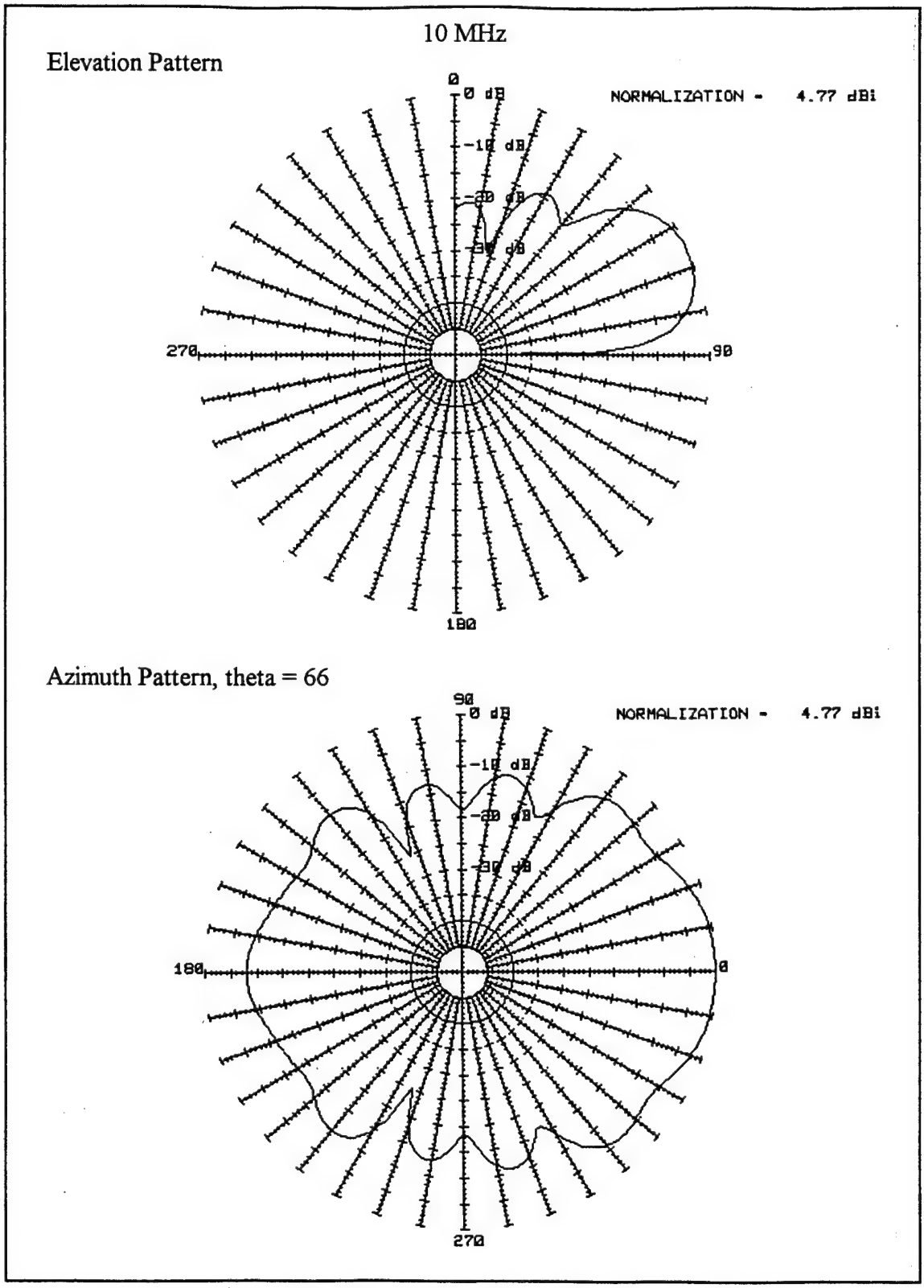

Figure 40. NEC-4 Sloping V Radiation Patterns, 10 MHz.

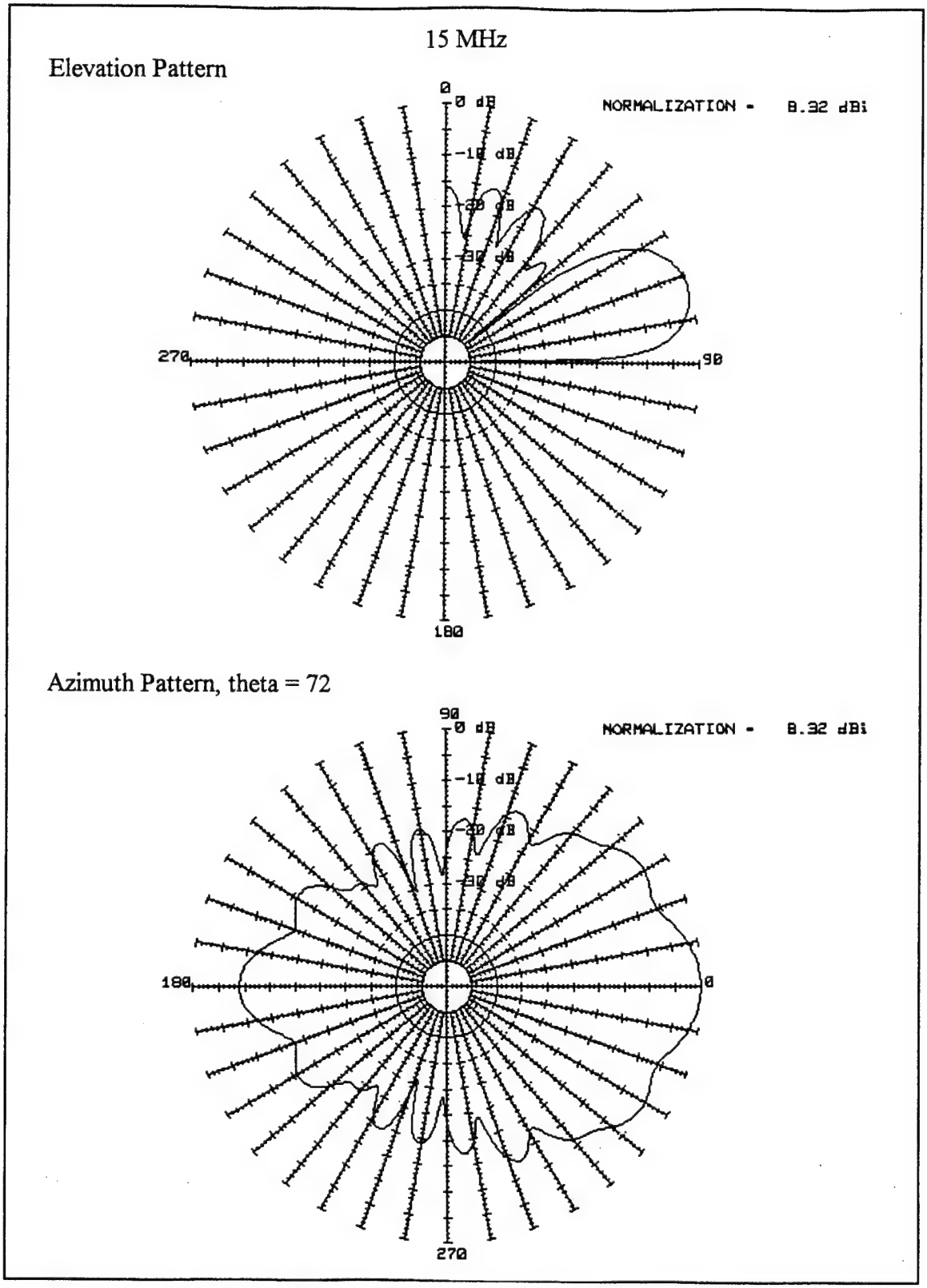

Figure 41. NEC-4 Sloping V Radiation Patterns, 15 MHz.

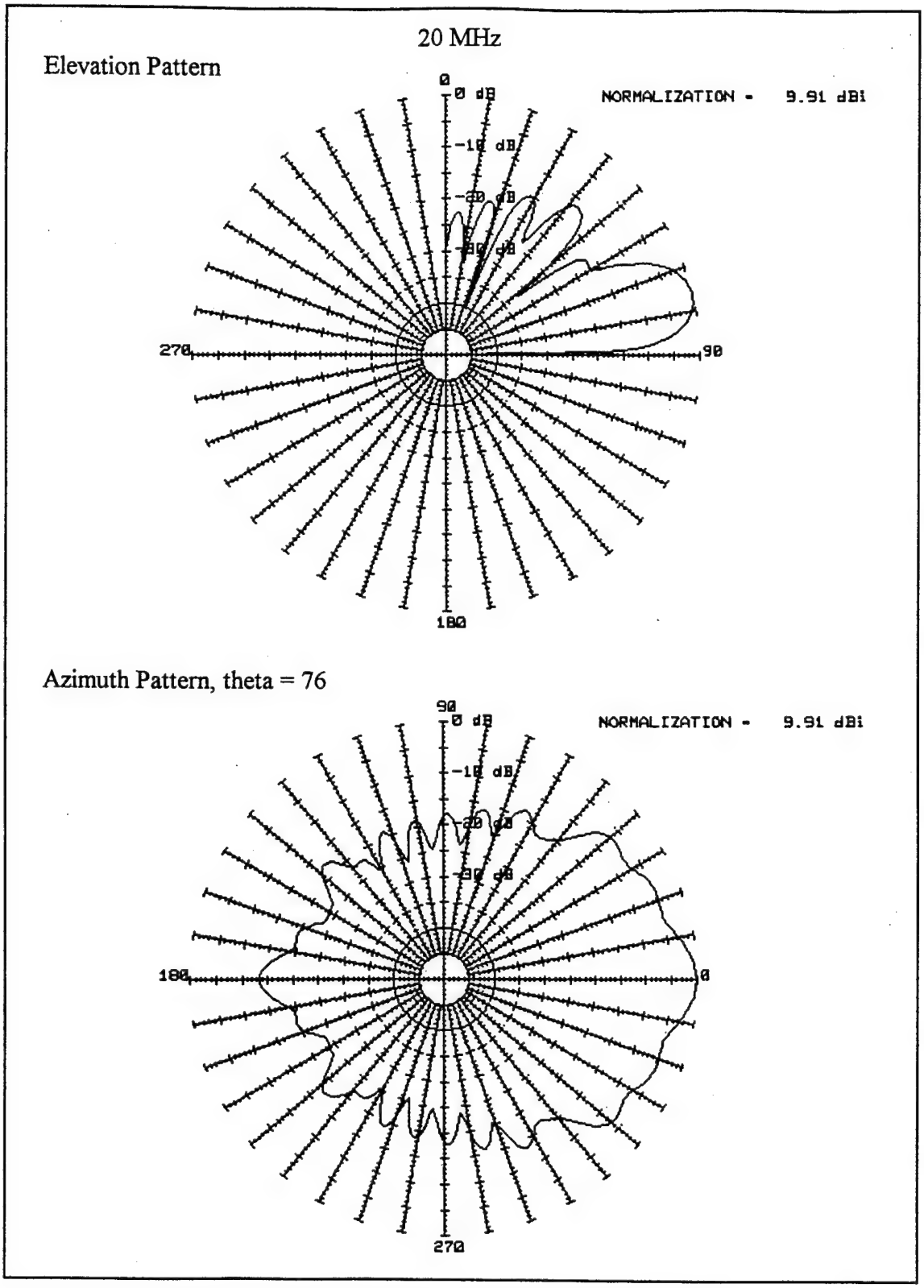

Figure 42. NEC-4 Sloping V Radiation Patterns, 20 MHz.

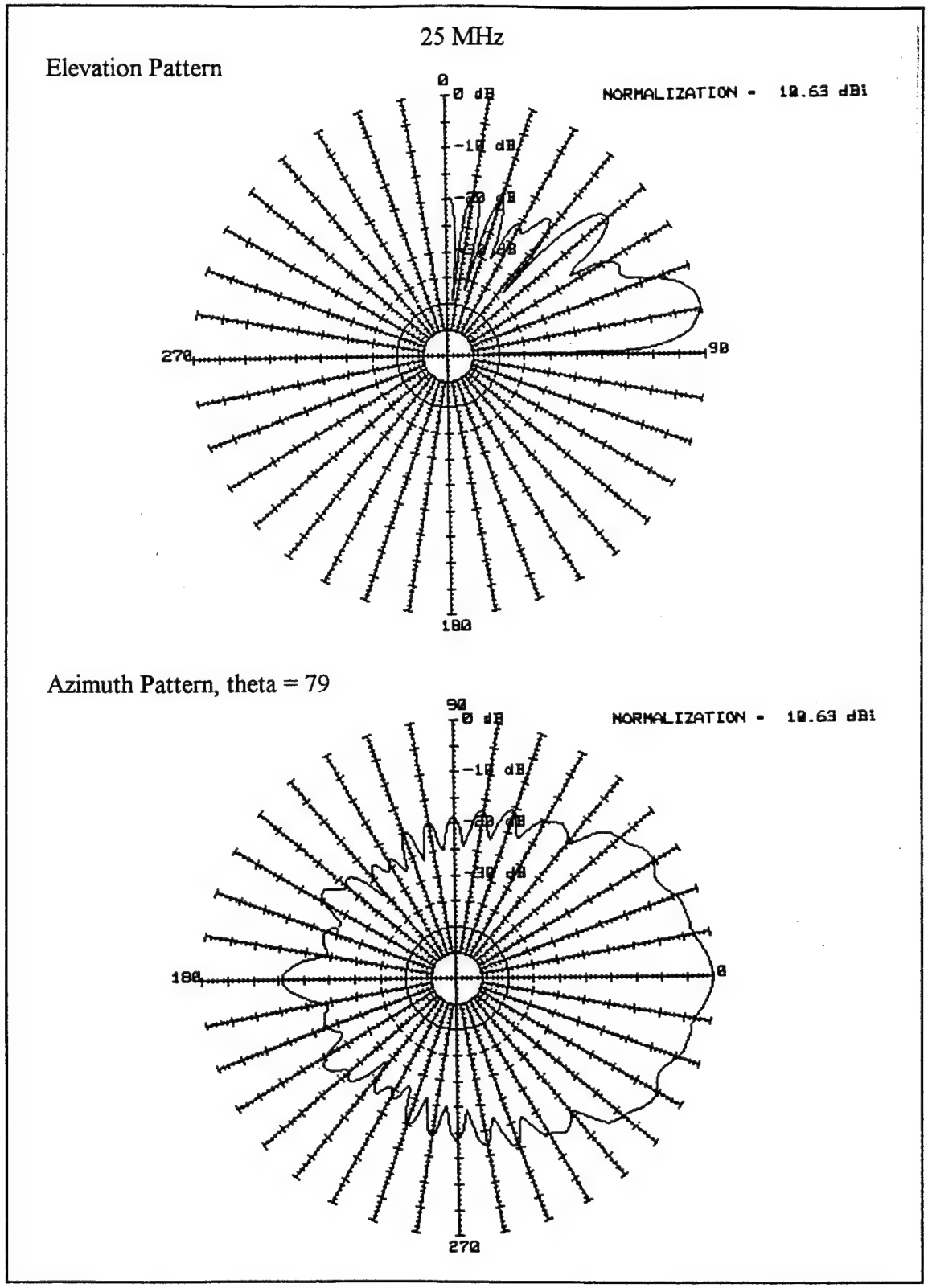

Figure 43. NEC-4 Sloping V Radiation Patterns, 25 MHz.

VI. TERRAIN MODELING

A. OAHU SITE

1. PAINT Results

The PAINT software was used to read digital terrain data from a Defense Mapping Agency CD-ROM for the Oahu site. The coordinates for the site are 21 degrees 31' N and 158 degrees 00' W. Figure 44 shows a contour of the site created from the CD-ROM data. The arrow in the center of the 1600 m x 1600 m area is the location of the antennas.

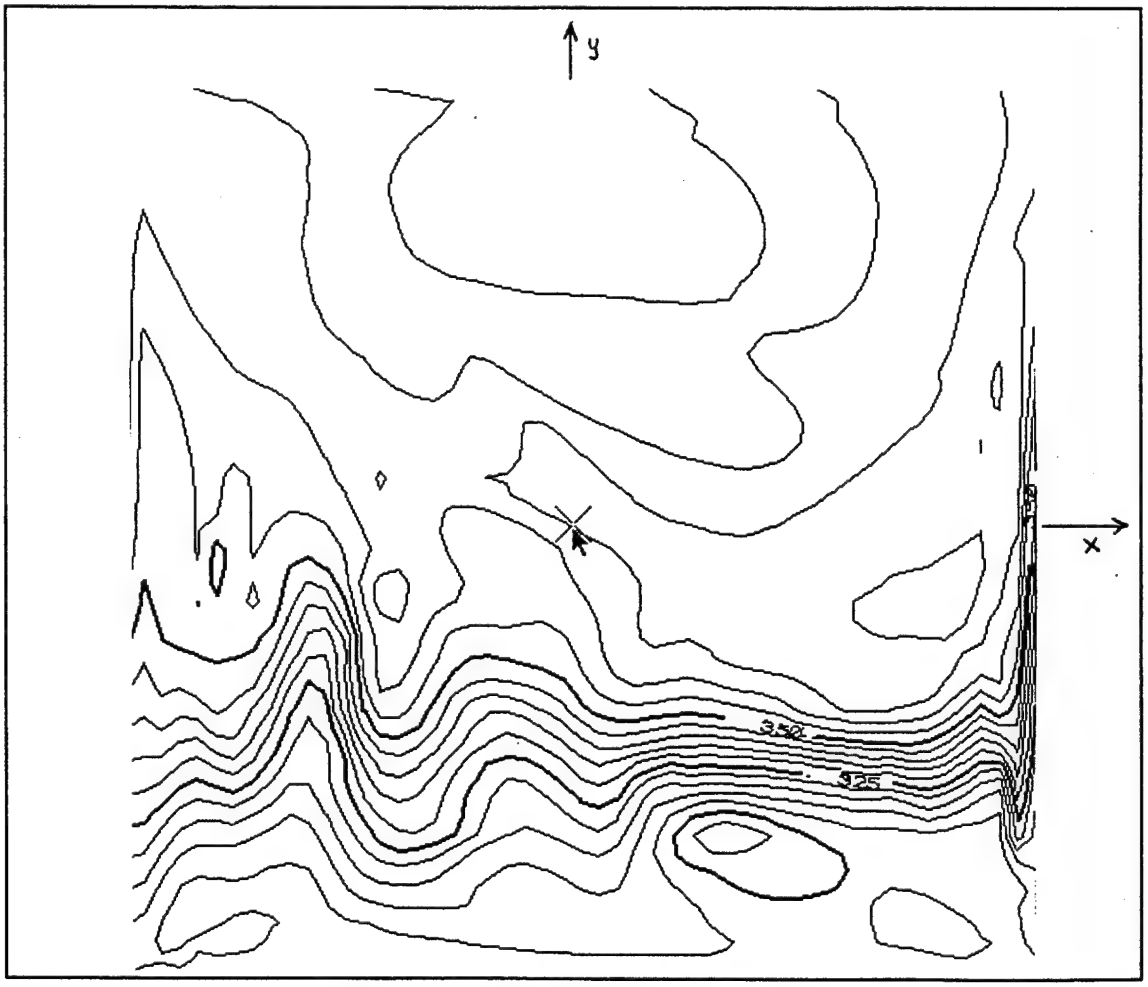

Figure 44. Oahu Antenna Site Contour.

True North is located at the top center along the y-axis. The propagation azimuth toward Rarotonga is approximately 268 degrees from the x-axis or 2 degrees short of due South. Figure 45 shows the top view of the 3-D triangular plate file created by PAINT to model the terrain.

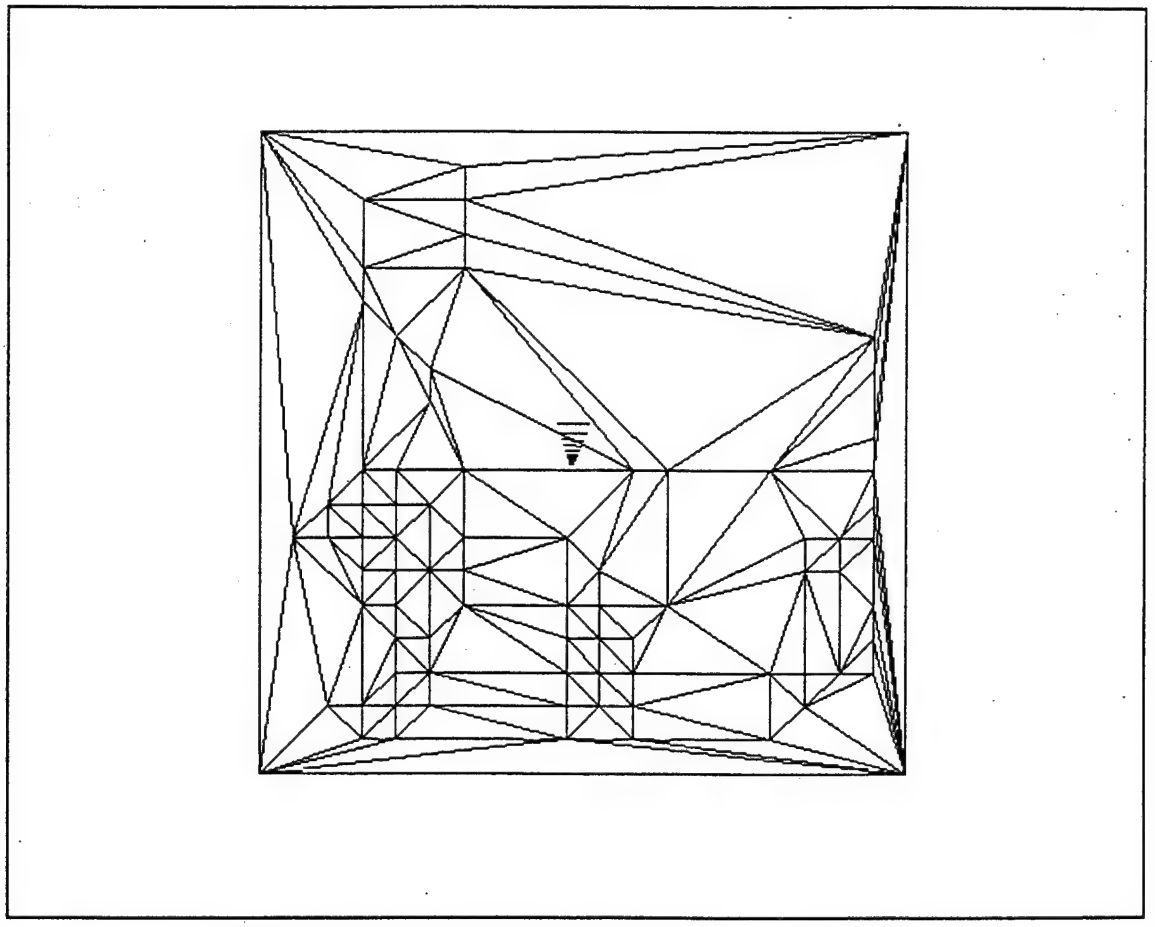

Figure 45. PAINT 3-D Oahu Terrain Plates, Top View.

This file consists of 154 dielectric covered plates. The HF Log-periodic antenna is shown in the center oriented toward Rarotonga. PAINT uses terrain plate files and currents from NEC output files as inputs to the NEC - BSC program. The output patterns can be displayed on screen and printed.

a. HF Log-periodic Results

Figures 46 and 47 show PAINT elevation pattern results for the HF log-periodic antenna modeled with NEC-4 in the last chapter. There are pronounced terrain effects at lower elevation angles of the plots due to the downslope in front of the antenna. A problem with the PAINT array source placement algorithm has been identified. The problem was discussed in Reference 14. The source array is placed at a height specified by the user above one of the corners of the plate or plates under the desired source location. Sometimes the code buries part of the antenna under the model terrain. This occurs in the case where array elements are at different heights as in the HF log-periodic antenna being modeled here. The source height for these plots was adjusted so that the elements were not buried beneath the terrain surface.

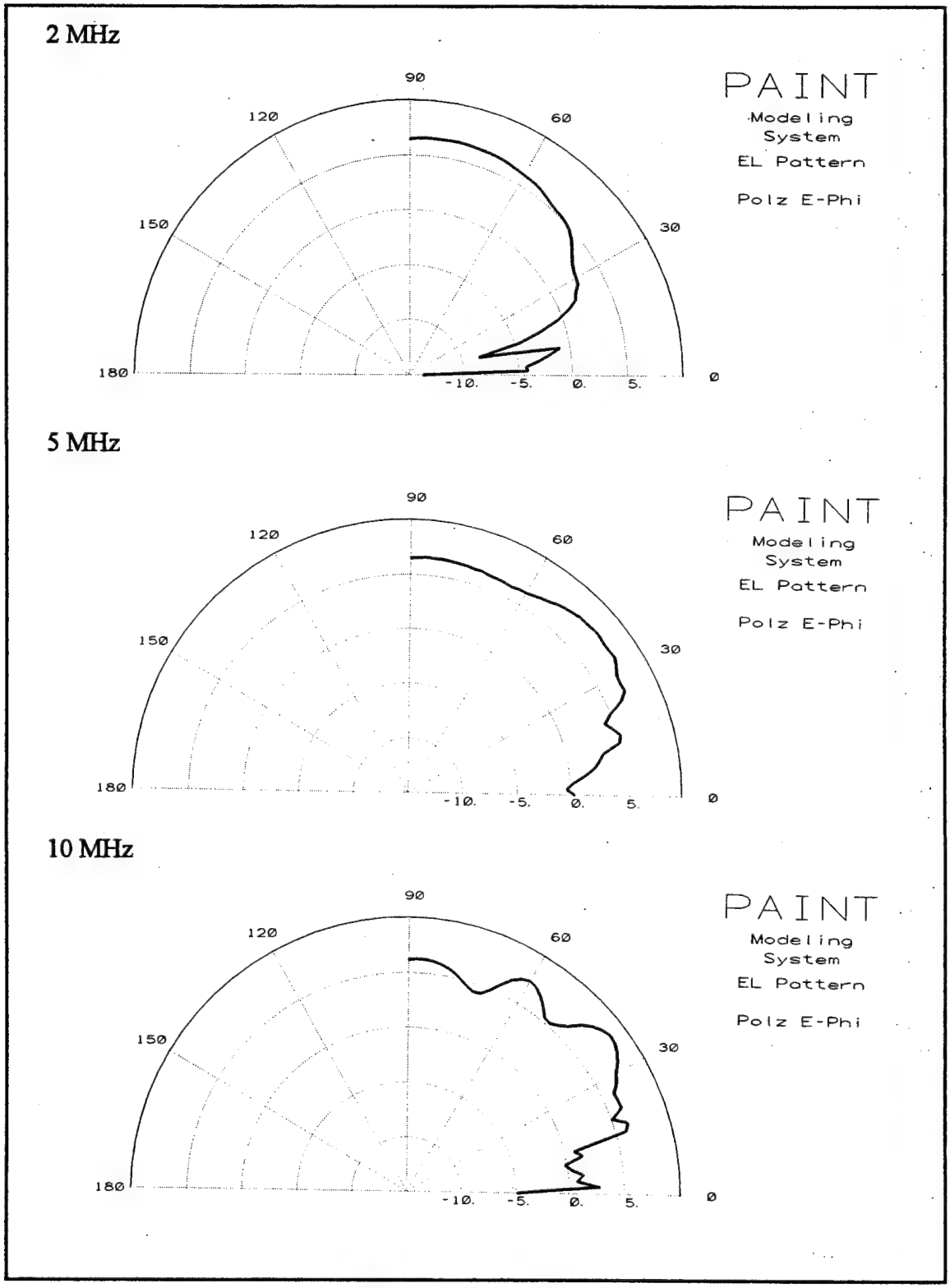

Figure 46. Oahu PAINT Results for HF Log-periodic Antenna.

15 MHz

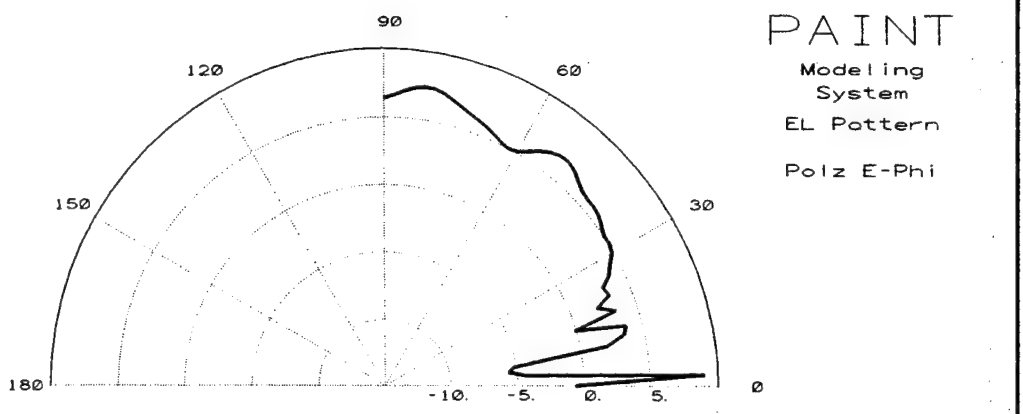

20 MHz

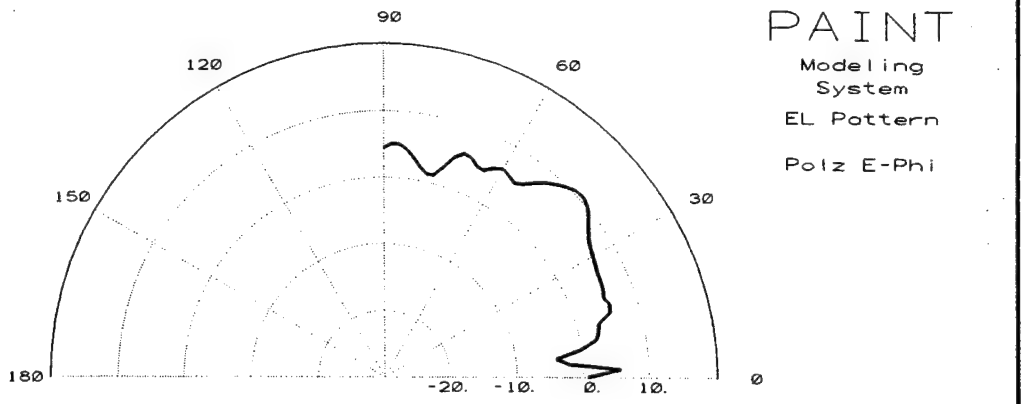

25 MHz

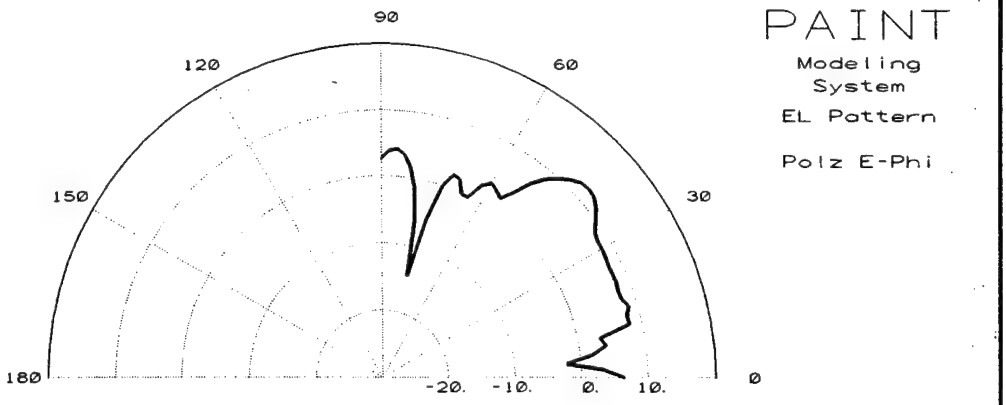

Figure 47. Oahu PAINT Results for HF Log-periodic Antenna (Continued).

b. VHF Log-Periodic Results

Figures 48 and 49 show PAINT elevation pattern results for the VHF log-periodic antenna modeled with NEC-4 in the last chapter. The results for the 25 MHz pattern are expected to be approximately the same as the HF log-periodic 25 MHz pattern because the radiating elements for both are at about the same height. Differences in patterns are attributed to the differences in antenna size. The HF log-periodic antenna is about 310 feet long along the ground and the VHF log-periodic antenna is 22.5 feet long. The centers for both antenna arrays are located at the same position. At 25 MHz, this places the radiating elements for the HF log-periodic antenna approximately 160 feet closer to the downslope in front of the antennas and ground effects are observed in the elevation patterns. The VHF antenna is located 10 feet above a large plate and no ground effects are observed in the elevation patterns.

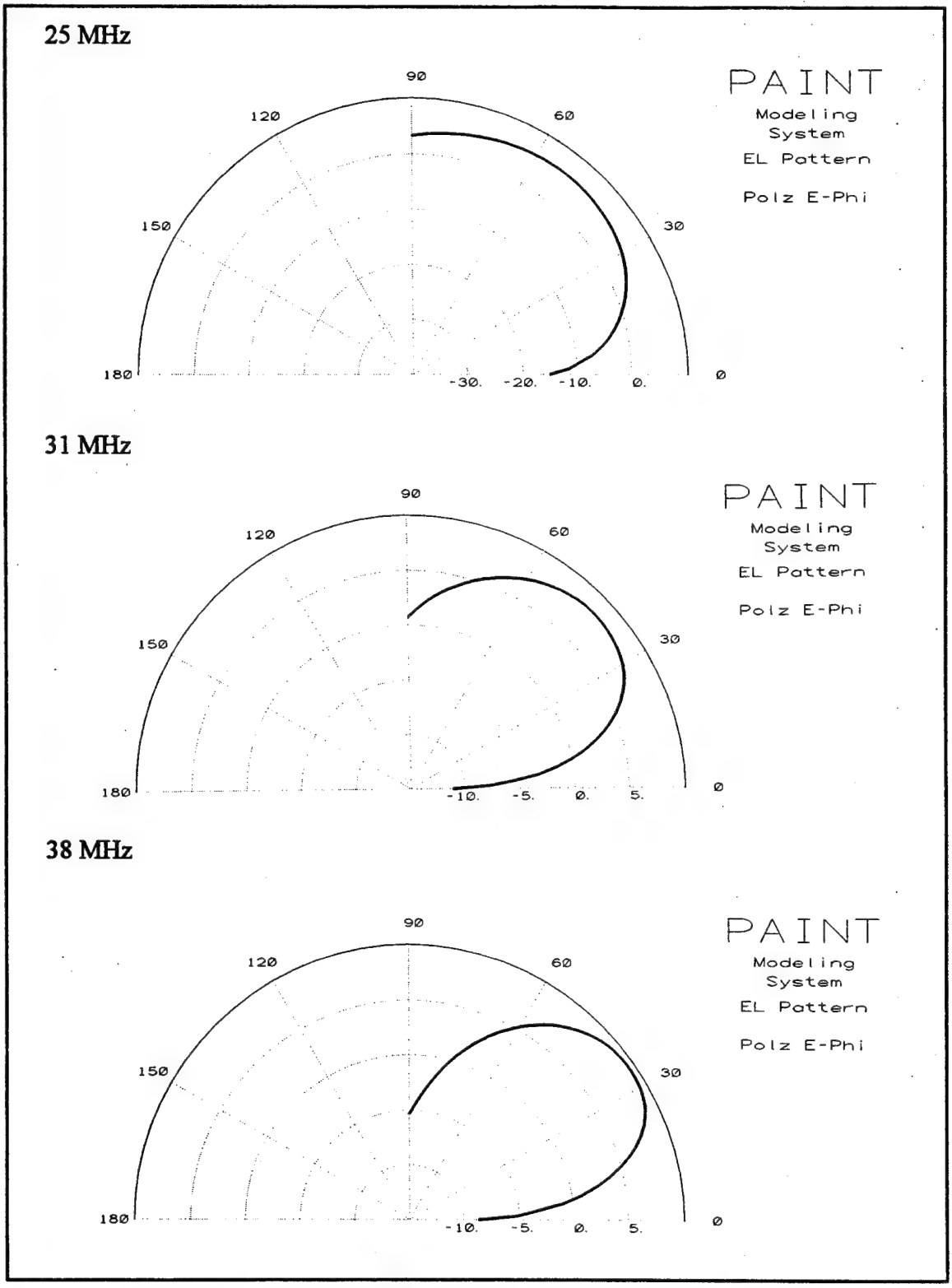

Figure 48. Oahu PAINT Results for VHF Log-periodic Antenna.

45 MHz

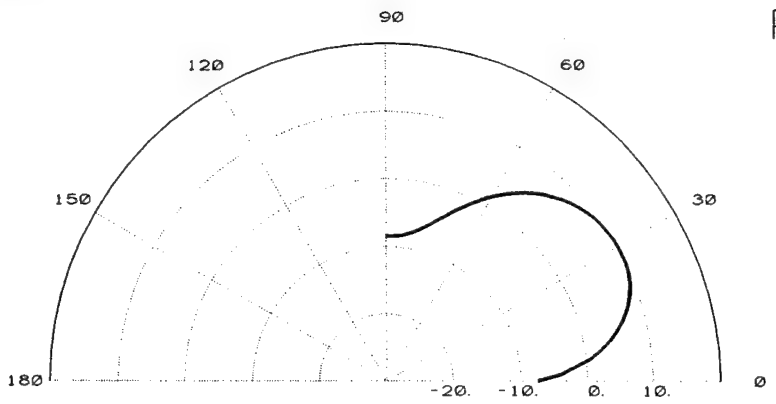

PAINT
Modeling
System
EL Pattern
Polz E-Phi

52 MHz

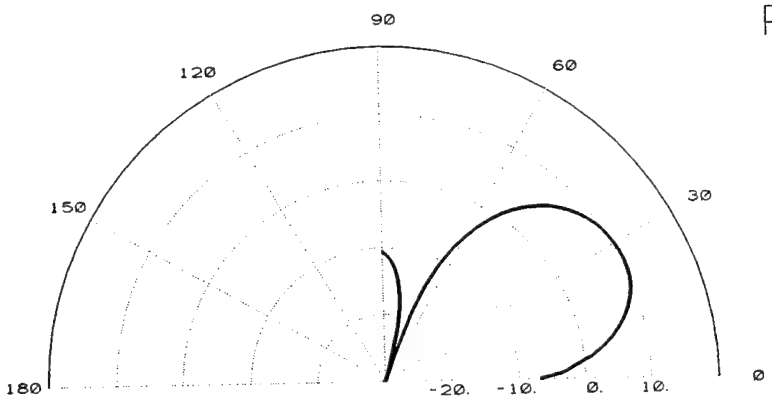

PAINT
Modeling
System
EL Pattern
Polz E-Phi

60 MHz

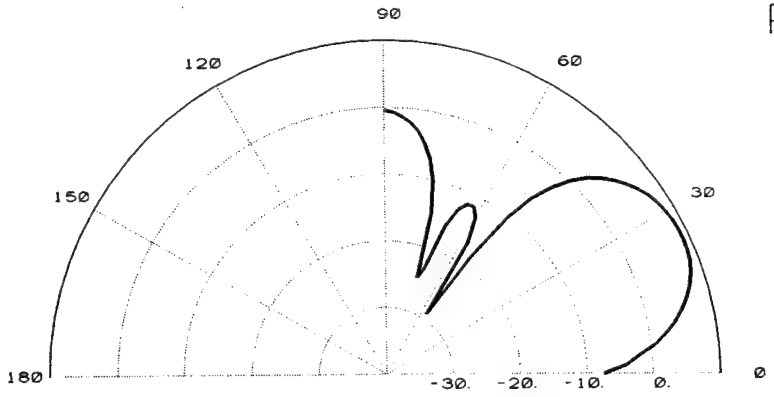

PAINT
Modeling
System
EL Pattern
Polz E-Phi

Figure 49. Oahu PAINT Results for VHF Log-periodic Antenna (Continued).

2. TA Results

MN software was used to create freespace radiation patterns to be used with TA for terrain modeling. Appendix H contains the MN input file for a 6 element VHF log-periodic antenna.

The 12 element HF log-periodic antenna could not be adequately modeled by MN as the maximum number of pulses MN can handle is 127. This is not enough pulses for the 47 wires required to model the HF log-periodic elements and transmission lines.

Figures 50 through 52 show the TA elevation plots for the VHF log-periodic antenna on Oahu. The 2-D terrain profiles are shown under each elevation pattern. The arrow points to the antenna location. These results were obtained using 1/4 degree pattern resolution and the TA filter option to suppress spikes. The TA pattern results show ground effects at the low elevation angles where the pattern is stronger than predicted by ELNEC and NEC-4 flat ground planes. TA terrain files are in Appendix I.

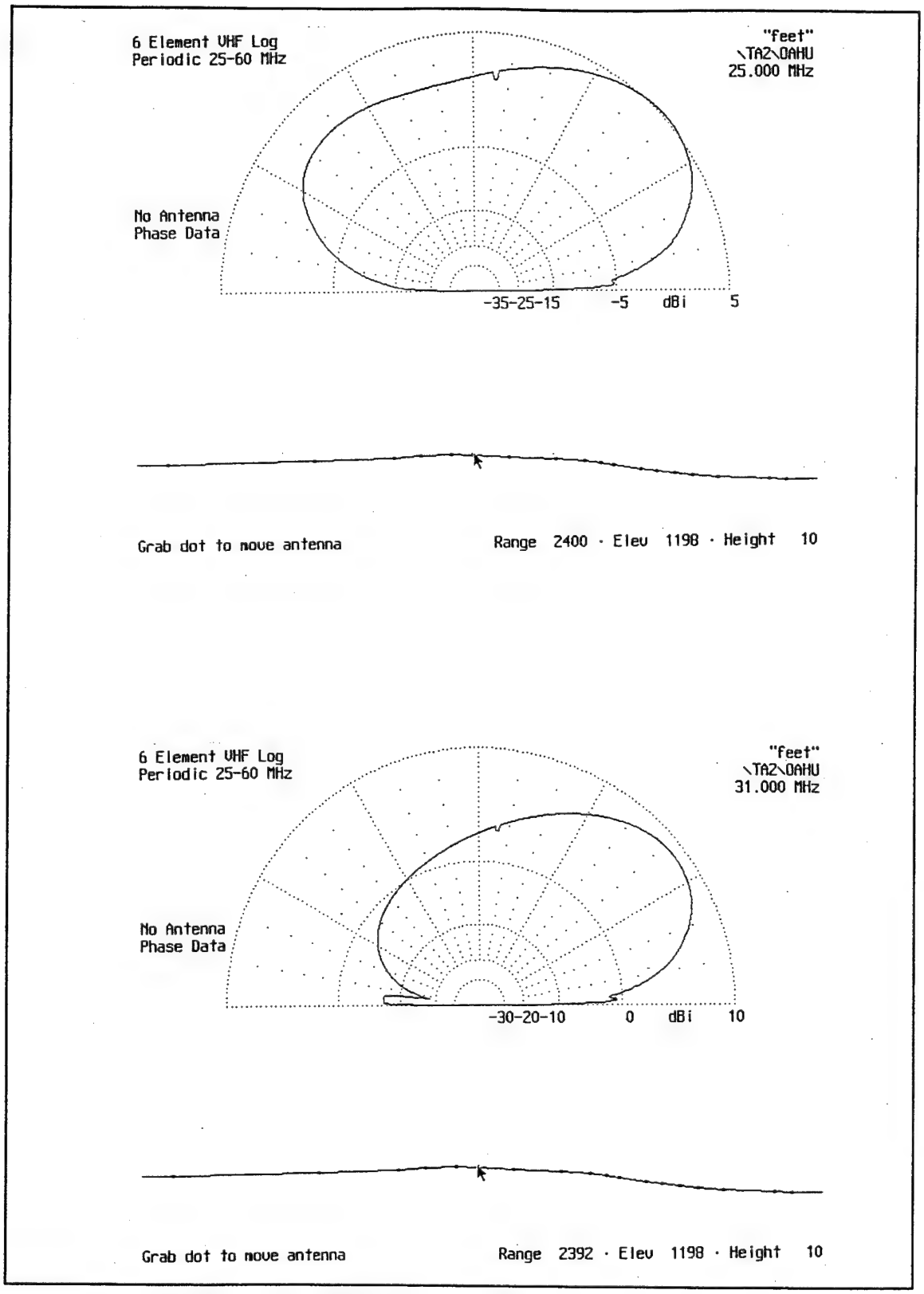

Figure 50. Oahu TA Results for VHF Log-periodic Antenna.

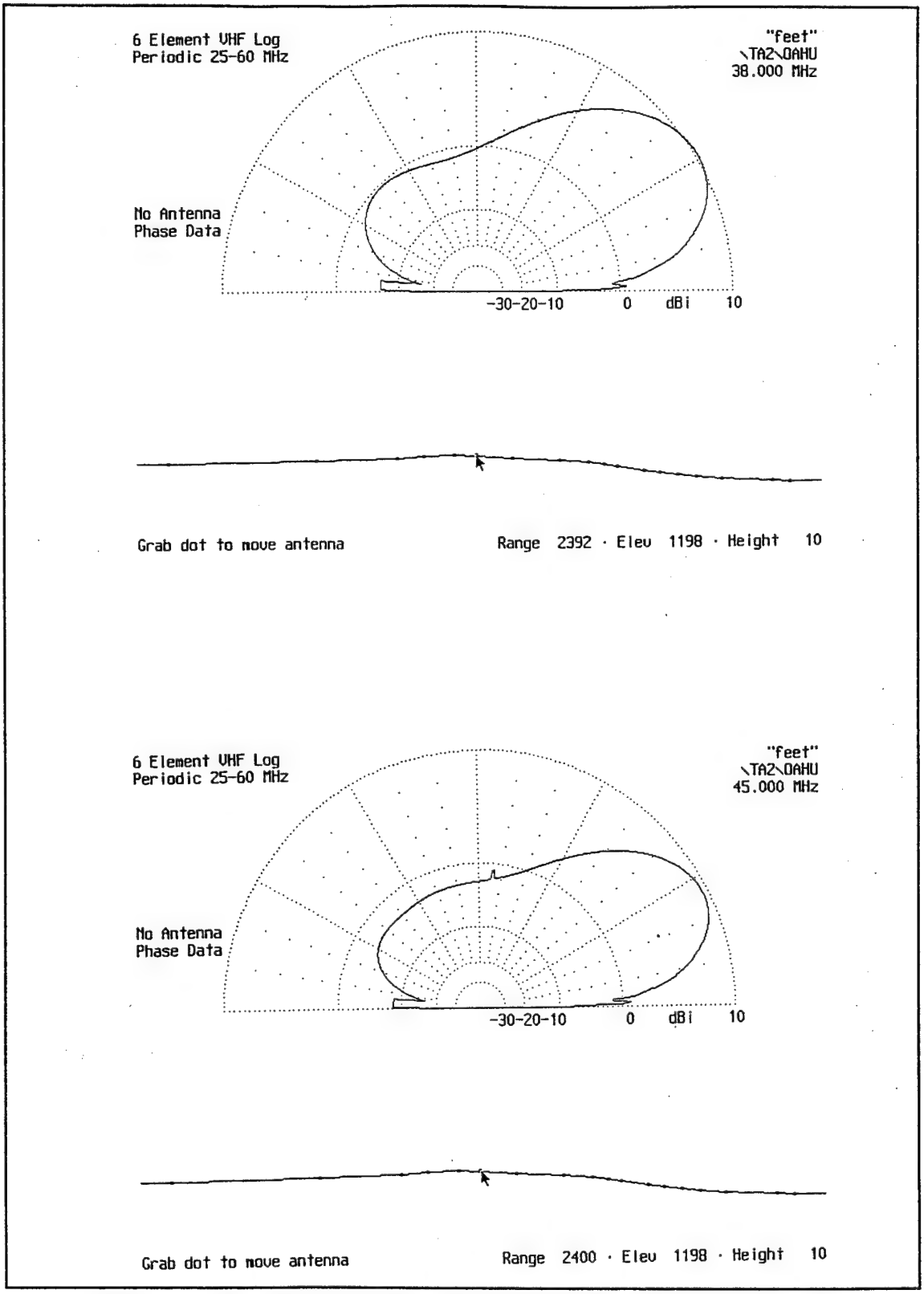

Figure 51. Oahu TA Results for VHF Log-periodic Antenna (Continued).

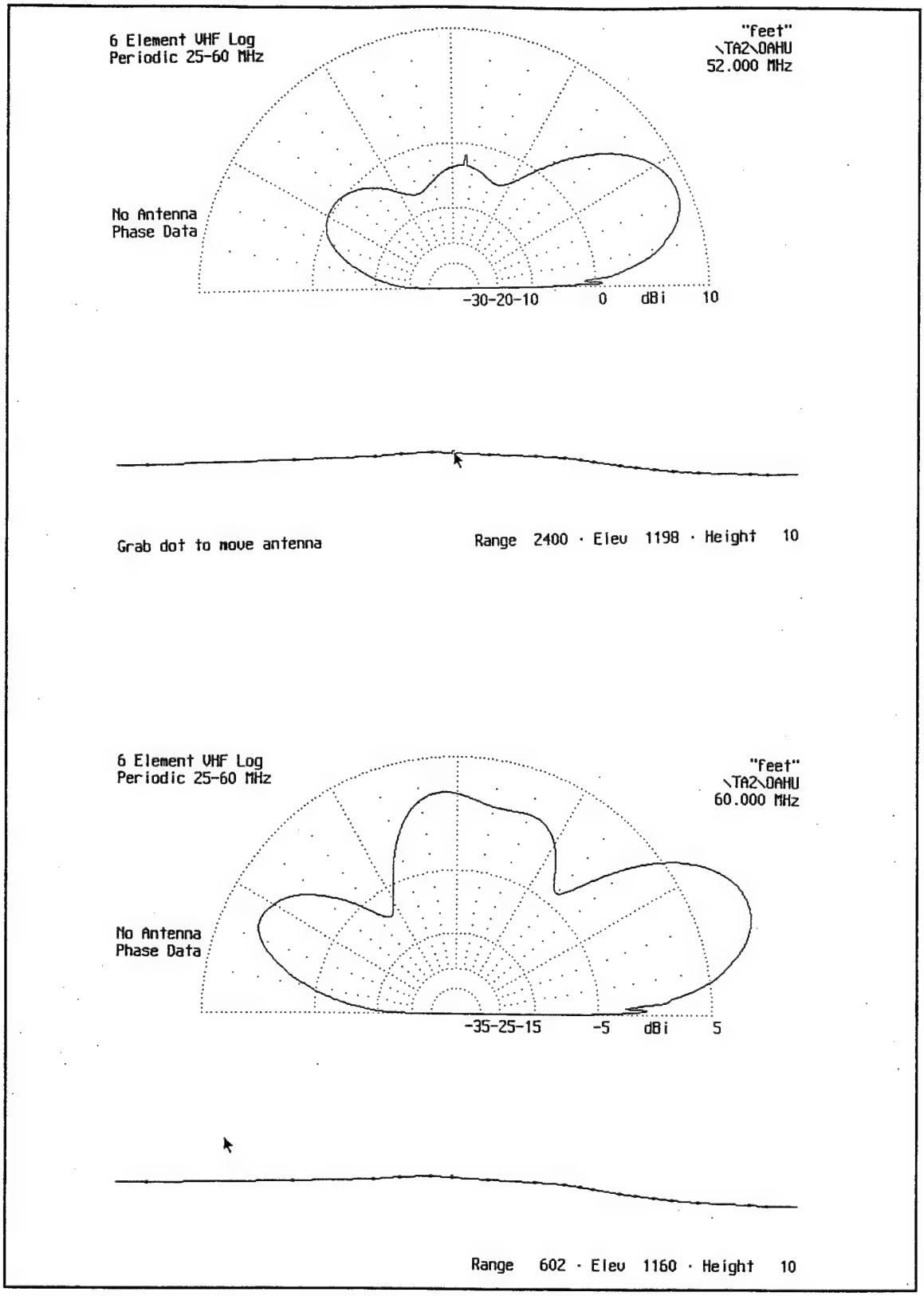

Figure 52. Oahu TA Results for VHF Log-periodic Antenna (Continued).

B. RAROTONGA SITE

1. PAINT Results

The Rarotonga terrain file was created from a contour map instead of a DMA CD-ROM. The contour map of Rarotonga was used to create a grid with 189 elevation data points of the site location. A data point file was used to create a PAINT terrain file. Figure 53 shows a contour of the site. The arrow in the center shows the antenna location in the 1600 x 1600 meter square. The antenna is located on the north shore of the island

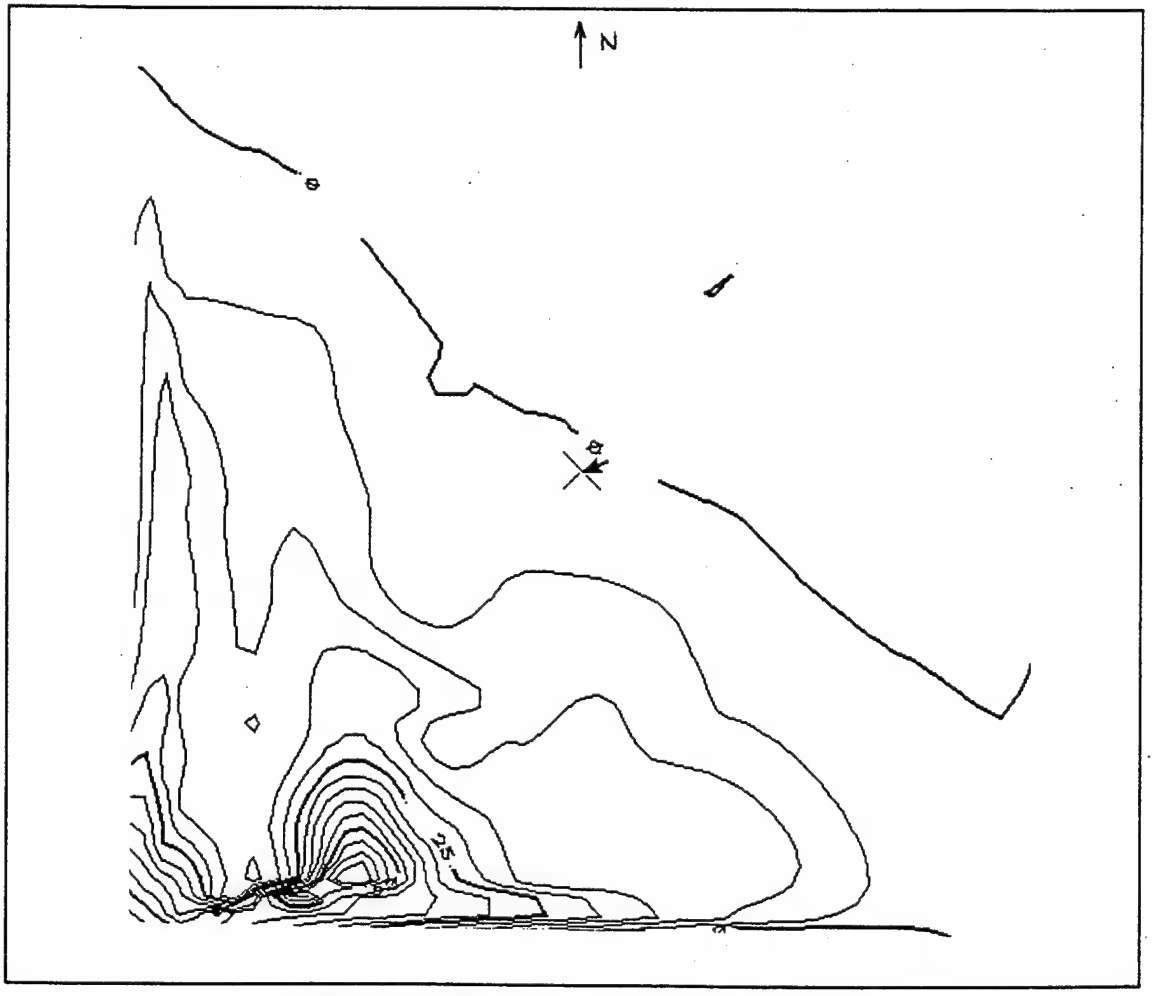

Figure 53. Rarotonga Antenna Site Contour.

near the ocean. The direction towards Oahu is approximately 2 degrees east of true north, which is straight up in the figure.

Figure 54 shows the top view of the 3-D triangular plate file created by PAINT with the sloping V antenna near the center. The file consists of 102 triangular plates.

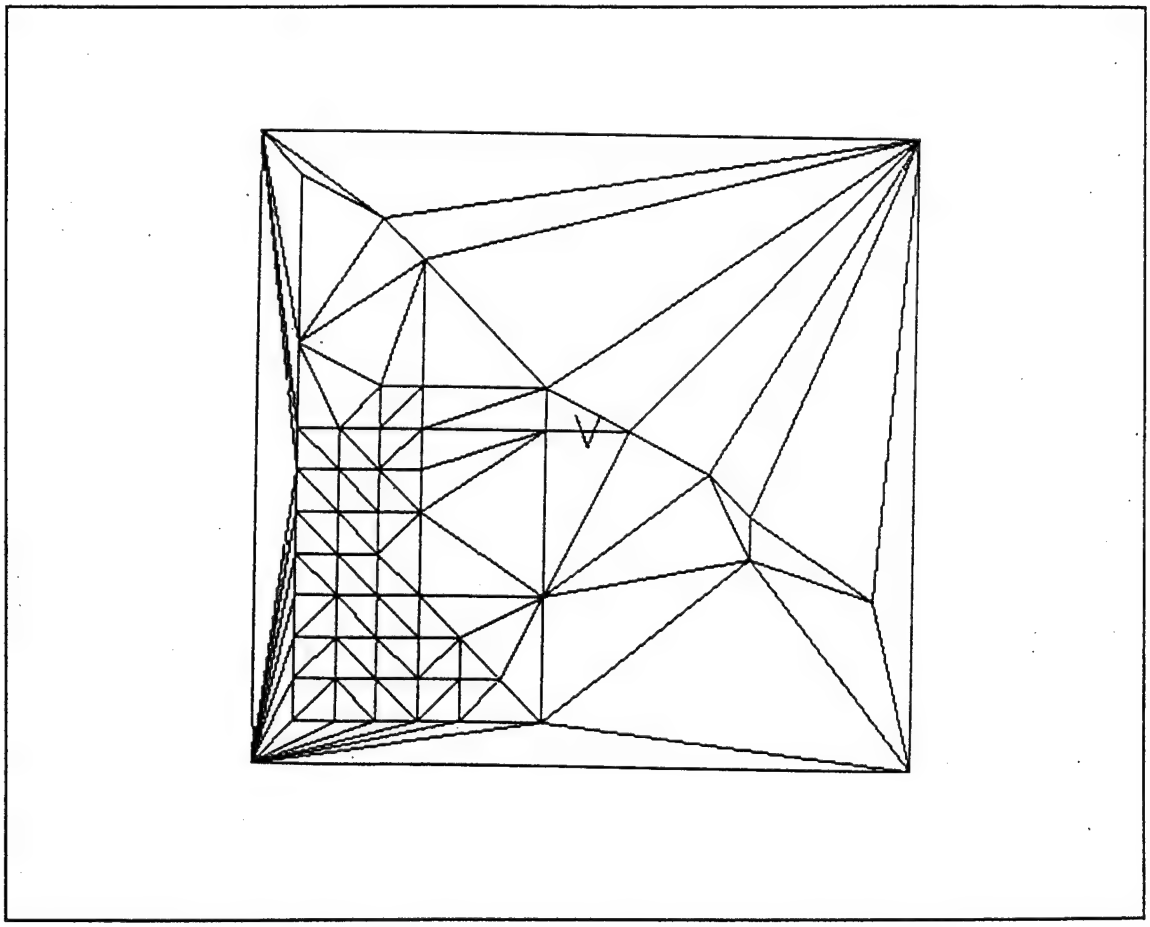

Figure 54. PAINT 3-D Rarotonga Terrain Plates, Top View.

a. Sloping V Results

Figures 55 and 56 show PAINT elevation pattern results for the sloping V antenna modeled with NEC-4 in the last chapter. Problems were also encountered with determining a height for this antenna so that elements were not buried.

2 MHz

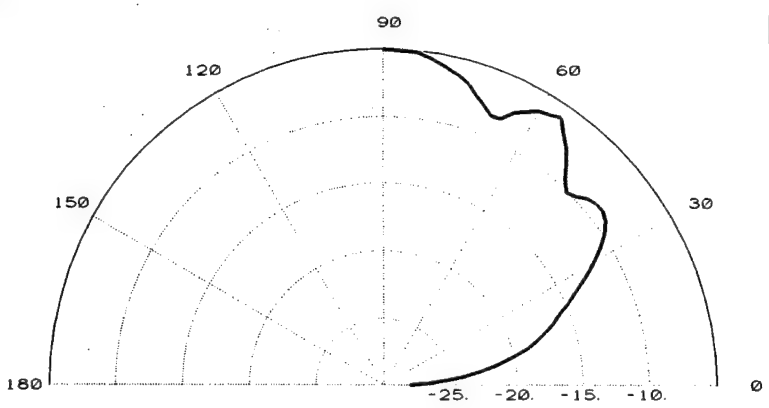

5 MHz

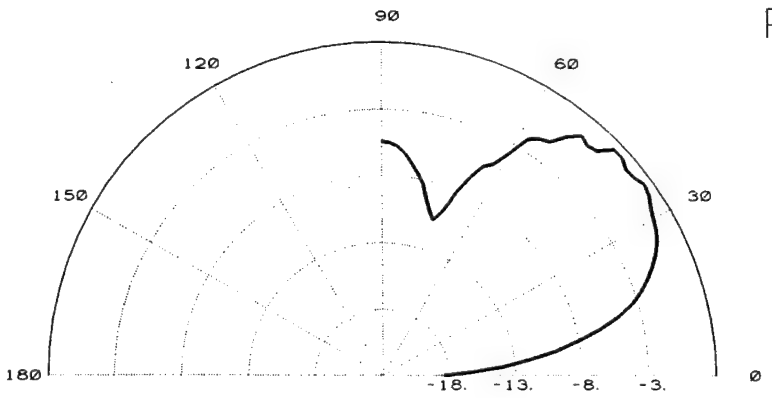

10 MHz

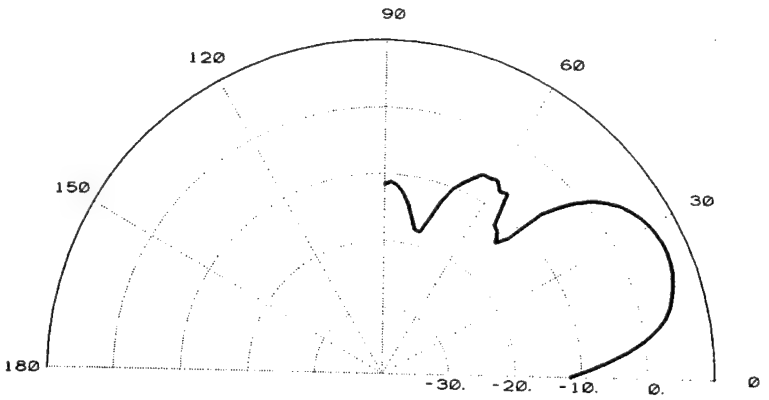

Figure 55. Rarotonga PAINT Results for Sloping V Antenna.

15 MHz

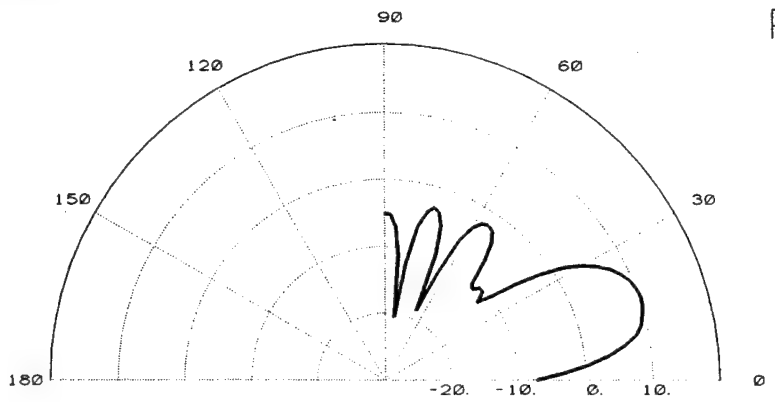

20 MHz

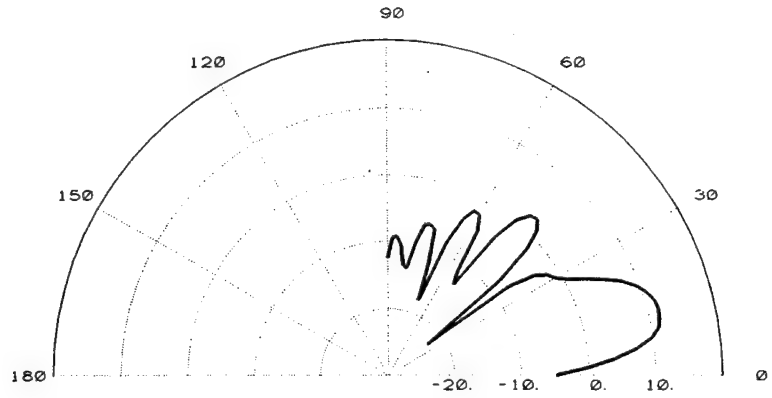

25 MHz

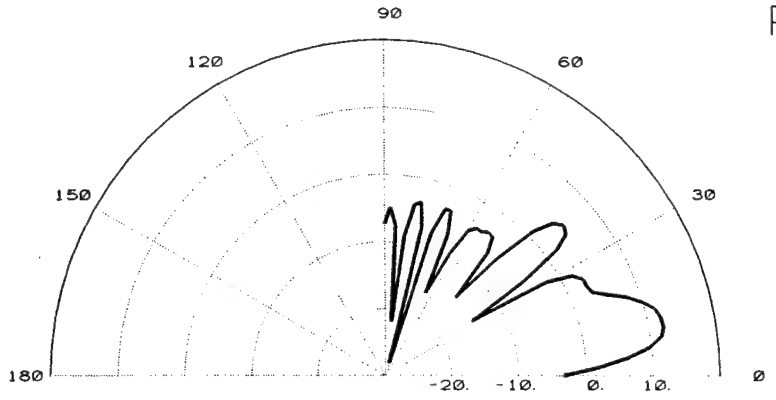

Figure 56. Rarotonga PAINT Results for Sloping V Antenna (Continued).

b. VHF Log-periodic Results

Figures 57 and 58 show PAINT elevation pattern results for the VHF log-periodic antenna.

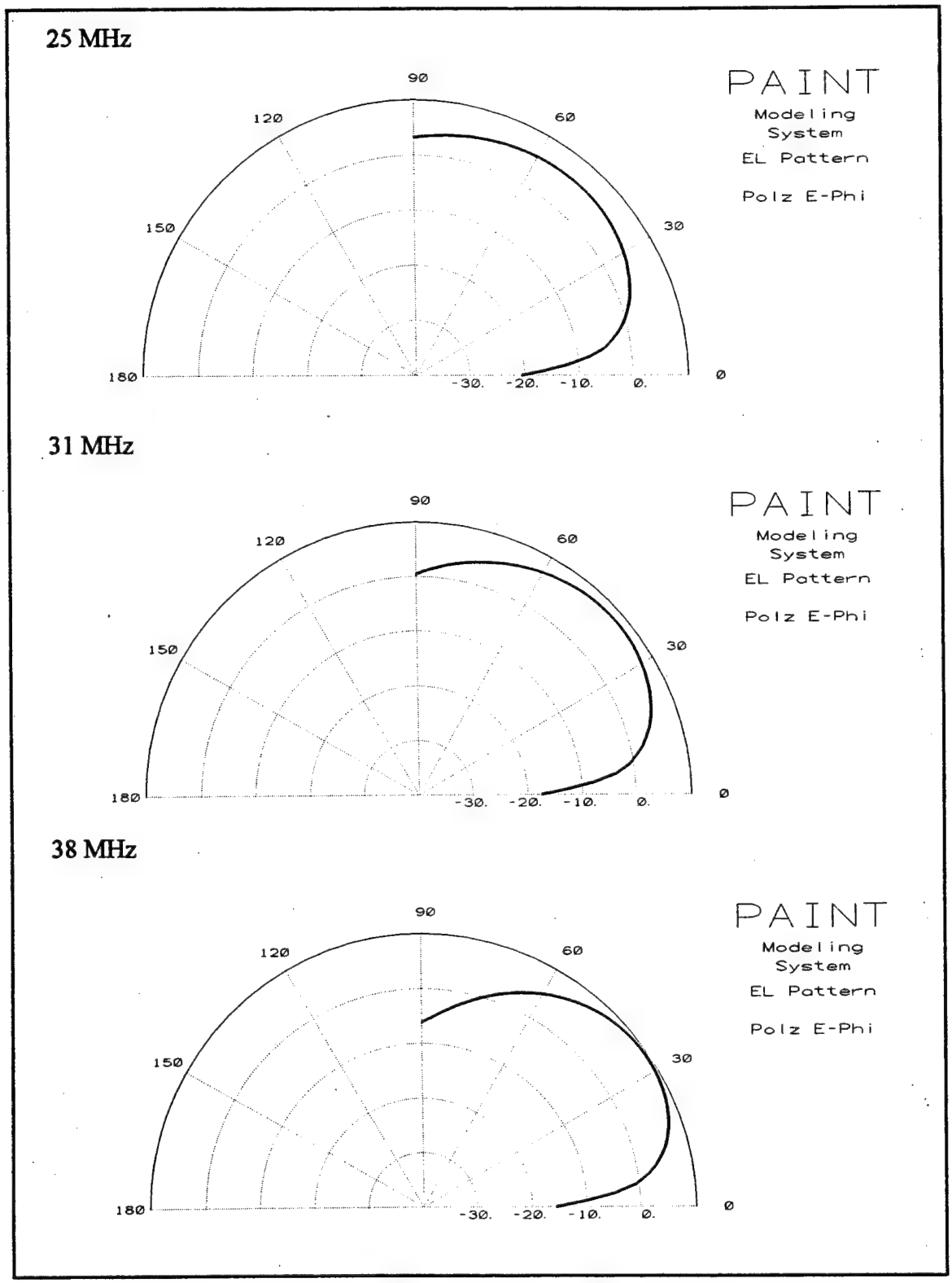

Figure 57. Rarotonga PAINT Results for VHF Log-periodic Antenna.

45 MHz

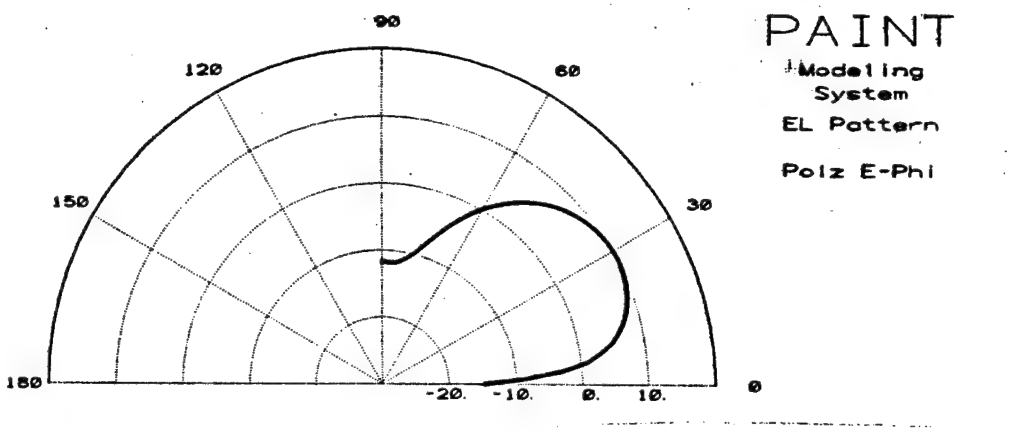

52 MHz

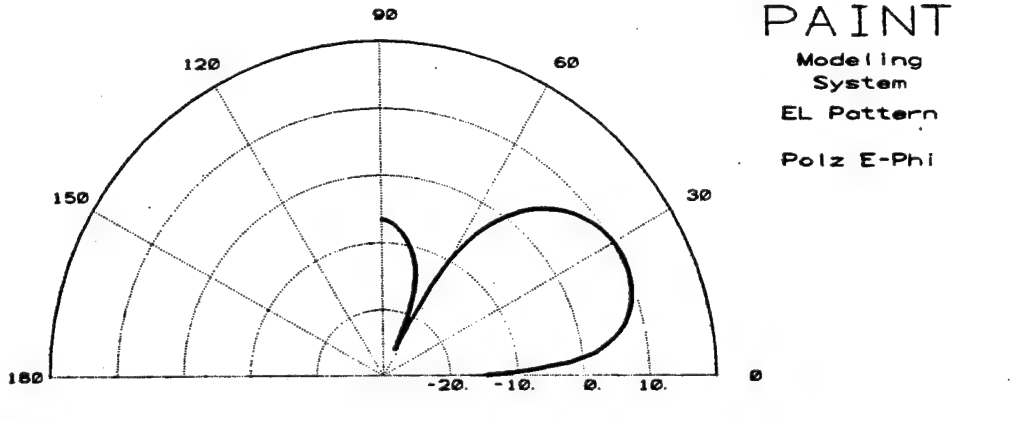

60 MHz

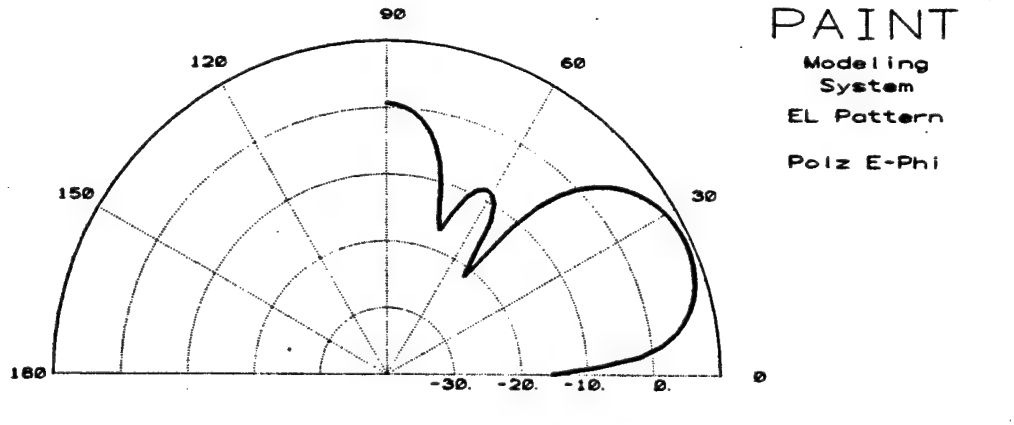

Figure 58. Rarotonga PAINT Results for VHF Log-periodic Antenna (Continued).

2. TA Results

A 2-D terrain model was created for the Rarotonga site. This was used with the MN model of the VHF log-periodic antenna. The sloping V could not be modeled with MN as it was is not possible to model the grounded terminating resistors in a freespace antenna model.

Figures 59 through 61 show the TA elevation plots for the VHF log-periodic antenna on Rarotonga. The 2-D terrain profiles are shown under each elevation pattern. The arrow points to the antenna location. The TA results do not show ground effects in the pattern at low elevation angle that occured with the TA Oahu terrain profile.

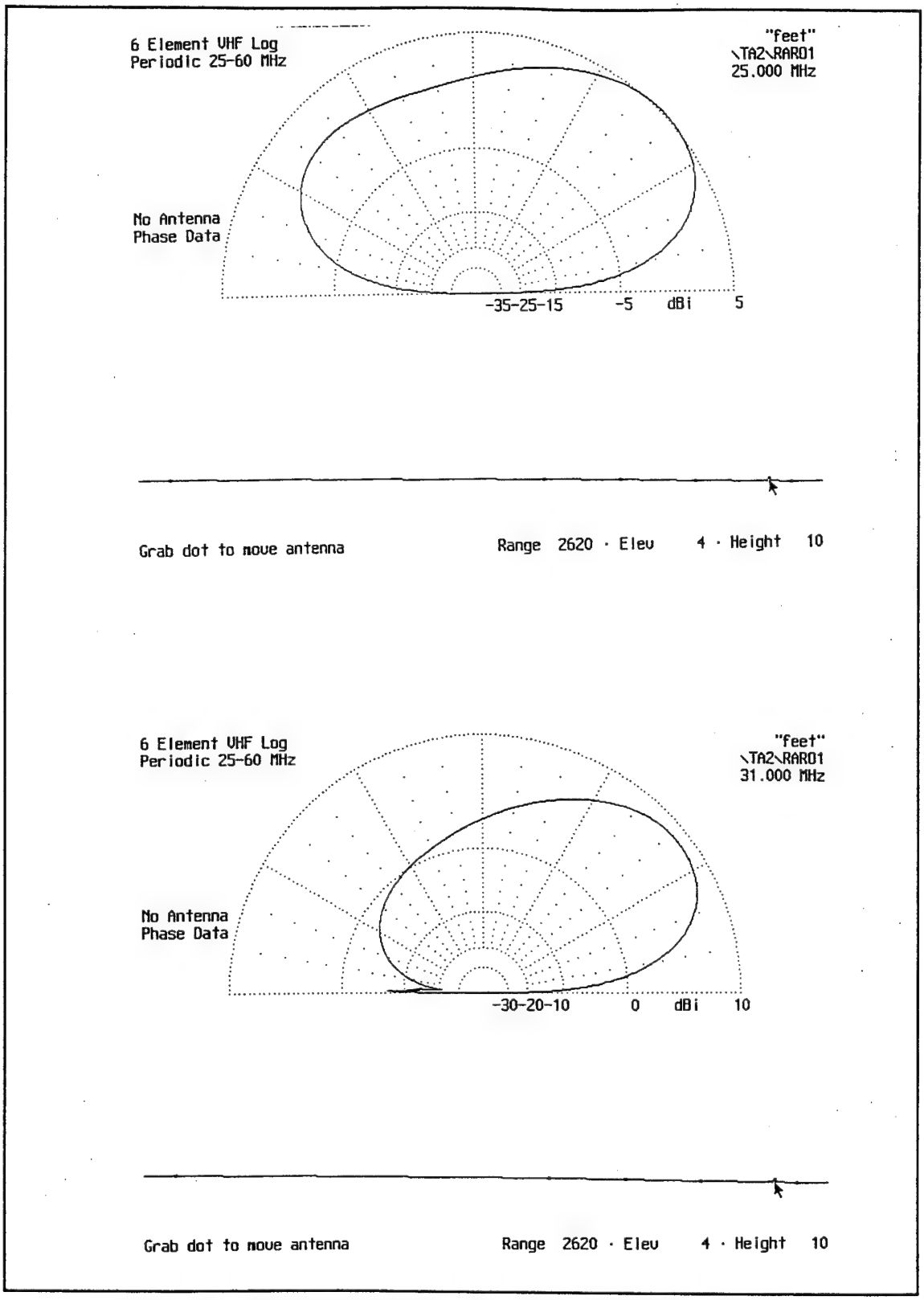

Figure 59. Rarotonga TA Results for VHF Log-periodic Antenna.

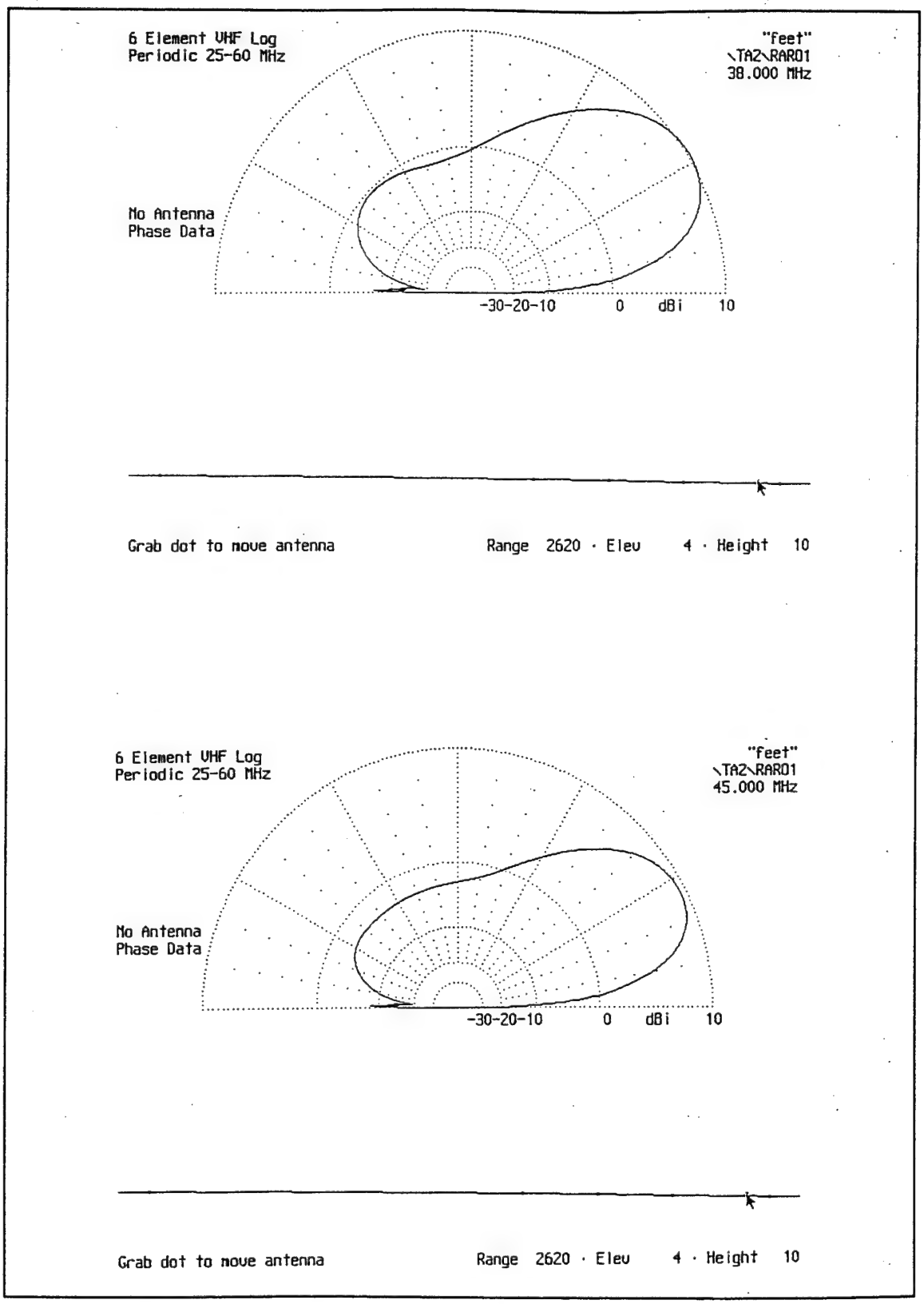

Figure 60. Rarotonga TA Results for VHF Log-periodic Antenna (Continued).

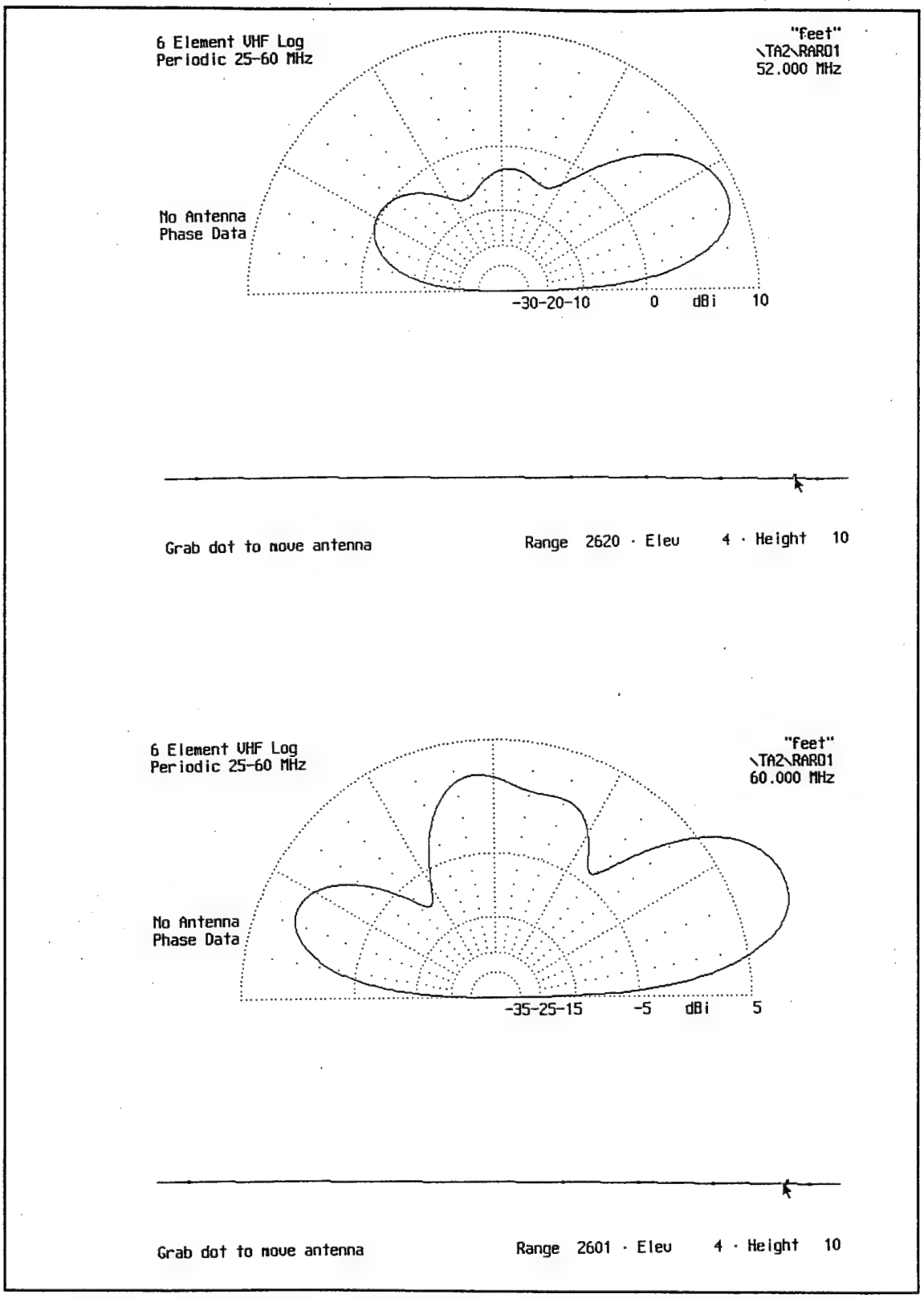

Figure 61. Rarotonga TA Results for VHF Log-periodic Antenna (Continued).

VII. CONCLUSIONS AND RECOMMENDATIONS

A. CONCLUSIONS

A four step process for antenna design was outlined: theoretical design, preliminary analysis with ELNEC software, detailed analysis with NEC-4 software and finally terrain modeling with PAINT, MN and TA software. A rhombic antenna configuration was rejected after the preliminary design stage revealed bandwidth limitations. A VHF log-periodic antenna was chosen for the 25-60 MHz band at both sites. A sloping V configuration was chosen for the 2-25 MHz band at the Rarotonga site and an HF log-periodic antenna was chosen for the 2-25 MHz band at the Oahu site.

The PAINT results show that a downslope in front of the antenna, as is the case at the Oahu site, affects the low angle elevation pattern for the HF log-periodic antenna. The VHF log-periodic antenna patterns do not show ground effects because the antenna is positioned further back away from the downslope.

The TA results indicate that a downslope in front of the antenna at Oahu strengthens the low elevation angle radiation compared to the pattern results from the nearly flat Rarotonga site.

A sample comparative analysis is provided for each antenna at one frequency. All results are compared to the NEC-4 results and the percent deviation is shown. Table 10 shows comparisons for the 6 element VHF log-periodic antenna at 25 MHz.

	Maximum Gain, dBi (deviation)	Takeoff Angle, degrees (deviation)	Beamwidth, degrees (deviation)
NEC-4	4.37	46	66
ELNEC	4.28 (-2.1 %)	46 (0 %)	64 (-3.0 %)
PAINT Oahu	5.92 (42.9 %)	52 (13.0 %)	65 (-1.5 %)
PAINT Raro.	5.92 (42.9 %)	50 (8.7 %)	58 (-12.1 %)
TA Oahu	5.20 (21.1 %)	41 (-10.9 %)	66 (0 %)
TA Raro.	5.10 (18.3 %)	45 (-2.2 %)	68 (3.0 %)

Table 10. VHF Log-periodic Comparative Analysis, 25 MHz.

Table 11 shows a comparison of results for the HF log-periodic antenna at 25 MHz. All results are compared to NEC-4. As previously explained, the antenna was not modeled with MN and TA due to the excessive number of wires required for modeling.

	Maximum Gain, dBi (deviation)	Takeoff Angle, degrees (deviation)	Beamwidth, degrees (deviation)
NEC-4	11.33	41	33
ELNEC	10.26 (-21.8 %)	42 (2.4 %)	34 (3.0 %)
PAINT Oahu	12.04 (17.8 %)	42 (2.4 %)	33 (0 %)

Table 11. HF Log-periodic Comparative Analysis, 25 MHz.

Table 12 shows a comparative analysis for the sloping V antenna. The antenna was not modeled with MN and TA.

	Maximum Gain, dBi (deviation)	Takeoff Angle, degrees (deviation)	Beamwidth, degrees (deviation)
NEC-4	10.63	11	11.5
ELNEC	9.57 (-21.7 %)	10 (-9.1 %)	10 (-13.0 %)
PAINT Raro.	10.94 (7.4 %)	18 (63.6 %)	15 (30.4 %)

Table 12. Sloping V Comparative Analysis, 25 MHz.

A sample of program run times is presented for comparison. The 6 element VHF log-periodic antenna is modeled. The programs were all run with a 90 MHz Pentium processor. Table 13 shows the run time results.

PROGRAM	Time (min:sec)
NEC-4, 96 segments	0:22
ELNEC, 96 segments	0:41
PAINT, 96 segments and 154 plates.	9:16
MN, 96 segments TA	0:28 < 0:01

Table 13. Sample Run Times.

TA is the fastest of the programs to use if a freespace pattern of the antenna has been created. It is easy to change the terrain and antenna location. If a change of frequency is required the MN antenna program has to be run for the new frequency.

B. RECOMMENDATIONS FOR FUTURE RESEARCH

It is recommended that the PAINT source array definition problem be corrected. Special consideration should be given to the problem of positioning a current array that has elements at different heights. Until corrections are made, one suggestion is to flatten the plate or plates directly under the antenna. Another suggestion is to increase the number of plates used until the terrain under the antenna is well defined.

APPENDIX A. ELNEC RHOMBIC INPUT DATA

ELNEC ver. A1.02

Rhombic, L=50.7 m, 45 deg apex 10-27-1995 08:21:16

Frequency = 15 MHz.

Wire Loss: Zero

---------- WIRES ----------

Wire	Conn.	--- End 1 (x,y,z : m)	Conn.	--- End 2 (x,y,z : m)	Dia(mm)	Seg
1	W5E1	-46.800, 0.010, 13.100	W2E1	0.000, 19.400, 13.100	2.00E+00	55
2	W1E2	0.000, 19.400, 13.100	W6E2	46.800, 0.010, 13.100	2.00E+00	55
3	W4E2	0.000,-19.400, 13.100	W6E1	46.800, -0.010, 13.100	2.00E+00	55
4	W5E2	-46.800, -0.010, 13.100	W3E1	0.000,-19.400, 13.100	2.00E+00	55
5	W1E1	-46.800, 0.010, 13.100	W4E1	-46.800, -0.010, 13.100	2.00E+00	1
6	W3E2	46.800, -0.010, 13.100	W2E2	46.800, 0.010, 13.100	2.00E+00	1

---------- SOURCES ----------

Source	Pulse	Wire #/Pct From End 1 Actual	(Specified)	Ampl.(V, A)	Phase(Deg.)	Type
1	220	5 /100.00	(5 / 50.00)	1.000	0.000	I

---------- LOADS ----------

Load	Pulse	Wire #/Pct From End 1 Actual	(Specified)	R (Ohms)	X(Ohms)
1	222	6 /100.00	(6 / 50.00)	600.000	0.000

Ground type is Real

---------- RADIALS ----------

Number of Radials = 0 Wire Dia. = 0 mm.

---------- MEDIA ----------

Medium	Conductivity(S/m)	Dielectric Const.	Ht(m)	R Coord(m)
1	5.000E-03	13.00	0 (def)	0 (def)

APPENDIX B. ELNEC SLOPING V INPUT DATA

ELNEC ver. A1.02

Sloping V, 45 deg, L=80m 12-02-1995 12:13:42

Frequency = 15 MHz.

Wire Loss: Zero

---------- WIRES ----------

Wire	Conn.	End 1 (x,y,z : m)	Conn.	End 2 (x,y,z : m)	Dia(mm)	Seg
1	W5E1	0.000, -0.100, 14.000	W3E1	72.900,-28.280, 1.800	4.00E+00	100
2	W5E2	0.000, 0.100, 14.000	W4E1	72.900, 28.280, 1.800	4.00E+00	100
3	W1E2	72.900,-28.280, 1.800	G	72.900,-28.280, 0.000	4.00E+00	4
4	W2E2	72.900, 28.280, 1.800	G	72.900, 28.280, 0.000	4.00E+00	4
5	W1E1	0.000, -0.100, 14.000	W2E1	0.000, 0.100, 14.000	4.00E+00	2

---------- SOURCES ----------

Source	Pulse	Wire #/Pct From End 1 Actual	(Specified)	Ampl.(V, A)	Phase(Deg.)	Type
1	210	5 / 50.00	(5 / 50.00)	1.000	0.000	V

---------- LOADS ----------

Load	Pulse	Wire #/Pct From End 1 Actual	(Specified)	R (Ohms)	X(Ohms)
1	203	3 /100.00	(3 /100.00)	600.000	0.000
2	208	4 /100.00	(4 /100.00)	600.000	0.000

Ground type is Real

---------- RADIALS ----------

Number of Radials = 0 Wire Dia. = 0 mm.

---------- MEDIA ----------

Medium	Conductivity(S/m)	Dielectric Const.	Ht(m)	R Coord(m)
1	5.000E-03	13.00	0 (def)	0 (def)

APPENDIX C. ELNEC HF LOG-PERIODIC INPUT DATA

ELNEC ver. A1.02

HF Log Periodic 12-02-1995 14:25:15

Frequency = 2 MHz.

Wire Loss: Zero

---------- WIRES ----------

Wire	Conn.	End 1 (x,y,z : ft)	Conn.	End 2 (x,y,z : ft)	Dia(in)	Seg
1	W2E1	0.000, 0.000,100.169		0.000,123.000,100.169	1.57E-01	5
2	W1E1	0.000, 0.000,100.169	W3E2	68.200, 0.000, 80.469	1.57E-01	4
3		68.200,-98.500, 80.469	W2E2	68.200, 0.000, 80.469	1.57E-01	5
4	W2E2	68.200, 0.000, 80.469	W5E1	123.000, 0.000, 64.569	1.57E-01	4
5	W4E2	123.000, 0.000, 64.569		123.000, 78.500, 64.569	1.57E-01	5
6	W4E2	123.000, 0.000, 64.569	W7E2	166.200, 0.000, 52.069	1.57E-01	4
7		166.200,-63.000, 52.069	W6E2	166.200, 0.000, 52.069	1.57E-01	5
8	W6E2	166.200, 0.000, 52.069	W9E1	200.800, 0.000, 42.069	1.57E-01	4
9	W8E2	200.800, 0.000, 42.069		200.800, 50.500, 42.069	1.57E-01	5
10	W8E2	200.800, 0.000, 42.069	W11E2	228.700, 0.000, 33.969	1.57E-01	4
11		228.700,-40.500, 33.969	W10E2	228.700, 0.000, 33.969	1.57E-01	5
12	W10E2	228.700, 0.000, 33.969	W13E1	250.800, 0.000, 27.569	1.57E-01	4
13	W12E2	250.800, 0.000, 27.569		250.800, 32.000, 27.569	1.57E-01	5
14	W12E2	250.800, 0.000, 27.569	W15E2	269.100, 0.000, 22.269	1.57E-01	4
15		269.100,-26.000, 22.269	W14E2	269.100, 0.000, 22.269	1.57E-01	5
16	W14E2	269.100, 0.000, 22.269	W17E1	283.500, 0.000, 18.069	1.57E-01	4
17	W16E2	283.500, 0.000, 18.069		283.500, 20.500, 18.069	1.57E-01	5
18	W16E2	283.500, 0.000, 18.069	W19E2	295.000, 0.000, 14.769	1.57E-01	4
19		295.000,-16.500, 14.769	W18E2	295.000, 0.000, 14.769	1.57E-01	5
20	W18E2	295.000, 0.000, 14.769	W21E1	304.600, 0.000, 11.969	1.57E-01	4
21	W20E2	304.600, 0.000, 11.969		304.600, 13.000, 11.969	1.57E-01	5
22	W20E2	304.600, 0.000, 11.969	W23E2	311.900, 0.000, 9.869	1.57E-01	4
23		311.900,-10.500, 9.869	W22E2	311.900, 0.000, 9.869	1.57E-01	5
24		0.000,-123.00,100.000	W25E1	0.000, 0.000,100.000	1.57E-01	5
25	W24E2	0.000, 0.000,100.000	W26E1	68.200, 0.000, 80.300	1.57E-01	4
26	W25E2	68.200, 0.000, 80.300		68.200, 98.500, 80.300	1.57E-01	5
27	W25E2	68.200, 0.000, 80.300	W28E2	123.000, 0.000, 64.400	1.57E-01	4
28		123.000,-78.500, 64.400	W27E2	123.000, 0.000, 64.400	1.57E-01	5
29	W27E2	123.000, 0.000, 64.400	W30E1	166.200, 0.000, 51.900	1.57E-01	4
30	W29E2	166.200, 0.000, 51.900		166.200, 63.000, 51.900	1.57E-01	5
31	W29E2	166.200, 0.000, 51.900	W32E2	200.800, 0.000, 41.900	1.57E-01	4
32		200.800,-50.500, 41.900	W31E2	200.800, 0.000, 41.900	1.57E-01	5

APPENDIX C. ELNEC HF LOG-PERIODIC INPUT DATA (CONTINUED)

```
33 W31E2 200.800,  0.000, 41.900 W34E1 228.700,  0.000, 33.800  1.57E-01   4
34 W33E2 228.700,  0.000, 33.800       228.700, 40.500, 33.800  1.57E-01   5
35 W33E2 228.700,  0.000, 33.800 W36E2 250.800,  0.000, 27.400  1.57E-01   4
36       250.800,-32.000, 27.400 W35E2 250.800,  0.000, 27.400  1.57E-01   5
37 W35E2 250.800,  0.000, 27.400 W38E1 269.100,  0.000, 22.100  1.57E-01   4
38 W37E2 269.100,  0.000, 22.100       269.100, 26.000, 22.100  1.57E-01   5
39 W37E2 269.100,  0.000, 22.100 W40E2 283.500,  0.000, 17.900  1.57E-01   4
40       283.500,-20.500, 17.900 W39E2 283.500,  0.000, 17.900  1.57E-01   5
41 W39E2 283.500,  0.000, 17.900 W42E1 295.000,  0.000, 14.600  1.57E-01   4
42 W41E2 295.000,  0.000, 14.600       295.000, 16.500, 14.600  1.57E-01   5
43 W41E2 295.000,  0.000, 14.600 W44E2 304.600,  0.000, 11.800  1.57E-01   4
44       304.600,-13.000, 11.800 W43E2 304.600,  0.000, 11.800  1.57E-01   5
45 W43E2 304.600,  0.000, 11.800 W46E1 311.900,  0.000,  9.700  1.57E-01   4
46 W45E2 311.900,  0.000,  9.700       311.900, 10.500,  9.700  1.57E-01   5
47 W45E2 311.900,  0.000,  9.700 W22E2 311.900,  0.000,  9.869  1.57E-01   2


 48  W1E1   0.000,  0.000,100.169 W24E2   0.000,  0.000,100.000  1.57E-01   2

             ------------- SOURCES -------------

Source    Pulse     Wire #/Pct From End 1    Ampl.(V, A)  Phase(Deg.)  Type
                   Actual      (Specified)

 1        208    47 / 50.00   ( 47 / 50.00)      1.000       0.000       I

             -------------- LOADS --------------

Load      Pulse     Wire #/Pct From End 1      R (Ohms)       X(Ohms)
                   Actual      (Specified)

 1        211    48 / 50.00   ( 48 / 50.00)     300.000         0.000

Ground type is Real

             -------------- RADIALS --------------

Number of Radials = 0      Wire Dia. = 0 in.

             -------------- MEDIA --------------

Medium          Conductivity(S/m)   Dielectric Const.    Ht(ft)    R Coord(ft)

 1                 9.000E-03            13.00          0 (def)     0 (def)
```

APPENDIX D. ELNEC VHF LOG-PERIODIC INPUT DATA

ELNEC ver. A1.02

VHF LP, 6 element 12-02-1995 11:25:35

Frequency = 60 MHz.

Wire Loss: Zero

---------- WIRES ----------

Wire	Conn.	End 1 (x,y,z : in)	Conn.	End 2 (x,y,z : in)	Dia(in)	Seg
1	W2E1	0.000, 0.000,120.158		0.000,118.100,120.158	1.57E-01	11
2	W1E1	0.000, 0.000,120.158	W3E1	74.200, 0.000,120.158	1.57E-01	8
3	W2E2	74.200, 0.000,120.158		74.200,-99.200,120.158	1.57E-01	10
4	W2E2	74.200, 0.000,120.158	W5E1	136.500, 0.000,120.158	1.57E-01	6
5	W4E2	136.500, 0.000,120.158		136.500, 83.300,120.158	1.57E-01	9
6	W4E2	136.500, 0.000,120.158	W7E1	188.900, 0.000,120.158	1.57E-01	6
7	W6E2	188.900, 0.000,120.158		188.900,-70.000,120.158	1.57E-01	8
8	W6E2	188.900, 0.000,120.158	W9E1	232.900, 0.000,120.158	1.57E-01	6
9	W8E2	232.900, 0.000,120.158		232.900, 58.800,120.158	1.57E-01	7
10	W8E2	232.900, 0.000,120.158	W11E1	269.800, 0.000,120.158	1.57E-01	4
11	W10E2	269.800, 0.000,120.158		269.800,-49.400,120.158	1.57E-01	6
12	W13E1	0.000, 0.000,120.000		0.000,-118.10,120.000	1.57E-01	11
13	W12E1	0.000, 0.000,120.000	W14E1	74.200, 0.000,120.000	1.57E-01	8
14	W13E2	74.200, 0.000,120.000		74.200, 99.200,120.000	1.57E-01	10
15	W13E2	74.200, 0.000,120.000	W16E1	136.600, 0.000,120.000	1.57E-01	6
16	W15E2	136.600, 0.000,120.000		136.600,-83.300,120.000	1.57E-01	9
17	W15E2	136.600, 0.000,120.000	W18E1	188.900, 0.000,120.000	1.57E-01	6
18	W17E2	188.900, 0.000,120.000		188.900, 70.000,120.000	1.57E-01	8
19	W17E2	188.900, 0.000,120.000	W20E1	232.900, 0.000,120.000	1.57E-01	6
20	W19E2	232.900, 0.000,120.000		232.900,-58.800,120.000	1.57E-01	7
21	W19E2	232.900, 0.000,120.000	W22E1	269.800, 0.000,120.000	1.57E-01	4
22	W21E2	269.800, 0.000,120.000		269.800, 49.400,120.000	1.57E-01	6
23	W21E2	269.800, 0.000,120.000	W10E2	269.800, 0.000,120.158	1.57E-01	2
24	W1E1	0.000, 0.000,120.158	W12E1	0.000, 0.000,120.000	1.57E-01	2

APPENDIX D. ELNEC VHF LOG-PERIODIC INPUT DATA (CONTINUED)

---------- SOURCES ----------

Source	Pulse	Wire #/Pct From End 1 Actual	(Specified)	Ampl.(V, A)	Phase(Deg.)	Type
1	162	23 / 50.00	(23 / 50.00)	1.000	0.000	V

---------- LOADS ----------

Load	Pulse	Wire #/Pct From End 1 Actual	(Specified)	R (Ohms)	X(Ohms)
1	165	24 / 50.00	(24 / 50.00)	50.000	0.000

Ground type is Real

---------- RADIALS ----------

Number of Radials = 0 Wire Dia. = 0 in.

---------- MEDIA ----------

Medium	Conductivity(S/m)	Dielectric Const.	Ht(in)	R Coord(in)
1	5.000E-03	13.00	0 (def)	0 (def)

APPENDIX E. NEC-4 VHF LOG-PERIODIC INPUT FILE

```
CM    6 element VHF Log Periodic 25-60 MHz
CM    10' high over real ground
CM      f/n: vhf60.inp
CE
GW  1  21    0.   -118.1    120.0     0.     118.1    120.0    .079
GW  2  19   74.2   -99.2    120.0    74.2     99.2    120.0    .079
GW  3  17  136.5   -83.3    120.0   136.5     83.3    120.0    .079
GW  4  15  188.9   -70.0    120.0   188.9     70.0    120.0    .079
GW  5  13  232.9   -58.8    120.0   232.9     58.8    120.0    .079
GW  6  11  269.8   -49.4    120.0   269.8     49.4    120.0    .079
GS  0  0  0.0254
GE -1.  0.  0.
GN  2  0  0  0  13.0  0.005
TL  1  11  2  10  -50.  0  .02  0  0  0
TL  2  10  3  9   -50.
TL  3  9   4  8   -50.
TL  4  8   5  7   -50.
TL  5  7   6  6   -50.
EX  0  6  6  0  1  0.
FR  0  0  0  0  60  0.
XQ  1.
RP  0  1  360  1000  66  0  0  1  0  0.
EN
```

APPENDIX F. NEC-4 HF LOG-PERIODIC INPUT FILE

```
CM     12 Element HF Log Periodic  2-25 MHz
CM     Ground Plane present
CM       f/n: LP25.inp
CM       wire coordinates in feet
CE
GW  1  33    0.0    -123.0    100.0     0.0    123.0    100.0   0.00656
GW  2  31   68.2     -98.5     80.3    68.2     98.5     80.3   0.00656
GW  3  29  123.0     -78.5     64.4   123.0     78.5     64.4   0.00656
GW  4  27  166.2     -63.0     51.9   166.2     63.0     51.9   0.00656
GW  5  25  200.8     -50.5     41.9   200.8     50.5     41.9   0.00656
GW  6  23  228.7     -40.5     33.8   228.7     40.5     33.8   0.00656
GW  7  21  250.8     -32.0     27.4   250.8     32.0     27.4   0.00656
GW  8  19  269.1     -26.0     22.1   269.1     26.0     22.1   0.00656
GW  9  17  283.5     -20.5     17.9   283.5     20.5     17.9   0.00656
GW 10  15  295.0     -16.5     14.6   295.0     16.5     14.6   0.00656
GW 11  13  304.6     -13.0     11.8   304.6     13.0     11.8   0.00656
GW 12  11  311.9     -10.5      9.7   311.9     10.5      9.7   0.00656
GS  0   0   0.3048
GE  -1.  0.  0.
GN  2.   0.  0.  0.  13.0  0.005
TL  1  17  2  16  -300.  0  .0033  0  0  0
TL  2  16  3  15  -300.
TL  3  15  4  14  -300.
TL  4  14  5  13  -300.
TL  5  13  6  12  -300.
TL  6  12  7  11  -300.
TL  7  11  8  10  -300.
TL  8  10  9   9  -300.
TL  9   9  10  8  -300.
TL  10  8  11  7  -300.
TL  11  7  12  6  -300.
EX  0  12  6  0  1  0.
FR  0  0  0  0  25  0.
XQ  1.
RP  0  1  360  1000  49  0  0  1  0  0
EN
```

APPENDIX G. NEC-4 SLOPING V INPUT FILE

```
CM    Sloping Vee Antenna  2-25 MHz
CM    Apex height = 14.5 m, Interior Angle = 45 degrees
CM    Leg length = 80 m, 600 ohm terminating resisters
CM    Terminated end height = 1.8 m
CM    f/n: v15.inp
CE
GW1, 100,  0.,  -0.1,  14.0,   72.9, -28.28, 1.8,   0.002,
GW2, 100,  0.,  0.1,  14.0,   72.9,  28.28, 1.8,   0.002,
GW3,  4, 72.9, -28.28, 1.8, 72.9, -28.28, 0.,  0.002,
GW4,  4, 72.9,  28.28, 1.8, 72.9,  28.28, 0.,  0.002,
GW5,  3,  0.,  -0.1,  14.0,   0.,  0.1,  14.0,  0.002,
GE-1, 0, 0,
LD4, 1, 100, 100, 600, 0,
LD4, 2, 100, 100, 600, 0,
FR0, 0, 0, 0, 15, 0,
GN2, 0, 0, 0, 13.0, 0.005,
EX0, 5, 2, 1, 1.0, 0, 0,
XQ1,
RP0, 1, 360, 1000, 72, 0, 0, 1, 0, 0,
EN
```

APPENDIX H. MN VHF LOG-PERIODIC INPUT FILE

```
6 Element VHF Log Periodic 25-60 MHz
Free Space
60 MHz
23 wires, inches
6    0      0    1      0      118.1    1    .079
4    0      0    1     74.2    0        1    .079
6    74.2   0    1     74.2    -99.2    1    .079
4    74.2   0    1     136.5   0        1    .079
6    136.5  0    1     136.5   83.3     1    .079
4    136.5  0    1     188.9   0        1    .079
6    188.9  0    1     188.9   -70.0    1    .079
4    188.9  0    1     232.9   0        1    .079
6    232.9  0    1     232.9   58.8     1    .079
4    232.9  0    1     269.8   0        1    .079
6    269.8  0    1     269.8   -49.4    1    .070
6    0      0    0     0       -118.1   0    .079
4    0      0    0     74.2    0        0    .079
6    74.2   0    0     74.2    99.2     0    .079
4    74.2   0    0     136.5   0        0    .079
6    136.5  0    0     136.5   -83.3    0    .079
4    136.5  0    0     188.9   0        0    .079
6    188.9  0    0     188.9   70.0     0    .079
4    188.9  0    0     232.9   0        0    .079
6    232.9  0    0     232.9   -58.8    0    .079
4    232.9  0    0     269.8   0        0    .079
6    269.8  0    0     269.8   49.4     0    .079
4    269.8  0    0     269.8   0        1    .079
1 source
wire 23, center
```

APPENDIX I. TA TERRAIN FILES

```
"Oahu Terrain Profile"
vhf25.pf,2398,10
"feet"
0,1155
1148,1165
1785,1181
1988,1198
2234,1207
2398,1198
2687,1181
3054,1165
3281,1148
3406,1132
3507,1115
3609,1099
3711,1083
3835,1066
3978,1050
4121,1033
4327,1017
4728,1001
4859,991
```

```
"Rarotonga Terrain Profile"
vhf25.pf,2625,10
"feet"
0,45
328,41
656,37
984,33
1312,29
1640,25
1967,18
2297,10
2620,4
2723,0
5249,0
```

LIST OF REFERENCES

1. McNamara, L. F., *The Ionosphere: Communications, Surveillance, and Direction Finding*, Krieger Publishing Company, Melbourne, FL 1991.

2. Davies, K., *Ionospheric Radio,* Peter Peregrinus Ltd., London, United Kingdom 1990.

3. Kingan, S. G., "A Study of the Behaviour and Geographical Distribution of Nighttime VHF Transequatorial Propagation in the Central Pacific," *TENERP Conference Proceedings June 22-24*, 1993, NPS Monterey, CA.

4. Collin, R. E., *Antennas and Radiowave Propagation,* McGraw-Hill Inc., Los Angeles, CA 1985.

5. Rudge, A. W., Milne, K., Olver, A. D., and Knight, P., *The Handbook of Antenna Design,* Peter Peregrinus Ltd., London, United Kingdom 1983.

6. Milligan, T. A., *Modern Antenna Design,* McGraw-Hill Inc., Los Angeles, CA 1985.

7. Stutzman, W. L., and Thiele, G. A., *Antenna Theory and Design,* John Wiley & Sons, New York, NY 1981.

8. Jasik, H. and Johnson, R. C., *Antenna Engineering Handbook 2nd Edition,* McGraw-Hill Inc., Los Angeles, CA 1984.

9. Young, J. S., "Simulation of Antenna Patterns Over 3-Dimentional Irregular Terrain Using the Uniform Geometrical Theory of Diffraction (UTD) [Development of the PAINT System]," PhD. Thesis, The Pennsylvania State University, 1994.

10. Burke G. J., *Numerical Electromagnetic Code - NEC-4 Methods of Moments Part I: User's Manual,* Lawrence Livermore National Laboratory, January 1992.

11. Lewallen R. W., *ELNEC Manual,* 1993.

12. Beezley B., *MN Antenna Analysis Manual,* 1990.

13. Beezley B., *TA 1.11 Terrain Analyzer Manual,* 1995.

14. Phoncon, between Theodore Kline, The Naval Postgraduate School and Keith Lysak, The Pennsylvania State University, 29 November 1995.

INITIAL DISTRIBUTION LIST

1. Defense Technical Information Center 2
   8725 John J. Kingman Rd., STE 0944
   Ft. Belvoir, VA 22060-6218

2. Library, Code 013 2
   Naval Postgraduate School
   Monterey, CA 93943-5101

3. Director, Training and Education 1
   MCCDC, Code C46
   1019 Elliot Rd.
   Quantico, VA 22134-5027

4. Chairman, Code EC 1
   Department of Electrical and Computer Engineering
   Naval Postgraduate School
   Monterey, CA 93943-5101

5. Dr. Richard W. Adler, Code EC/Ab 2
   Department of Electrical and Computer Engineering
   Naval Postgraduate School
   Monterey, CA 93943-5101

6. Rasler W. Smith, Code EC/Sr 2
   Department of Electrical and Computer Engineering
   Naval Postgraduate School
   Monterey, CA 93943-5101

7. Captain Theodore S. Kline 2
   MCCDC
   Quantico, VA 22134-5001

8. Brian Beezley 1
   3532 Linda Vista Dr.
   San Marcos, CA 92069-6310

9. Dr. James K. Breakall 1
Applied Research Lab
Pennsylvania State University
University Park, PA 16801

10. Dr. Joel S. Young 1
2740 Bowman Ln.
Conway, AZ 72032-6760

11. Cdr. John ODwyer 1
Naval Information Warfare Activity
Code N9
9800 Savage Rd.
Ft. Meade, MD 20755-6000

12. Jim Zmyslow 1
5507 Lake Ridge Terrace
Bowie, MD 20720

13. Bob Rose 1
15514 E. Richwood Ave.
Fountain Hill, AZ 85268

14. Stuart Kingan 1
Edgewater, Matavera Village
Avura
Rarotonga, Cooke Islands

15. Robert Hunsucker 1
7917 Gearhardt
Klamath Falls, OR 97603

16. Roy Lewellan 1
Box 6658
Beaverton, OR 97007